To the Graduate Council:

I am submitting herewith a thesis written by Donald Kim Sickafoose entitled "Ecostratigraphy of the Lower Middle Ordovician and Paleoecology of Porterfieldian and Wildernessian Biotas at Evans Ferry, Tennessee." I recommend that it be accepted in partial fulfillment of the requirements for the degree of Master of Science, with a major in Geology.

Kenneth R. Walker
Major Professor

We have read this thesis and
recommend its acceptance:

Fred B. Zeller

R. E. McLaughlin

Accepted for the Council:

L. Evans Edgell
Vice Chancellor
Graduate Studies and Research

Thesis
79
S624
cop. 2

ECOSTRATIGRAPHY OF THE LOWER MIDDLE ORDOVICIAN AND PALEOECOLOGY OF PORTERFIELDIAN AND WILDERNESSIAN BIOTAS AT EVANS FERRY, TENNESSEE

A Thesis

Presented for the

Master of Science

Degree

The University of Tennessee, Knoxville

Donald Kim Sickafoose

June 1979

139[illegible]6

ACKNOWLEDGEMENTS

The writer expresses great appreciation to Dr. Kenneth R. Walker who guided the writer in this problem, supplied financial aid (from a National Science Foundation research grant) for summer field work, and provided great encouragement toward the completion of this paper. Appreciation is also given to Dr. R. E. McLaughlin and F. B. Keller for reviewing this thesis and for offering helpful criticisms.

The writer would also like to thank Drs. T. W. Broadhead and F. K. McKinney for their valuable assistance in the taxonomic identification of echinoderms and bryozoans respectively. Appreciation is also extended to M. R. Maitland who is responsible for most of the trilobite identifications and for the construction of the trilobite plate.

The writer also extends his appreciation to F. C. Breland who printed many of the photographs for this thesis, and to S. C. Ruppel who suggested this problem and provided invaluable assistance in the early stages of field work. Finally, the writer expresses great appreciation to his parents, Donald and Amelia Sickafoose, for making it possible for the writer to complete his education.

ABSTRACT

This study is an ecostratigraphic and paleoecologic analysis of a part of the complex facies in Middle Ordovician carbonate shelf sediments at Evans Ferry, Tennessee. The 330 meter stratigraphic section begins at the Post-Knox unconformity and comprises in ascending order: the Tumbez Formation, the Eidson and Hogskin members of the Lincolnshire Formation and the Rockdell, Benbolt and Wardell formations. This study consists of two parts. First, a petrographic analysis of 146 thin sections from the stratigraphic section to establish a paleoenvironmental framework. Using this framework, two fossiliferous intervals (A and B), representing different environments, were selected for paleoecologic study.

Deposition of the Evans Ferry section began in the supratidal-intertidal environment, progressed to a stable offshore subtidal environment and ended with a return to peritidal conditions. The Tumbez Formation represents a supratidal-high intertidal environment at its base and a low intertidal algal flat environment at its top. Algal flats were maintained throughout the deposition of the lower Eidson Member, but were succeeded by shallow subtidal conditions in the middle and upper units. Stable subtidal conditions are inferred for the deposition of the Hogskin Member with occasional interruptions by storm or tidal channel deposits. The Rockdell Formation was deposited in a subtidal environment with semirestricted water circulation. The upper units of the Rockdell Formation and the lower units of the

Benbolt Formation represent interacting stable subtidal environments characterized by intermittent deposition of mud and decreasing water depth. The remainder of the Benbolt Formation includes deposits of tidal skeletal sand bars, algal mud mounds and deeper subtidal intermound areas. A gradual change from shallow nearshore subtidal to high intertidal-supratidal environments is inferred for the Wardell Formation.

Interval A composes the lower 21 meters of the Benbolt Formation (171.3-192.3 meters from the base of the section) and is divisible into three lithologic zones based on the packstone to shale (pk:sh) ratio. Zone I (9 m thick) has a 2:1 ratio and exhibits the highest species variety of any studied interval. Fossil assemblages represent gradual environmental changes, and are dominated by stenohaline epifaunal suspension feeders. A parameter was devised (uniformity index), which characterizes the distribution of species within fossil Classes. Zone I has high uniformity indices indicating a monotonic decrease in numbers of species within Classes.

Zone II (4.5 m thick) has a 1:2 pk:sh ratio, lower species variety, and low uniformity indices suggesting less environmental stability. Abundance of epifaunal suspension feeders decreases concomitant with an increase in vagile deposit feeders and browsers. Zone III (7.5 m thick) has a variable pk:sh ratio of 5:1 at the base to 2:1 at the top. The less exposed and weathered outcrop of zone III may account for the few species identified other than in thin sections, and indicates

a large sample collecting bias. All of interval A represents a stable offshore, level bottom, subtidal environment.

Interval B contains 47.2 meters of rock of which the lower 26.4 meters is fossiliferous; the remainder is composed of intertidal mudstone and calcareous shale laminae. The fossiliferous rock sequence contains five paleocommunities, which represent an offshore to onshore regression, these are: (1) Hesperorthis community; (2) Strophomena-Hesperorthis community; (3) Tetradium-Girvanella community; (4) Chaulistomella-Stophomena community; and (5) Strophomena-Rostricellula community. The Strophomena-Hesperorthis assemblages resemble an ecotonal community between the Hesperorthis community (furthest offshore) and the Tetradium-Girvanella wave baffle community. The Chaulistomella-Strophomena and Strophomena-Rostricellula assemblages represent shallow nearshore subtidal communities interstratified with intertidally deposited sediments.

Total species diversity of the biota in interval B decreases up the section (toward nearer-shore environments). The uniformity indices for the communities are very low reflecting the dominance of species variety by one class. The biota displays two trends with decreasing distance from shore, which are: (1) a progressive change from sessile suspension feeders to vagile deposit feeders and (2) a change toward increasing salinity tolerances. Consequently, interval B represents communities exhibiting compositional changes in response to increasingly harsh physical conditions.

TABLE OF CONTENTS

CHAPTER		PAGE
I.	INTRODUCTION	1
	General Background	1
	Study Area	2
	Purpose and Limitations of the Study	4
	Previous Investigations (1943-1973)	6
	Recent Investigations (1973-Present)	10
	Methods	15
II.	STRATIGRAPHY AND INFERRED PALEODEPOSITIONAL ENVIRONMENTS OF THE UNITS IN THE EVANS FERRY SECTION	17
	Introduction	17
	Post-Knox Unconformity	18
	Tumbez Formation	19
	General description	19
	Lithology T1	19
	Thin section analysis	19
	Paleoenvironmental interpretation	22
	Lithology T2	25
	Thin section analysis	25
	Paleoenvironmental interpretation	26
	Lithology T3	27
	Thin section analysis	27
	Paleoenvironmental interpretation	28
	Lithology T4	29
	Thin section analysis	29
	Paleoenvironmental interpretation	33
	Eidson Member of the Lincolnshire Formation	34
	General description	34
	Lithology E1	34
	Thin section analysis	34
	Paleoenvironmental interpretation	37
	Lithology E2	38
	Thin section analysis	38
	Paleoenvironmental interpretation	39
	Lithology E3	40
	Thin section analysis	40
	Paleoenvironmental interpretation	44
	Hogskin Member of the Lincolnshire Formation	44
	General description	44
	Lithology H1	45
	Thin section analysis	45
	Paleoenvironmental interpretation	49

CHAPTER PAGE

Lithology H2 52
Thin section analysis 52
Paleoenvironmental interpretation 53
Rockdell Formation 53
General description 53
Lithology R1 54
Thin section analysis 54
Paleoenvironmental interpretation 59
Lithology R2 60
Thin section analysis 60
Paleoenvironmental interpretation 61
Benbolt Formation 62
General description 62
Lithology B1 63
Thin section analysis 63
Paleoenvironmental interpretation 65
Lithology B2 66
Thin section analysis 66
Paleoenvironmental interpretation 66
Lithology B3 67
Thin section analysis 67
Paleoenvironmental interpretation 70
Lithology B4 72
Thin section analysis 72
Paleoenvironmental interpretation 72
Wardell Formation 73
General description 73
Lithology W1 74
Thin section analysis 74
Paleoenvironmental interpretation 77
Lithology W2 78
Thin section analysis 78
Paleoenvironmental interpretation 81
Lithology W3 83
Thin section analysis 83
Paleoenvironmental interpretation 84
Summary 85

III. PALEOECOLOGY OF INTERVAL A (PORTERFIELDIAN AGE) AND INTERVAL B (WILDERNESSIAN AGE) 86

Introduction 86
Interval A 91
General description 91
Lithologic zone I 93
General description 93
Species diversity 95

CHAPTER PAGE

Uniformity index 96
Analysis of autecologic parameters 99
Lithologic zone II 101
General description 101
Species diversity and the uniformity index 103
Analysis of autecologic parameters 105
Lithologic zone III 106
General description 106
Species diversity and the uniformity index 107
Analysis of autecologic parameters 107
Discussion of interval A 108
Interval B 110
General description 110
Hesperorthis community 111
Strophomena-Hesperorthis community 113
Tetradium-Girvanella oncolite community 117
Chaulistomella-Strophomena community 119
Strophomena-Rostricellula community 123
Analysis of autecologic parameters for interval B . . . 125
Discussion of interval B 128
Summary and Conclusions 131

REFERENCES CITED 136

APPENDICES 144

Appendix A 145
Appendix B 149
Appendix C 155

VITA 185

LIST OF TABLES

TABLE		PAGE
1.	Composition and Estimated Abundances of the Hesperorthis Community	112
2.	Composition and Estimated Abundances for the Strophomena-Hesperorthis Community	115
3.	Composition and Estimated Abundances for the Tetradium-Girvanella Oncolite Community	118
4.	Composition and Estimated Abundances for the Chaulistomella-Strophomena Community	120
5.	Composition and Estimated Abundances for the Strophomena-Rostricellula Community	124
A-1.	Constituent Particle Analyses (Rock Volume Percent) for Selected Thin Sections	146
B-1.	Descriptions of Gastropods Found in Intervals A and B	150
B-2.	Descriptions of Cephalopods Found in Interval A	150
B-3.	Autecologic Parameters of the Taxa Present in Intervals A and B of the Benbolt and Wardell Formations, Respectively, at Evans Ferry, Tennessee	151
C-1.	Fossils Present in EF'18-A	156
C-2.	Fossils Present in EF'18-B	156
C-3.	Fossils Present in EF'18-C	156
C-4.	Fossils Present in EF'18-D	157
C-5.	Fossils Present in EF'18-E	157
C-6.	Fossils Present in EF'18-F	157
C-7.	Fossils Present in EF'18-G	158
C-8.	Fossils Present in EF'18-H	158
C-9.	Fossils Present in EF'18-I	158

TABLE PAGE

C-10. Fossils Present in EF'19-J 159

C-11. Fossils Present in EF'19-K 159

C-12. Fossils Present in EF-19-L 159

C-13. Fossils Present in EF'19-M 160

C-14. Fossils Present in EF'19-N 160

C-15. Fossils Present in EF'23-A 160

C-16. Fossils Present in EF'23-B 161

C-17. Fossils Present in EF'23-C 161

C-18. Fossils Present in EF'23-D 162

C-19. Fossils Present in EF'24-A 162

C-20. Fossils Present in EF'24-B 162

C-21. Fossils Present in EF'24-C 163

C-22. Fossils Present in EF'25-A 163

C-23. Fossils Present in EF'25-B 163

C-24. Fossils Present in EF'25-C 164

C-25. Fossils Present in EF'25-D 164

C-26. Fossils Present in EF'26-A 164

C-27. Fossils Present in EF'26-B 164

C-28. Fossils Present in EF'26-C 165

C-29. Fossils Present in EF'26-D 165

C-30. Fossils Present in EF'26-E 165

C-31. Fossils Present in EF'26-F 165

C-32. Fossils Present in EF'26-G 166

LIST OF FIGURES

FIGURE		PAGE
1.	Location Map of the Study Area at Evans Ferry, Tennessee	3
2.	Stratigraphic Section for the Units at Evans Ferry, Tennessee	5
3.	Correlation Chart for the Schemes of Stratigraphic Terminology Applied to the Middle Ordovician Units in the St. Paul Strike Belt of Northeast Tennessee	8
4.	Environmental Model during Late Porterfieldian Time	11
5.	Environments of Deposition for the Middle Ordovician Rocks of East Tennessee and Southwest Virginia	12
6.	Diagram Showing the Areas Studied by Various Workers Involved in the University of Tennessee Research Program and Printed in Theses and Dissertations	13
7.	Types of Stylolites	18
8.	Photomicrographs of the Lower and Upper Tumbez Formation	20
9.	Stratigraphic Distribution of Allochems for Evans Ferry, Tennessee	24
10.	Photomicrographs of the Upper Tumbez Formation	31
11.	Stratigraphic Distribution of Detrital Quartz Silt for Evans Ferry, Tennessee	32
12.	Photomicrographs of the Lower Eidson Member	36
13.	Photographs of Lithologies within the Eidson and Hogskin Members of the Lincolnshire Formation	41
14.	Photomicrographs of Shale Laminae within the Hogskin Member and Associated Diagenesis	47
15.	Location of Algae in the Stratigraphic Section at Evans Ferry, Tennessee	50

FIGURE PAGE

16. Photomicrographs and Field Photograph of the Rockdell Formation 55

17. Stratigraphic Distribution of the Alga Girvanella for Evans Ferry, Tennessee 58

18. Field Photograph and Photomicrographs of the Middle and Upper Benbolt Formation 68

19. Photomicrographs and Hand Specimen of the Lower Wardell Formation 76

20. Photomicrographs of Thin Sections within the Middle and Upper Wardell Formation 79

21. Field Photographs of Interval A in the Benbolt Formation 92

22. Stratigraphic Distribution of Species Diversity within Each Major Taxon for Interval A, Evans Ferry, Tennessee . . 94

23. Series of Histograms Illustrating Species Diversity within Classes for Selected Sample Intervals within Interval A . . 97

24. Classification of Trophic Categories and Mobility Relationships for Species Occurring in Interval A 100

25. Percent Euryhaline Species versus Percent Stenohaline Species for the Biota of Intervals A and B 102

26. Total Species Diversity for Interval A toward the Top of the Evans Ferry Section 109

27. Series of Histograms Illustrating Species Diversity within Classes for Selected Sample Intervals within Interval B . . 114

28. Stratigraphic Distribution of the Varietal Aspect of Species Diversity within Each Major Taxon for Interval B, Evans Ferry, Tennessee 122

29. Classification of Trophic Categories and Mobility Relationships for Species Occurring in Interval B 126

30. Total Species Diversity for Interval B toward the Top of the Evans Ferry Section 129

LIST OF PLATES

PLATE		PAGE
C-1.	Gymnolaemata	167
C-2.	Gymnolaemata: Cryptostomata and Trepostomata	169
C-3.	Inarticulata and Articulata	171
C-4.	Articulata	173
C-5.	Cephalopoda and Gastropoda	175
C-6.	Trilobita	177
C-7.	Rhombifera, Paracrinoidea, Eocrinoidea, Parablastoidea and Cyclocystoidea	179
C-8.	Crinoidea	181
C-9.	Chlorophyceae, Problematical Algae, Rhodophyceae and Schizophyceae	183

CHAPTER I

INTRODUCTION

I. GENERAL BACKGROUND

The Middle Ordovician rocks of the Southern Appalachians display a complex mosaic of carbonate rocks and intercalated terrigenous clastic rocks. These rocks crop out in somewhat linear strike belts, which trend northeast to southwest and are separated from adjacent belts by a series of southeasterly dipping thrust faults. Attempts by previous workers to correlate these rocks from strike belt regionally across the Southern Appalachians have generally relied on lithostratigraphic criteria and biostratigraphic data derived from the study of single taxa. The lithostratigraphic data, however, has been problematical because of the previously unrecognized complexity of the environmental facies present in the Middle Ordovician sequence. Likewise, since megafossils may be environmentally controlled (McLaughlin, 1973), biostratigraphic correlations across facies boundaries may also be questioned.

To answer these problems a research program initiated at the University of Tennessee has employed an ecostratigraphic approach to the analysis of the Middle Ordovician succession in East Tennessee. The initial work, centered mainly in strike belts southeast of the Saltville fault, has revealed a network of complex facies displaying rapid lateral and vertical changes. Similar facies complexes have been

observed in the strike belts northwest of the Saltville fault, but detailed ecostratigraphic studies are lacking. This investigation is an attempt to unravel the carbonate succession in a part of one such northwestern belt.

II. STUDY AREA

The Evans Ferry section is located about 6.4 kilometers north of the town of Thorn Hill, Tennessee, along Highway 25 East as shown in the southcentral portion of the Howard Quarter Quadrangle, 162-NW. It is adjacent to a large meander-loop in the Clinch River (Figure 1). According to Prouty (1946), the Middle Ordovician sequence at Evans Ferry is in the St. Paul strike belt. This strike belt is bounded by the Copper Creek thrust fault on the southeast and the Clinchport thrust fault on the northwest.

Recent highway construction on Route 25 East (near Evans Ferry) has removed a sharp curve and as a result has provided fresh exposures of the Middle Ordovician rocks above the Eidson Member of the Lincolnshire Formation. The severed curve of the old Route 25 East still remains and exhibits weathered rocks of the same formations. These aspects of the study area are ideal because: (1) the fresh outcrops allow unobstructed measurement of the section, and (2) the weathered outcrops expose fossiliferous rock slabs and individual specimens for use in paleoecologic study.

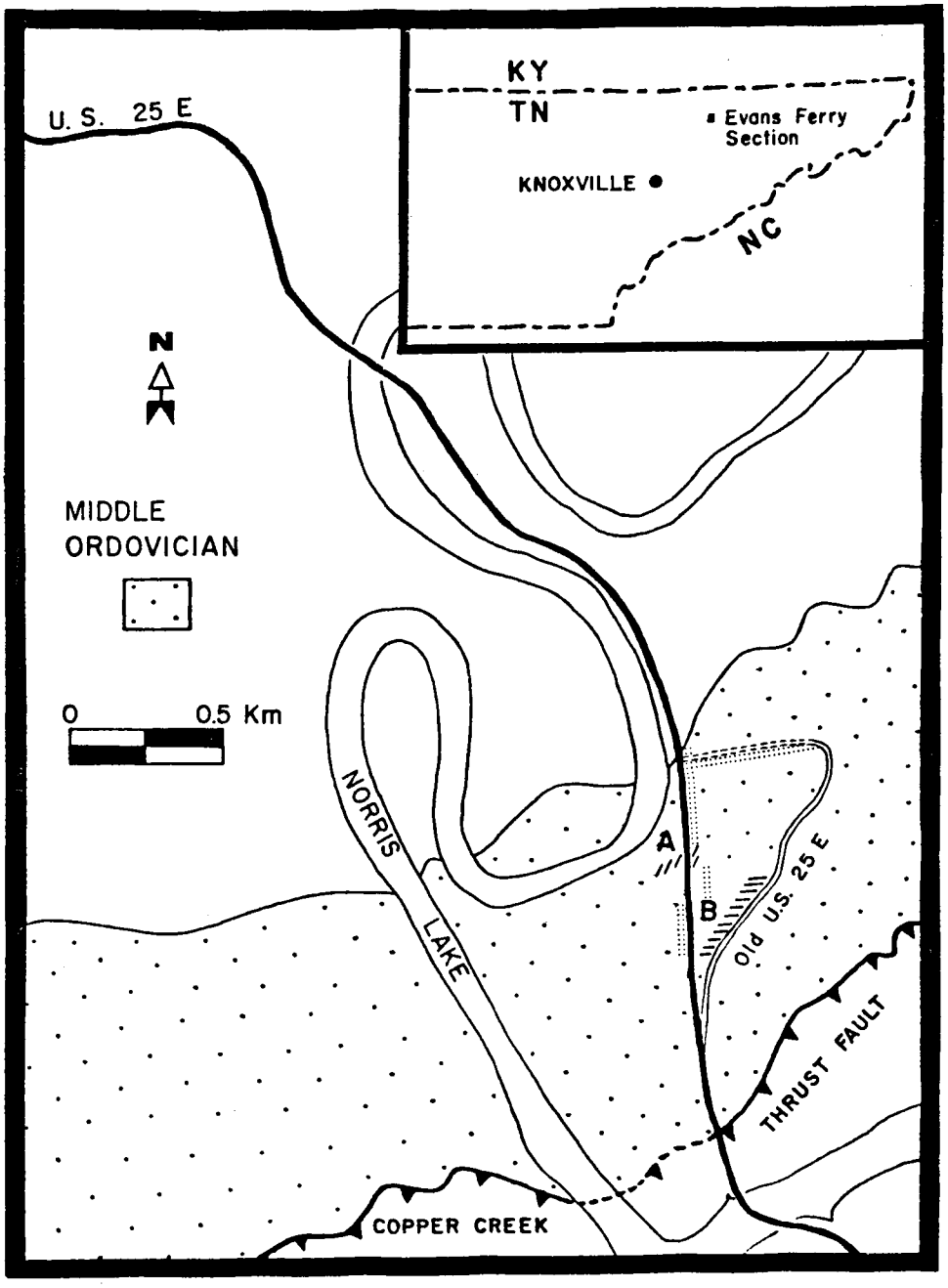


Figure 1. Location map of the study area at Evans Ferry, Tennessee. Outcrop locations are illustrated by the stippled pattern. The sample collecting sites for the paleoecologic study are shown by cross hatching for each interval, A and B.

III. PURPOSE AND LIMITATIONS OF THE STUDY

This study is an ecostratigraphic analysis of the poorly understood carbonate shelf sediments and their complex facies relationships. The study consists of two parts. The first part is the description of the major lithologies exposed in the Evans Ferry section and an interpretation of their respective paleodepositional environments. The section analyzed here begins at the post-Knox unconformity and consists in ascending order of the Tumbez Formation, Eidson and Hogskin members of the Lincolnshire Formation, and the Rockdell, Benbolt, and Wardell formations (Figure 2, stratigraphic terminology after Prouty, 1946; and Cooper, 1956). The second aspect of the study is an analysis of the fossil communities from two selected intervals within the section. The lowermost of these intervals is in the basal portion of the Benbolt Formation (171.3 meters to 192.3 meters above the base of the section). This interval was chosen because, according to Cooper (1956, Chart 1), the fauna is typical of his Porterfieldian Stage. The upper interval consists of the bulk of the Wardell Formation (282.9 meters to 330.1 meters above the base of the section), which is characterized by a fauna of Wilderness age (Cooper, 1956, Chart 1). On the basis of conodonts, Carnes (1975) has suggested that the entire Evans Ferry section is of Porterfieldian to Wildernessian age. More importantly, however, the two faunas clearly represent an offshore to onshore environmental transect. They therefore afford an opportunity to study the effect of changing environmental conditions

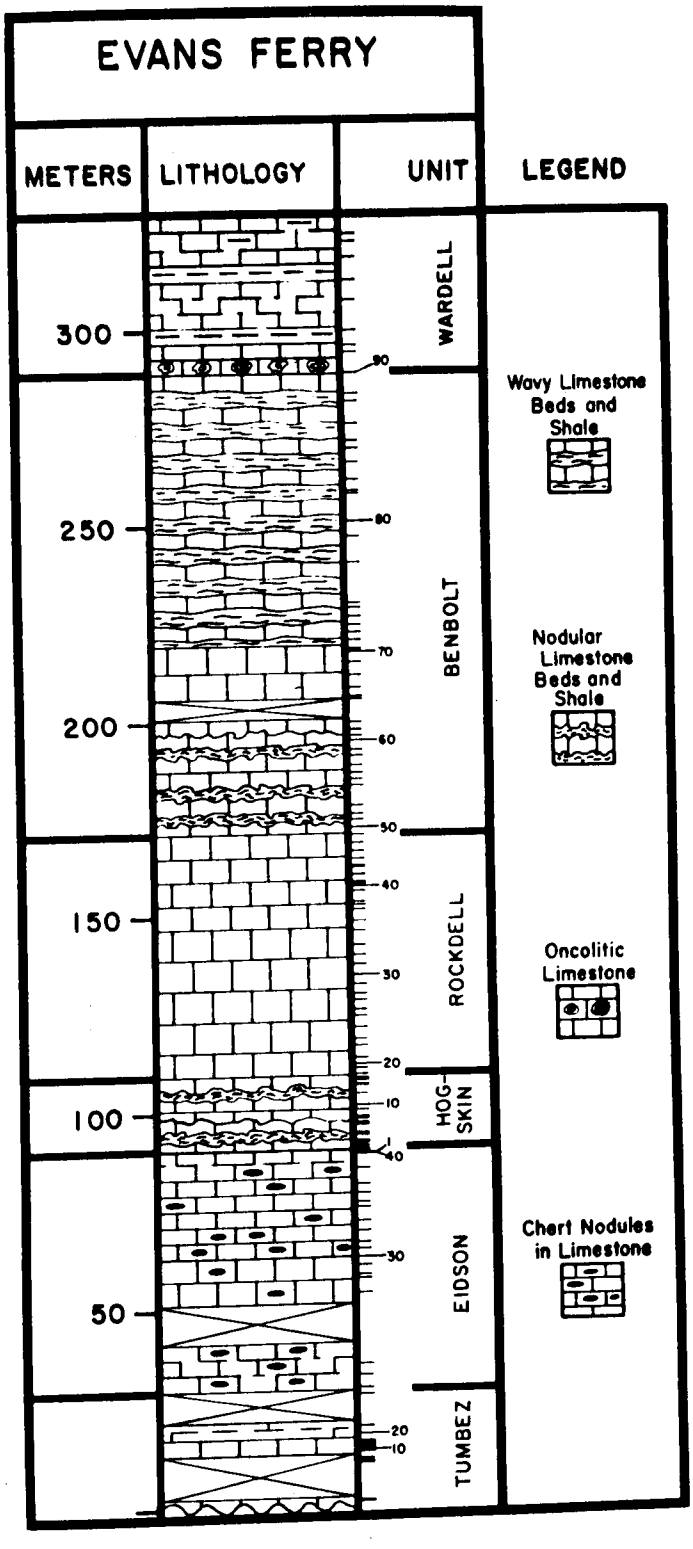


Figure 2. Stratigraphic section for the units at Evans Ferry, Tennessee. Location of the samples for petrologic analysis are shown on the right side of the stratigraphic column, associated numerals represent sample numbers.

on a large sample of typical Middle Ordovician biotas. The lower and upper biota (here interpreted as a suite of paleocommunities) are separated by 90.6 meters of stratigraphic section, probably representing no more than 1-3 million years. This time interval is sufficiently short so that the overall effects of evolution on community composition are much less significant than environmental change. Thus, changes in the communities can be related directly to paleoenvironmental conditions inferred from sedimentologic evidence.

One of the major limitations of whole-biota community analyses is the variable level of taxonomic information available in the literature on various major taxa. For example, whereas the brachiopods of the biota studied at Evans Ferry have been magnificently monographed by G. A. Cooper (1956), the gastropods in this section have not previously been studied. For this reason, many of the major taxa are treated here at the generic and familial levels.

IV. PREVIOUS INVESTIGATIONS (1943-1973)

In southwest Virginia and northeast Tennessee, 25 new names were proposed for the lower Middle Ordovician units within a span of 10 years (Rodgers, 1953). Subdivision of these rocks has been problematical because they represent environments that changed rapidly in space and time. Consequently, formations and members that were described in one county could not be applied in a neighboring county. Despite differences in correlations caused by this facies complex, the past subdivisions are useful on a local scale. The

following is a review of the classification schemes that have been applied to the lower Middle Ordovician rocks of the St. Paul belt (Figure 3) and a brief discussion of their applicability to the units exposed at Evans Ferry. This discussion is limited to terms employed after 1943 (see Carnes, 1975, pp. 10-22, for pre-1943 treatment).

One classification scheme was introduced by Cooper and Prouty (1943) for the lower Middle Ordovician succession of Tazewell County, in southwestern Virginia. They subdivided the rocks into 29 distinctive zones (based on faunal and lithologic features), which were then grouped into 13 formations and members. Only the first nine units apply to the present study. Listed in ascending order these are: the Blackford, Five Oaks, Lincolnshire, Ward Cove, and Peery members of the Cliffield Formation; the Shannondale and Burkes Garden members of the Benbolt Formation; the Gratton Limestone; and the Wardell Formation. This classification scheme was applied to the rocks in northeast Tennessee by Prouty (1946). He found it necessary to modify and regroup some of the formations because of the lateral lithologic changes. The units of interest are (in ascending order): the Blackford, Five Oaks, Lincolnshire, Thompson Valley, upper Peery, Benbolt and Wardell formations. Prouty used this classification for the units at Evans Ferry (Prouty, 1946, p. 1175), but I have not found it practical for the following reasons. The Five Oaks Formation is not present at Evans Ferry, and the Lincolnshire Formation is more appropriately divided into the Eidson and Hogskin members in the study area as suggested by Cooper (1956). The Thompson Valley and upper Peery

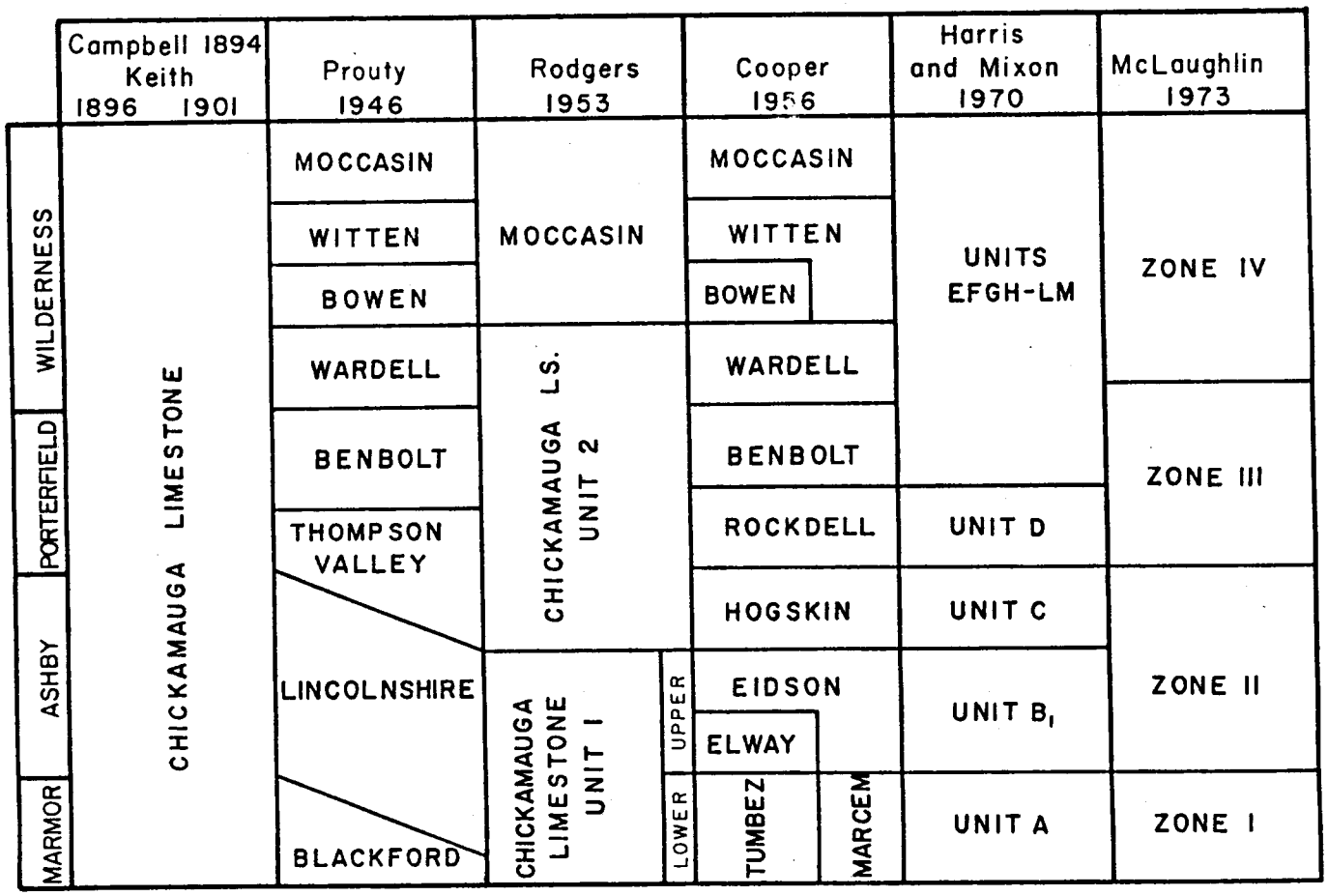


Figure 3. Correlation chart for the schemes of stratigraphic terminology applied to the Middle Ordovician units in the St. Paul strike belt of northeast Tennessee (after Carnes, 1975).

formations as used by Prouty (1946) are inseparable at Evans Ferry, and the term Rockdell Formation (B. N. Cooper, 1945; G. A. Cooper, 1956) is used here for equivalent units.

Rodgers (1953, p. 65) used older and more generalized terms for his map units, but described them completely so that they would "not be obscured by merely nomenclatorial difficulties." The three units that Rodgers used to characterize the middle belt between the Saltville fault and the Hunter Valley fault (which includes the Evans Ferry section) are the Chickamauga Limestone, unit 1; Chickamauga Limestone, unit 2; and Moccasin Formation. Rodgers' (1953) terms have not been used in this investigation, since they are inadequate to reflect my detailed measurements and numerous lithologic changes that are present.

The most comprehensive treatment given to the Middle Ordovician nomenclature of the Southern Applachians was undertaken by G. A. Cooper (1956). He described, in detail, every name that had been applied to the above succession. Cooper's (1956, Chart 1) terms designating units in Hogskin Valley can be related directly to the units in the Evans Ferry section. These two locations are in the same strike belt (24 kilometers apart) and display similar stratigraphic successions (see Carnes, 1975). For these reasons, Cooper's terms (Figure 3) are used for the present study.

In addition to the above classification schemes, Harris and Mixon (1970) mapped the Evans Ferry area (Geologic map of the Howard Quarter Quadrangle) and designated the units, in accordance with Rodgers and Kent (1948), by letters of the alphabet. Also, McLaughlin (1973) devised a biostratigraphic zonation (Figure 3) for the

Raccoon Valley section, which is about 40 kilometers southwest of Evans Ferry in the St. Paul strike belt. McLaughlin's (1973, p. 54) zonation is based on "recurrent lithofacies cycles and distinctive faunal assemblages."

V. RECENT INVESTIGATIONS (1973-PRESENT)

Recent investigations using modern ecostratigraphic techniques have been undertaken as part of a research program at the University of Tennessee (Walker, 1977; Walker, in prep.). The purpose of this program is to determine the paleodepositional environments for the Middle Ordovician rocks of East Tennessee. As a result of this program, 8 large scale ecostratigraphic packages have been recognized in the Middle Ordovician succession (Walker, in prep.). Figure 4 shows an earlier environmental model for this succession, which was proposed by Walker and Alberstadt (1974). Figure 5 illustrates the revised model (Walker, in prep.). The various parts of this environmental pattern are diagrammatically related (Figure 6) to the published and unpublished literature produced by workers involved in the University of Tennessee research program. The present study was designed to analyze the shelf facies of Walker's ecostratigraphic package 7, which is described as "A semirestricted carbonate shelf-lagoon with variable though distal terrigenous clastic influence, and occasional reestablishment of a shelf edge barrier and shale basin, toward the southeast" (Walker, personal communication, 1979).

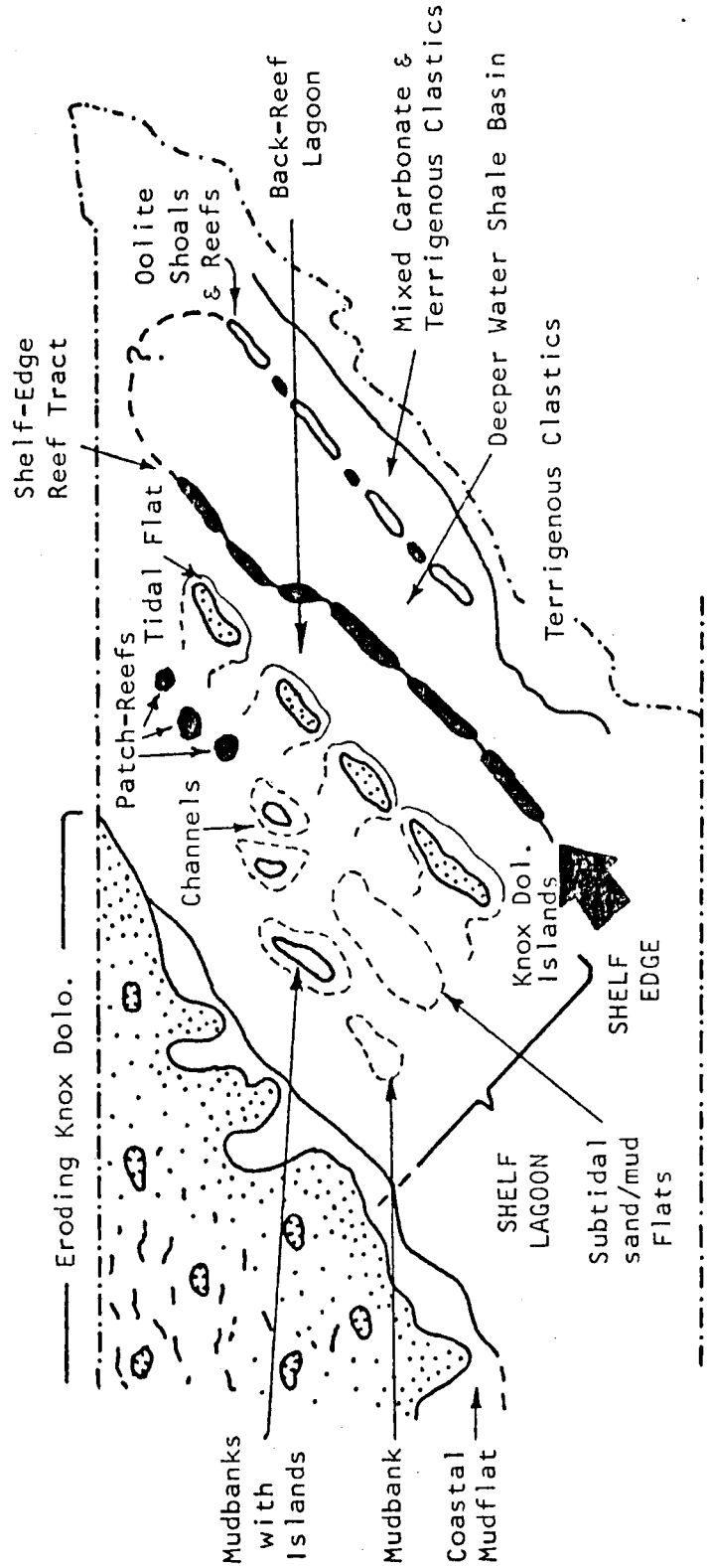


Figure 4. Environmental model during Late Porterfieldian time (after Walker and Alberstadt, 1974).

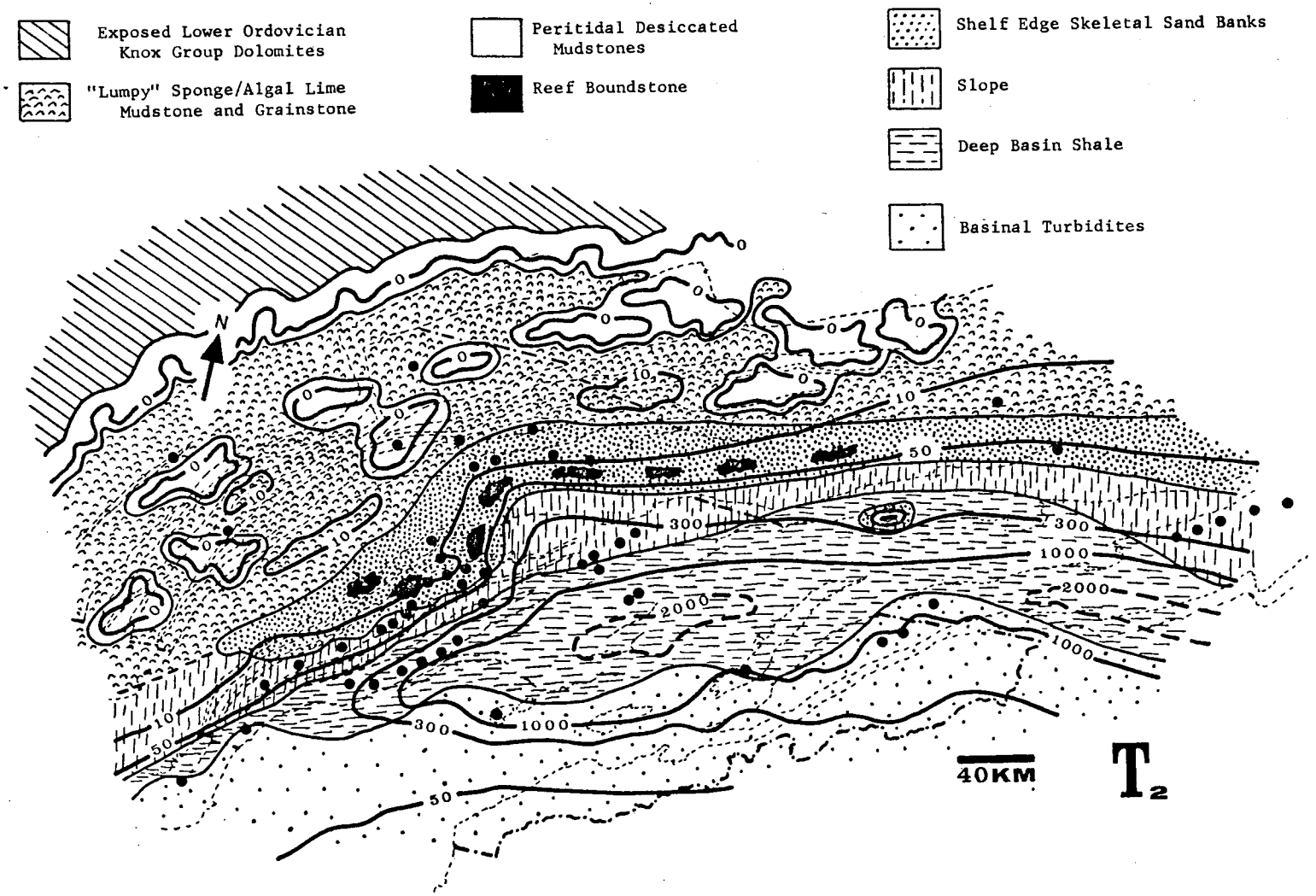


Figure 5. Environments of deposition for the Middle Ordovician rocks (time 2) of East Tennessee and southwest Virginia (modified after Walker, in prep.).

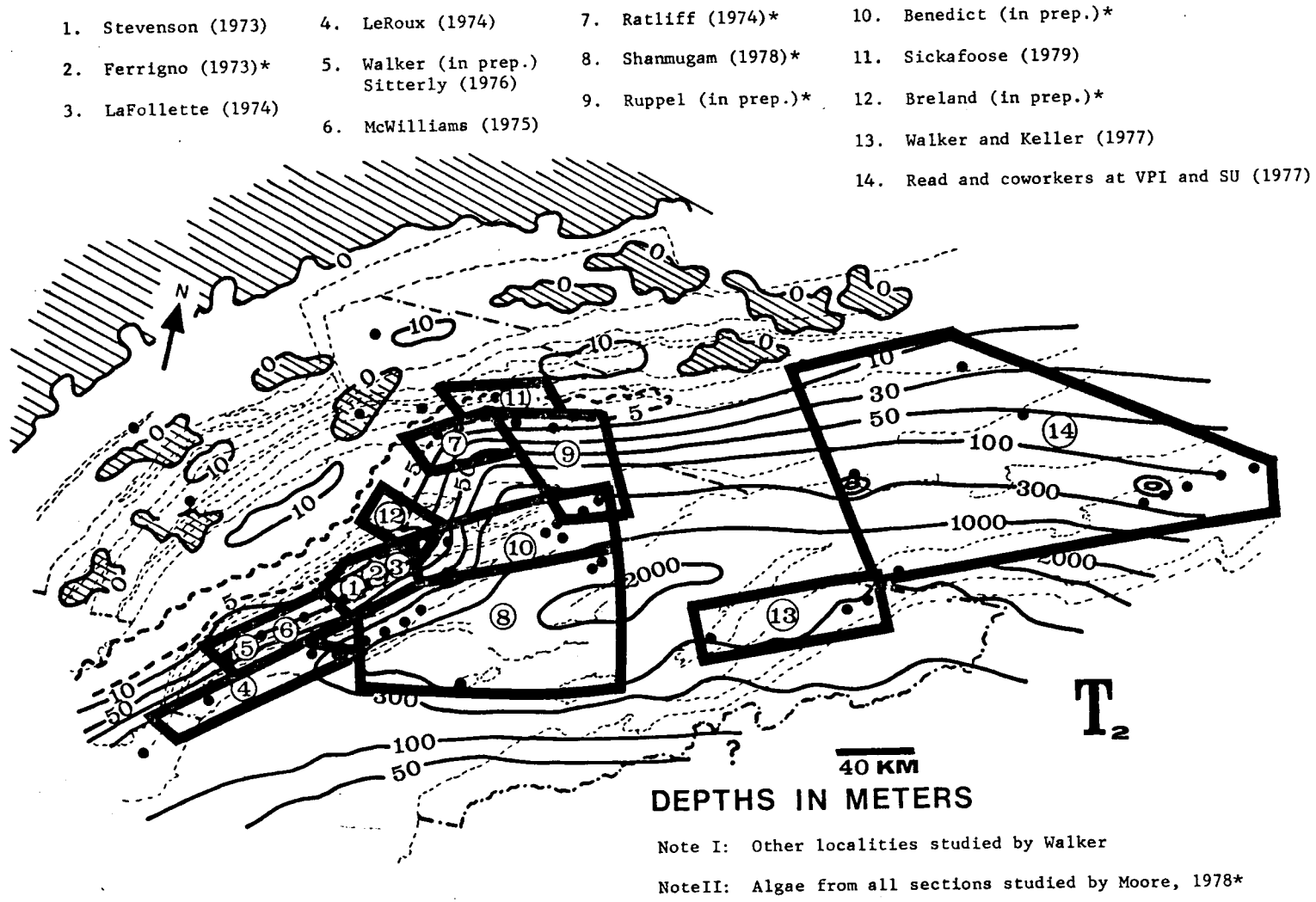


Figure 6. Diagram showing the areas studied by various workers involved in the University of Tennessee research program and printed in theses and dissertations (the latter marked by an asterisk). The paleobathymetric diagram was published by Benedict and Walker, 1978.

Certain biostratigraphic conclusions by other workers have been accepted for the Evans Ferry section in order to attach temporal significance to the units studied. Bergstrom and his coworkers have recently completed several works dealing with the conodont faunas in parts of this sequence. This work has helped to clarify many of the biostratigraphic problems. The most useful of these studies for the present analysis is Carnes (1975) because this work includes conodont information on the Evans Ferry section. McLaughlin (1973) has discussed the megafauna in the M. Ord. sequence in general terms and has pointed out the considerable inconsistency in previous correlations. Cooper (1956) studied the brachiopods in the St. Paul strike belt at Hogskin Valley, which is located about 24 kilometers southwest of the Evans Ferry section. These two areas display the same general succession of units (Cooper, 1956, Chart 1; Carnes, 1975). Therefore, the Marmor stage (Tumbez Fm.), Ashby stage (Eidson and Hogskin members), Porterfield stage (Rockdell and Benbolt Fms.) and the lower part of the Wilderness stage (Wardell Fm.) recognized at Hogskin Valley (Cooper, 1956) can also be correlated with the Evans Ferry section. More recent work on conodonts (Bergstrom, 1973) and trilobites (Shaw, 1974) has shown that Cooper's stages are, at least in part, time-correlative when traced from one area to another. Carnes (1975) concluded that the lower 45 meters of the Evans Ferry section is no younger than the lower part of the Prioniodus gerdae subzone of the Amorphognathus tvaerensis conodont zone. This is approximately equivalent to the Porterfield stage of Cooper's (1956)

classification and the Caradocian series of European usage (Bergstrom, 1971a, 1971b).

VI. METHODS

The initial field work consisted of a detailed study of the lower 330 meters of the Evans Ferry section. This portion of the section was divided into lithic units and each unit was sampled. No two samples were separated by more than 2.5 meters vertically and a total of 147 were taken. Study of the field lithologic descriptions coupled with laboratory petrographic analysis of sawn slabs and 50 × 75 mm thin sections of each lithic sample provided the data from which inferences of paleoenvironments were drawn. Constituent particle composition of selected samples was documented by point count technique (Table A-1, Appendix A). Four hundred points were counted per slide at intervals of one third of a millimeter. These data were used in both ternary diagrams and vertical plots in order to display the varying abundance of sample constituents in relation to their stratigraphic position. These two methods helped in the interpretation and illustration of the paleoenvironmental significance of constituent particle composition. Knowledge of the environments enabled the investigator to study the communities of the lower Benbolt and Wardell formations within the context of a well understood stratigraphic and environmental framework.

The second phase of the study consisted of the collection of fossil assemblages, including both fossils on rock slabs and individual

specimens. Samples obtained from localities A and B (Figure 1, p. 3) were carefully numbered and stored for future use. Polished sections and acetate peels were prepared for most of the fossiliferous slabs from locality B. The acetate peels were examined for biotic content with the aid of a binocular microscope and light table. Thin sections were used to supplement the biotic data from locality A. All paleontological as well as thin-section materials are catalogued and stored in the Collections of the Department of Geological Sciences at the University of Tennessee, Knoxville.

CHAPTER II

STRATIGRAPHY AND INFERRED PALEODEPOSITIONAL ENVIRONMENTS OF THE UNITS IN THE EVANS FERRY SECTION

I. INTRODUCTION

The treatment of the stratigraphy and inferred paleodepositional environments for the lithologic units at the Evans Ferry section begins at the post-Knox unconformity and ends with the upper unit of the Wardell Formation. Each formation or member is first discussed in general terms and is then divided into distinct lithologies, which are discussed in more detail. The presentation of data includes a thin section analysis accompanied by a paleoenvironmental interpretation. Percentages given in the thin section analysis are by volume unless otherwise specified. Descriptive terms for roundness and sorting were derived from Powers (1953) and Folk (1962), respectively. Carbonate rock terminology of both Dunham (1962) and Folk (1962) are given in the text. Dunham's terms are used in most discussions except where the term is too general, and then Folk's terms are substituted.

The paleoenvironmental interpretation includes a discussion of several early diagenetic features, if these features are prominently displayed within the lithologic unit. Stylolites are one such feature, and several types (Figure 7) occur in the rocks of the Evans Ferry section. The first three terms in Figure 7 were illustrated by Logan and Semeniuk (1976), but the latter term is introduced for this study.

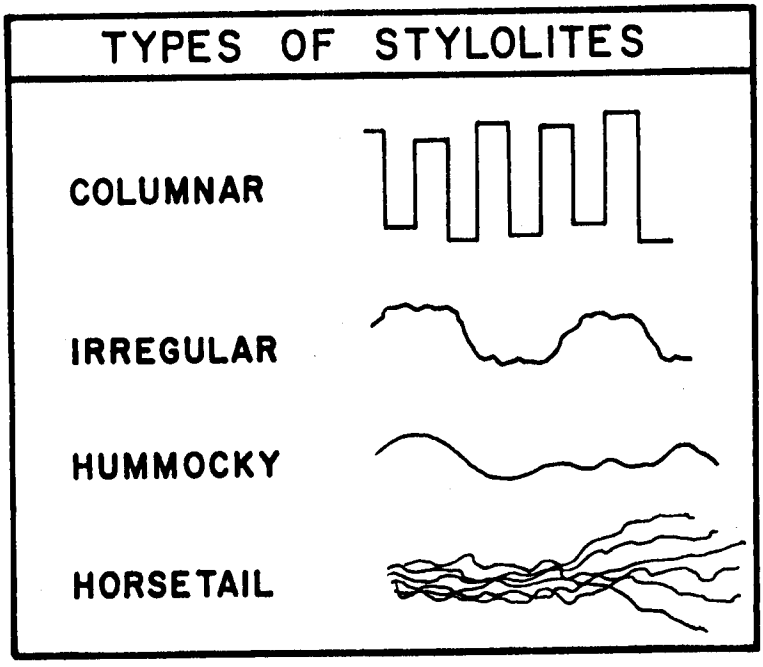


Figure 7. Types of stylolites.

II. POST-KNOX UNCONFORMITY

The post-Knox unconformity is poorly exposed on the north slope of Dry Valley just above a small creek, which trends parallel to the old state Route 25 East (Figure 1, p. 3). A dove gray dismicrite similar to the Mosheim directly overlies the Mascot Dolomite; though, the actual plane of contact is hidden from view. The dismicrite exhibits a fenestral fabric and contains abundant chert and dolomite clasts (3 mm-5 mm) near its base. This outcrop is the only exposure of the post-Knox unconformity found during field reconnaissance and therefore is taken as the base of the Evans Ferry section.

III. TUMBEZ FORMATION

General Description

The Tumbez Formation is poorly exposed along both sides of the old state route 25 East in Dry Valley (Figure 1, p. 3, dense stippled pattern represents the outcrops for the entire section). Based on detailed measurement of available outcrops and, where necessary, careful field approximations, the Tumbez Fm. is estimated to be 29 meters thick.

The Tumbez Fm. from bottom to top can be divided into the following four lithologies: (T1) a basal 0.5 m thick chert conglomerate and dismicrite, (T2) 12.8 m of thick bedded, fine sand grainstone containing red chert nodules, (T3) 4.6 m of gray limy shale interbedded with thin red-gray pelletal grainstone and red chert layers, and (T4) 11 m of laminated red micrite interbedded with undulating black chert. These lithologies are treated separately below.

Lithology T1

Thin section analysis. The dismicrites occur at the base of the section and are characterized by medium irregular fenestrae (0.01 mm to 0.4 mm thick), tabular fenestrae (1.6 mm wide) and a mixture of these two types (see Logan, 1974). A vertically bored erosional surface is present in one thin section (Figure 8A). These borings are filled with pellets from the overlying sediments. Other features clearly

Figure 8. Photomicrographs of the lower and upper Tumbez Formation.

A. Photomicrograph of a vertically bored erosional surface with pelletal infill from the overlying sediment, lithology T1, 13X (EF' 3).

B. Photomicrograph of a chert nodule exhibiting a dolomite replacement rim. Note the euhedral dolomite rhombs, lithology T1, 125X (EF' 3).

C. Photomicrograph of pelletal carbonate skeletal sand, lithology T2, 25X (EF' 4).

D. Photomicrograph of echinoderm debris with micrite envelopes, lithology T2, 25X (EF' 7).

E. Photomicrograph of a severely micritized trilobite fragment in spar cement, lithology T3, 100X (EF' 17).

F. Negative print of a thin section exhibiting wavy and irregular micritic clay laminae. The graded bed of figure, 8G, is at the top of this photo, lithology T3, 3X (EF' 10).

G. Photomicrograph of a graded skeletal carbonate layer between micritic clay laminae, lithology T3, 25X (EF' 10).

H. Photomicrograph of tabular intraclasts with a micrite rind (micrite envelope) in spar cement. Note the rounded edges of the intraclasts, lithology T3, 13X (EF' 17).

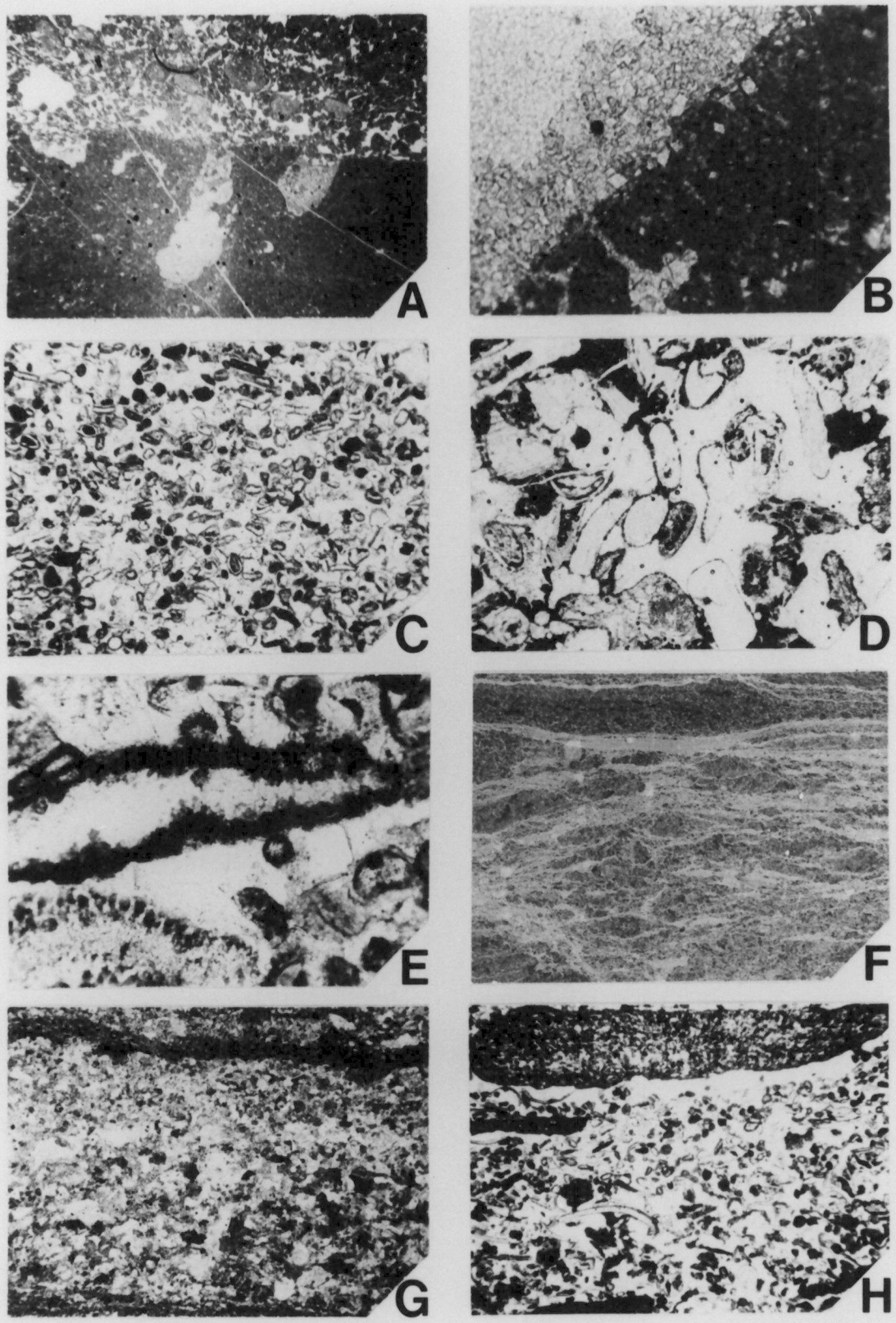


Figure 8

displayed in the dismicrites are grumeleuse structure, angular chert pebbles, angular dolomite granules, dolomite-rimmed chert pebbles, and widely distributed (3%) euhedral dolomite rhombs (0.01 mm to 0.16 mm). The fauna present in this lithology consist of ostracods and gastropods. The ostracods are represented by randomly oriented valves of which about one third are still articulated. The ostracods are abundant in one slide and sparsely distributed in another (some are partly dissolved). Therefore, they did not appear in the constituent analysis data. The gastropods were not thin-sectioned due to their wide dispersion. They are visible on the outcrop as flat spirals several centimeters in diameter, outlined on the weathered surface of the rock.

Paleoenvironmental interpretation. Logan (1974) states that medium irregular fenestral fabric is commonly formed by pustular algal mats in the upper and middle intertidal zones. Shinn (1968a) produced irregular fenestrae by drying nonlaminated lime mud and concluded that these structures were valuable supratidal indicators; algal mats are not necessary for their formation. Grover and Read (1978) noted very similar irregular fenestral fabrics in the New Market Limestone which they attributed to periodic desiccation. The descriptions of the associated sediment as described by Grover and Read (1978) and Logan et al. (1974) are similar to the sediment of lithology T1. The irregular fenestral fabric of lithology T1 is thus inferred to result from either periodic tidal flat desiccation (as in the New Market Limestone), or buckled intertidal algal mats (as in Recent sediments).

The tubular fenestrae in the Tumbez Formation are similar to burrow and root structures described by Shinn (1968b) and Logan et al. (1974) from Recent intertidal sediments, though the absence of Ordovician terrestrial plants precludes a plant root origin (Grover and Read, 1978). Several burrow-shaped (sediment-infilled) tubes (Figure 8A) associated with the tubular fenestrae, indicates that these fenestrae were formed by burrowing organisms.

The euhedral dolomite rhombs (silt and sand sized) found throughout the dismicrite appear to have formed in situ. Euhedral dolomite rhombs have replaced the edges and sometimes parts of the interior of detrital chert pebbles (Figure 8B). The dolomite rhombs project from the edges of the pebbles and are not abraded, indicating that the dolomite formed after the chert was deposited. Since dolomite rhombs found in the matrix have the same characteristics as those replacing the chert, they are believed to have formed at the same time and by similar processes. The hypersaline reflux mechanism described by Deffeyes et al. (1965) or the evaporative process presented by Illing et al. (1965) are each plausible processes for the formation of the dolomite rhombs in lithology T1.

Calcareous algae are not present in lithology T1, and the fauna is restricted (Figure 9). Gastropods and ostracods are euryhaline animals able to survive variable salinities (such as caused by evaporation and fresh-water runoff) characteristic of intertidal environments. Exclusion of stenohaline fauna from lithology T1 is an additional indication that sediment comprising these rocks was deposited in the intertidal or supratidal zone.

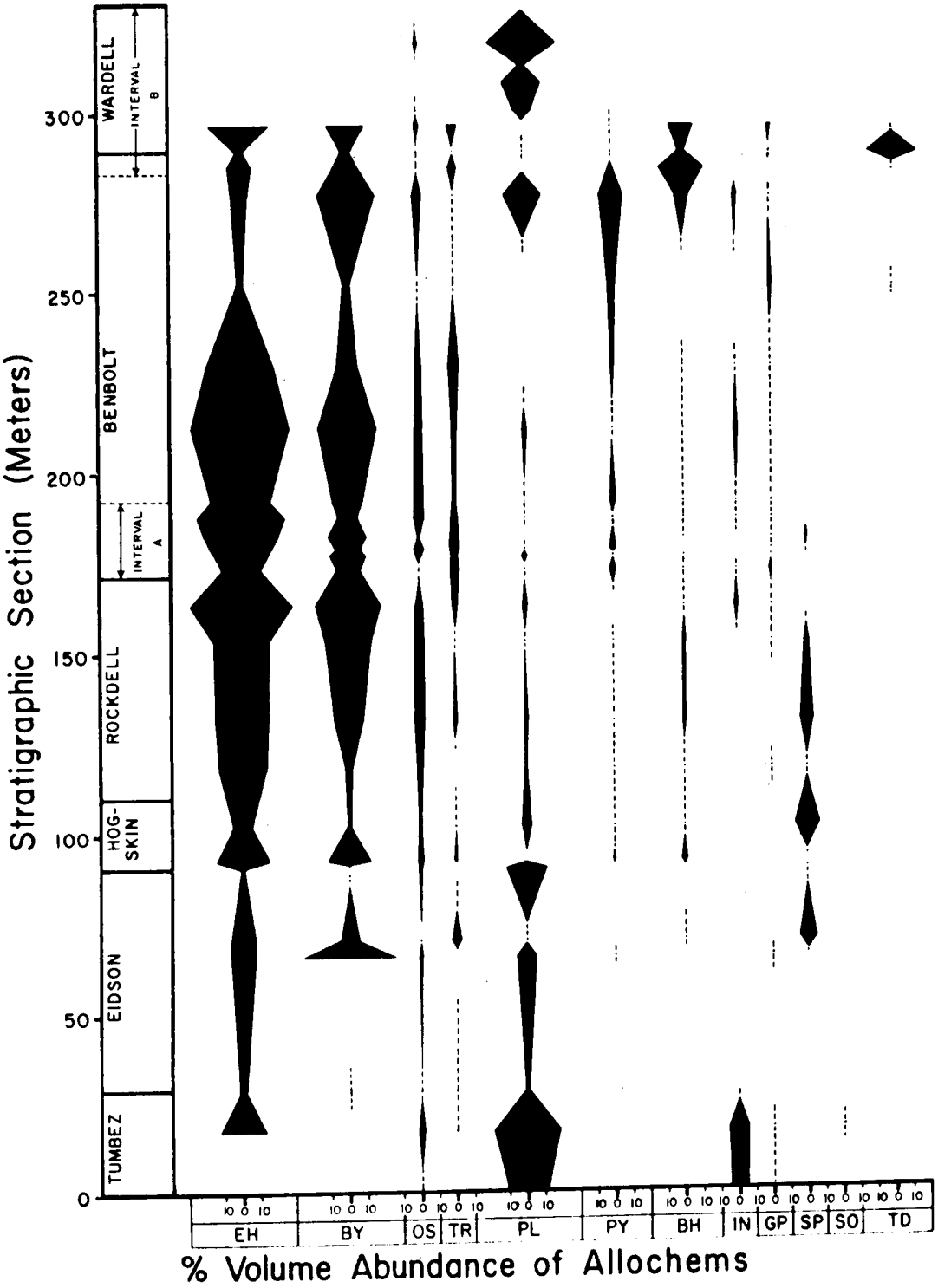


Figure 9. Stratigraphic distribution of allochems (omitting algae) for Evans Ferry, Tennessee. Volume percent was derived from point count data (see Table A-1, Appendix A).

Lithology T2

Thin section analysis. Thick-bedded, medium-grained limestones (lithology T2) generally occur above lithology T1. In thin section these rocks are grainstone (biosparite) and pelletal grainstone (biopelsparite). They contain sub-rounded and well sorted fine carbonate skeletal sand (Figure 8C, p. 21). The long axes of these fossil fragments are oriented parallel to bedding. The allochems, in order of decreasing abundance are: echinoderm debris (about 20%); peloids (about 10%); trilobites (about 3%); bryozoans ($\leq$ 2%); ostracods ($\leq$ 2%); intraclasts ($\leq$ 1%); superficial ooids ($\leq$ 1%); Hedstroemia (< 1%); and gastropods (< 1%). Trilobites are largely represented as silt-sized micrite-filled, circular cross sections of spines. The intraclasts consist of ellipsoidal, coarse sand packstones (biomicrite). The superficial ooids have 1 or 2 lamellae (0.008 mm to 0.012 mm thick), which are off white or slightly yellow-orange in plane polarized light. Minor (< 1%) coarse silt fragments of an amber, internally laminated substance appear to be chitino phosphatic shell debris from inarticulate brachiopods.

Micritization (Bathurst, 1966) is prevalent in lithology T2. A large portion of the peloids are probably micritized fossil fragments, as evidenced by the abundance of micrite envelopes in various stages of formation. Some fossil fragments have thin (0.08 mm) rims while other carbonate skeletal particles are almost completely micritized (Figures 8D and 8E, p. 21). Approximately 20% of the allochems have some form of micrite envelope.

In some samples, indiscriminate portions of the rock have been chertified, forming discrete chert nodules. The allochems from the original lithology are largely destroyed during the chertification process, though, their outlines and occasionally their internal structure are still discernible. No relationship between preexisting sedimentary structures and chertification could be determined.

Paleoenvironmental interpretation. The allochems of lithology T2 have been transported or were formed in an agitated environment. They have been subrounded by abrasion and have been size sorted by currents. Current activity is indicated by three lines of evidence: (1) the absence of micrite in the matrix (although present in hollow fossils), (2) the reduction of a diverse assemblage of fossils of several sizes to skeletal sand, and (3) the presence of superficial ooids indicates agitated or shoaling waters.

The presence of micrite envelopes around fossil fragments implies shallow water deposition only if one can prove that the borings in the shell have been made by photosynthetic algae and not fungi. Friedman (1971) states that this distinction is a hard one to make. However, this should not preclude the use of micrite envelopes as depth indicators. Swinchatt (1965) has shown that algal boring is abundant in the shallow shelf carbonate sediments of the Florida-Bahamas region, and Logan (1974) has observed a similar occurrence in the carbonate tidal flats of Shark Bay, Australia. Consequently, in conjunction with other lines of evidence, the presence of micrite envelopes should be a helpful indicator of shallow water conditions.

The occurrence of fragmented Hedstroemia indicates proximity to a shallow subtidal environment where calcareous algae were abundant (Moore, 1977). The lack of other calcareous algae in lithology T2 is notable. Moore (1977), in his study of Middle Ordovician algae of the Southern Appalachians, observed that calcareous algae were absent from tidal flat lithologies. Logan (1974) described a sequence in Shark Bay, Australia, where skeletal grains originating on the sublittoral platform were washed shoreward and were micritized, forming a pelletal grainstone near the strandline. Lithology T2 may have had a similar history. Tidal flat sediments derived from the adjacent marine environment have been documented by Ball, Shinn, and Stockman (1967) in Recent sediments deposited during hurricane Donna. These authors suggest that hurricanes were probably common occurrences during geologic history and similarly influenced the sedimentary record.

Lithology T3

Thin section analysis. Lithology T3 overlies lithology T2 and consists of dark orange-brown micritic clay shale laminae interbedded with fine to medium grained limestones and chert layers. Repeated attempts to thin section shalier beds failed because of severe weathering. The main carbonate rock type in lithology T3 is pelletal grainstone (pelsparite and biopelsparite). In thin section, the main differences between lithologies T2 and T3 are: (1) the greater abundance of micritic shale laminae in T3, and (2) the distinctly laminated character of the rock in T3.

The micritic clay shale laminae of lithology T3 (Figure 8F, p. 21) range in thickness from 0.04 mm to 2 mm and appear wavy, patchy and braided. Several slides contain intraclasts of these micritic clay laminae (tabular chips 0.7 mm to 2 mm long). The pelletal grainstone layers (0.4 mm to 7 mm thick) dominate the slides and consist of the following allochems: peloids (20%), echinoderm debris (13%), ostracod valves (about 3%), trilobite debris (about 1%), gastropods (< 1%), and Hedstroemia (< 1%). The skeletal debris is highly fragmented and well sorted (ranging in size from 0.03 mm to 0.1 mm). Graded layers (fining upward) occur rarely and only where micritic clay laminae are abundant (Figure 8G, p. 21). Fine laminoid fenestrae (0.1 mm to 0.4 mm thick) separate the pelletal grainstone layers where the micritic clay laminae are absent. Tubular fenestrae (0.7 mm diameter) are rare.

The average size of the allochems increases from 0.05 mm at the base of lithology T3 to 0.25 mm at the top. The top 0.5 meters of lithology T3 exhibits micritized skeletal debris (in several stages of formation) and large abraded tabular intraclasts (some with micrite envelopes, Figure 8H, p. 21). Superficial oolite sand is also present in this upper interval as a minor (< 1%) constituent (similar to lithology T2).

Paleoenvironmental interpretation. Except for the distinct laminations in lithology T3, it is very similar to lithology T2 and probably represents a similar depositional environment. Consequently, only the origin of the micritic clay laminae will be discussed. These

laminations are interpreted to represent sediment trapped by intertidal or subtidal blue-green algal mats. Modern intertidal algal mats are represented by continuous organic-rich laminae separated by layers of occasionally graded skeletal debris (Davies, 1970b) and fine laminoid fenestrae (Logan, 1974). The skeletal fragments are derived from the adjacent subtidal environment and are transported shoreward by storm tides. This description of modern intertidal algal mats agrees with features displayed in lithology T3.

Recent subtidal algal mats have been observed in shallow water (0.5 m to 2 m deep) carbonate environments in the Bahamas by several authors (Bathurst, 1967, and Neumann et al., 1970). However, Neumann et al. (1970) noted that laminations will be lacking in subtidal mat accumulations in contrast to intertidal or supratidal areas. In addition, rounded micritized tabular intraclasts (Figure 8H, p. 21) at the top of lithology T3 imply intertidal conditions because the clasts had to be indurated (most probably desiccated) before being bored and abraded. Low frequency of sediment exposure is inferred from the lack of abundant desiccation structures. Consequently, lithology T3 probably represents an ancient low intertidal algal flat frequented by storm deposits derived from the adjacent subtidal area.

Lithology T4

Thin section analysis. Laminated micrites are located at the top of the Tumbez Formation and grade into the overlying Eidson Member.

These rocks consist of micrite alternating with pelletal grainstone (biopelsparite), packstone (biomicrite) and dark orange-brown micritic clay laminae. The biopelsparite and biomicrite layers (range 0.07 mm to 1.6 mm thick) consist of severely abraded and moderately sorted echinoderm fragments (about 10%) and lesser amounts of peloids (about 5%), ostracod valves (about 2%) and trilobite debris (about 2%). These allochems range in size from 0.03 mm to 0.15 mm.

The dark brown micritic clay shale laminae range in thickness from 0.03 mm to 0.6 mm. In a silicified area of one slide, a dark micritic clay shale lamina remained partially intact while the skeletal debris and peloids of a biopelsparite layer were replaced and destroyed. The destruction of the micrite peloids helps illustrate that the micritic clay laminae are indeed composed of a substance other than micrite. In addition, micritic clay laminae were barely affected by etching with HCL, while the biopelsparite and biomicrite layers were dissolved (Figure 10A). The micritic shale laminae are very wavy in appearance, subparallel to bedding, and are oversteepened to form slopes of 30°. In one slide of lithology T4, a few of the micritic clay laminae are overfolded (Figure 10D). The laminae are occasionally disrupted by distinct vertical burrows (avg. 1.0 mm wide, Figure 10B) infilled with biomicrite or biopelsparite (Figure 10B and 10C).

Very fine, angular quartz sand and quartz silt are present in lithology T4. The abundance of the quartz increases from less than 1 volume percent near the base of T4 to 3.5 volume percent at the top (a slide from the latter was point counted and plotted on Figure 11).

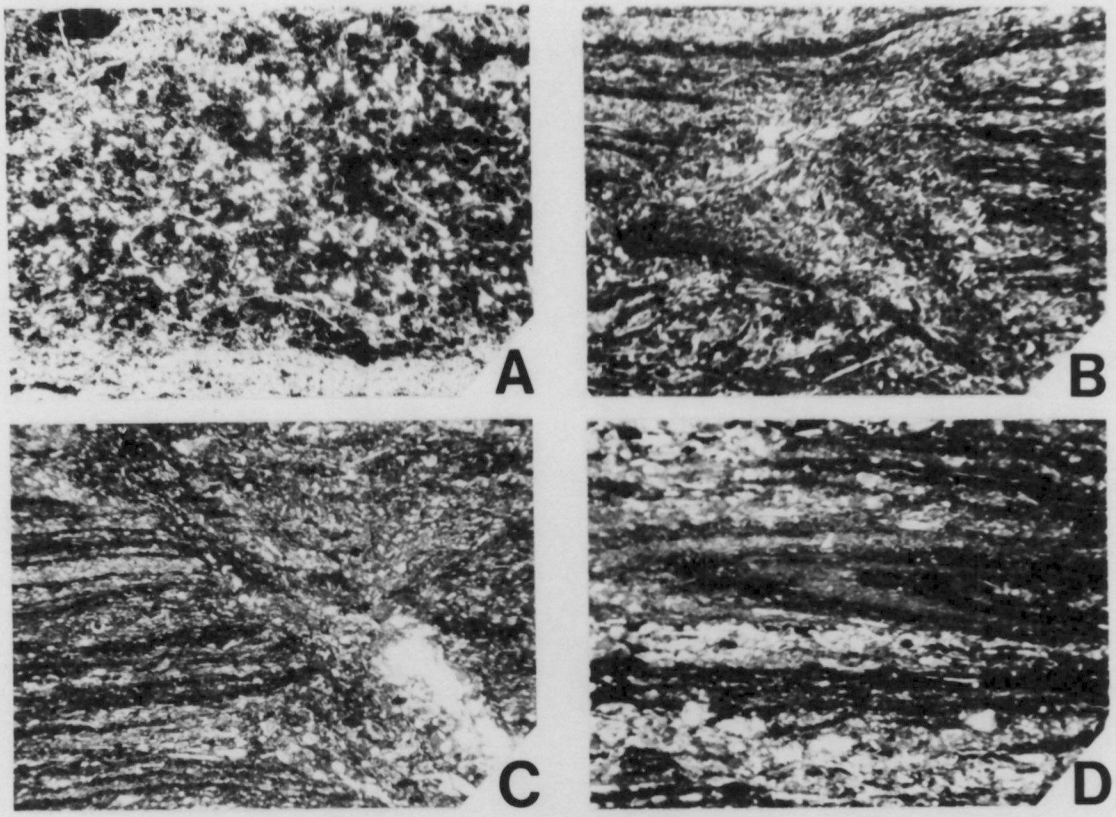


Figure 10. Photomicrographs of the upper Tumbez Formation (T4).

A. Photomicrograph (EF 22) of angular quartz silt (white dots) and clay laminae (wavy white lines, bottom) in a thin section etched with HCl acid. Crossed nichols, 25X.

B. Photomicrograph (EF 20) of micritic shale laminae disrupted by a steeply inclined burrow and filled with skeletal sand. 25X.

C. Photomicrograph (EF 20) of micritic shale laminae disrupted by a steeply inclined burrow and filled with spar cement, plus skeletal debris. 25X.

D. Photomicrograph (EF 20) of overfolded micritic shale laminae. 25X.

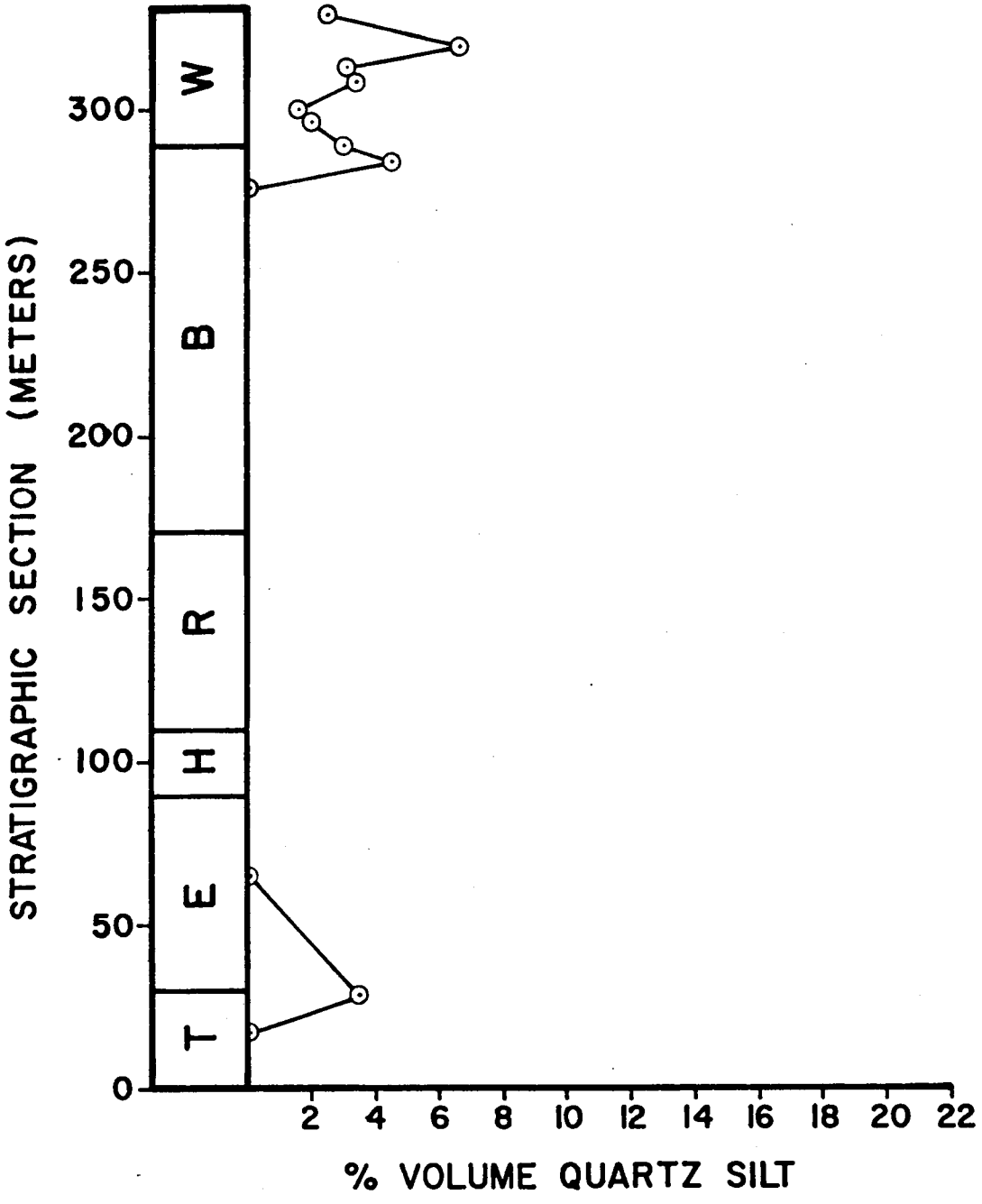


Figure 11. Stratigraphic distribution of detrital quartz silt for Evans Ferry, Tennessee. Volume percent was derived from point count data (see Table A-1, Appendix A).

The quartz sand and silt is concentrated in the biopelsparite layers (Figure 10A).

Paleoenvironmental interpretation. The dark wavy micritic clay laminae of lithology T4 are similar to the flat algal-laminated sediments described by Logan (1961) at Shark Bay, Australia. The overfolded and steeply inclined structures displayed by these micritic clay laminae are good indicators of algal binding (Davies, 1970b). Logan (1961) observed that the flat algal-laminated sediments occur in the intertidal mudflat environment, which is protected from wave action. Consequently, if lithology T4 had a similar history, the biopelsparite layers are probably indicative of a large influx of skeletal carbonate debris during storms and the associated higher energy conditions. The severe abrasion and moderate sorting of the allochems in lithology T4 supports the probability. An influx of skeletal debris from the adjacent sublittoral area has been observed by several authors (Logan, 1961; Davies, 1970b; Ginsburg and Hardie, 1975; Ball et al., 1967). The peloids and quartz silt were probably admixed with the storm deposited skeletal carbonate debris during high water (storm tides). The peloids may have originated locally from a pelleted intertidal flat and the quartz silt may have been derived from weathered Knox group rocks exposed in the supratidal environment. This could account for the concentration of quartz silt in the biopelsparite layers. The absence of desiccation structures indicates that the algal mats probably formed in a permanently covered low intertidal environment. Subtidal

algal mats as described by Neumann et al. (1970) do not possess the characteristics present in lithology T4.

IV. EIDSON MEMBER OF THE LINCOLNSHIRE FORMATION

General Description

The Eidson Member of the Lincolnshire Formation is largely exposed on the south side of the old state Route 25 East in Dry Valley (Figure 1, p. 3). Some of the lower units in the Eidson Member are poorly exposed and their thickness had to be approximated in the field. The total thickness of the Eidson Member is about 61 meters.

The Eidson Member is divisible into 3 separate lithologies. In ascending order, these are: (E1) 27.5 meters of thin-bedded, dark gray clayey micrite laminae interbedded with thick-bedded pelletal grainstone and chert layers; (E2) 9.4 meters of massive-bedded, blue-gray packstones and chert nodules; and (E3) 24.2 meters of brown-gray fossiliferous micrites interbedded with less abundant grainstones and chert nodules.

Lithology E1

Thin section analysis. The base of the Eidson Member (lithology E1) is very similar to the top of the Tumbez Formation (lithology T4). It contains finely laminated rocks with alternating clayey micrite laminae (0.08 mm to 0.8 mm thick) and pelletal grainstone (biopelsparite) laminae (0.12 mm to 2 mm thick). However, lithology E1 also contains thick (10 cm to 30 cm) interbeds of pelletal grainstone (biopelsparite).

The clayey micrite laminae are parallel to bedding and vary in appearance from wavy and oversteepened (30° slopes) to very straight. Possible algal filament molds were observed in one clayey micrite lamina. The laminations comprise 60% of the rock and rarely exhibit slight thickening on the crest of domes (Figure 12A). Shallow vertical burrows disrupt the clayey micrite laminae (discussed below), but they are uncommon. Laminae composed of biopelsparite are subparallel to bedding, appear undulose with irregular upper and lower boundaries and sometimes display positive grading (Figure 12B). Tabular clasts (1 mm to 2 mm long) composed of clayey micrite are numerous within the biopelsparite layers. Vertical burrows are filled by biopelsparite and are truncated by the biopelsparite laminae (Figure 12C). The skeletal composition of these laminae is the same as that for the thick biopelsparite beds discussed below.

The thick biopelsparite interbeds consist of echinoderm debris (about 25%), peloids (about 20%), ostracod valves (about 8%), trilobite debris (about 2%), other, unidentifiable, fossil debris (about 5%) and rare (much less than 1%) bryozoans and brachiopods all cemented by 40% calcite spar. The allochems are highly fragmented (0.03 mm to 0.3 mm), subrounded and moderately size sorted. Some of the silt allochems are vaguely concentrated into patches between sandier layers. Very coarse echinoderm sand debris is a minor constituent of these thick biopelsparite beds. In addition, the thick biopelsparites contain randomly distributed, very fine, angular, quartz sand (1%), vertical micrite-filled burrows (7 mm deep), and stylolites. The

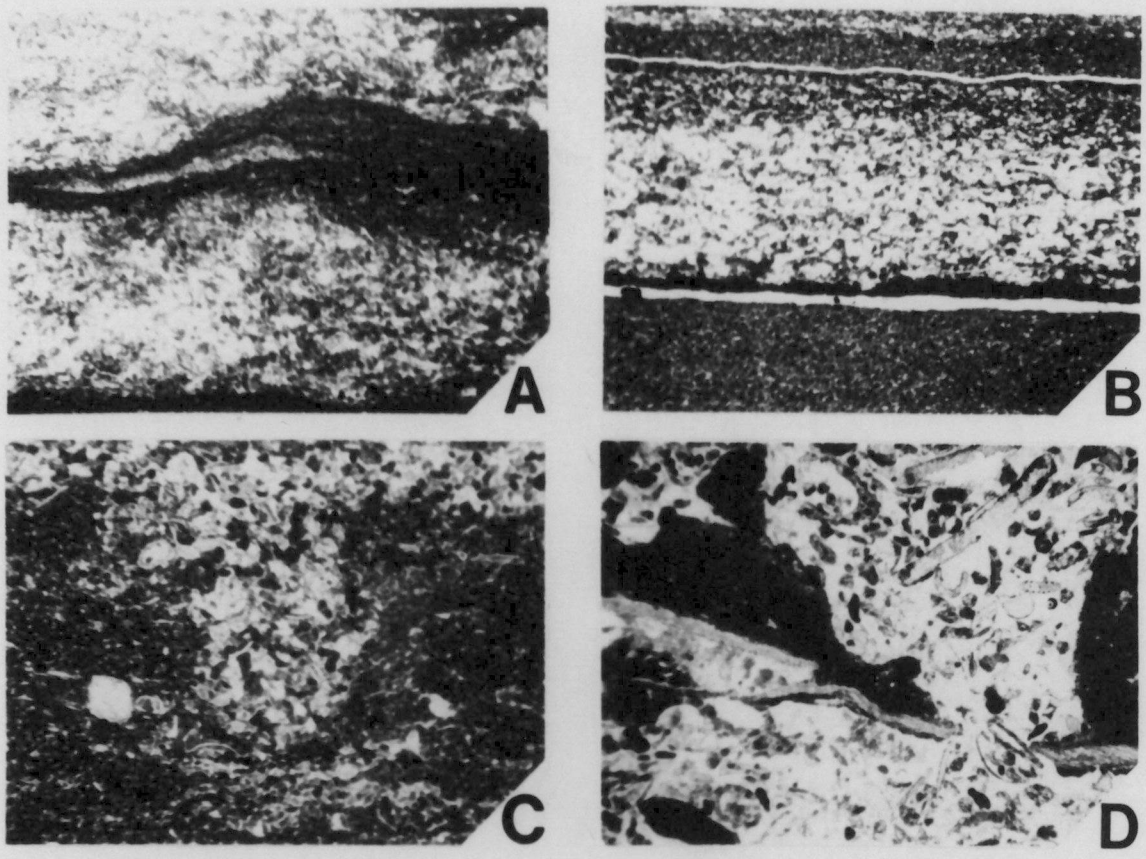


Figure 12. Photomicrographs of the lower Eidson Member (E1).

A. Photomicrograph (EF 25) of a clayey micrite lamina, which exhibits thickening at the arch of a dome. Sediment deposited laminae would show the thickening at the trough. 25X.

B. Photomicrograph (EF 25) of a positively graded skeletal lamina between clayey micrite laminae. 25X.

C. Photomicrograph (EF 23) of a vertical burrow in a micrite lamina filled by biopelsparite from the overlying lamina. 30X.

D. Photomicrograph (EF 30) of Girvanella coating only the top side of a brachiopod fragment, implying low current energy. 13X.

stylolites are roughly subparallel to bedding and are characterized by a thin, dark orange-brown residuum, a concentration of quartz sand, and an accumulation of sand size fragments of inarticulate brachiopods. The latter are also sparsely distributed throughout the rock.

Paleoenvironmental interpretation. The finely laminated rocks of lithology E1 were probably formed as a result of the activity of algal mats which were periodically buried by storm deposits (the biopelsparite laminae) in the intertidal environment. The truncation and infilling of vertical burrows by skeletal debris similar to that comprising the biopelsparite laminae illustrates the suddenness of deposition. In addition, graded skeletal layers could represent storm-derived debris that settled from suspension as the high tides dissipated (see Davies, 1970b). Tabular clasts of clayey micrite contained within the thin biopelsparite layers probably originated as broken pieces of desiccated, algally-trapped sediment laminae.

The thick biopelsparite interbeds of lithology E1 are interpreted as representing tidal channel deposits. The allochems contained in these beds exhibit definite signs of current transport (abrasion, sorting and lack of micrite). A peculiar feature of some biopelsparite beds is the sandwiching of layers of silt grains between layers of sand sized grains. This feature is inferred to be representative of a subtidal algal mat. Neumann et al. (1970) observed that subtidal algal mats preferentially trap finer particle sizes and can withstand current velocities 2 to 5 times higher than unbound sediment. Another feature that the

biopelsparite beds of E1 have in common with modern subtidal algal mat accumulations is the lack of laminations because of increased burrowing activity.

The alternation of the environmentally distinct units of lithology E1 (tidal channels and intertidal algal mats) could have resulted from the migration of a tidal channel that was adjacent to the intertidal flat. The migration of channel systems in tidal flat environments has been observed near Andros Island, Bahamas, by Shinn et al. (1969). They concluded that thin regressive and transgressive sequences could be formed in this manner without a change in sea level.

Lithology E2

Thin section analysis. Lithology E2 represents a sequence of changing rock types. The base of lithology E2 (57 m above the base of the section) is characterized by packstone (biomicrite), which contains allochems similar to those in lithology E1, but are less fragmented and abraded. The middle units of lithology E2 (58 m to 64 m from the base of the section) contain packstones (biomicrite and poorly washed biosparite). These middle units are characterized by a diverse faunal assemblage consisting of echinoderm debris (about 12%); bryozoan debris (about 12%); brachiopod fragments (about 6%); ostracod valves (about 2%); trilobite debris (about 2%); and rare (< 1%) gastropods and pelecypods. The rest of the rock usually consists largely of micrite. The fossils exhibit very little

abrasion and most of them are greater than 2 mm in size. Their association with abundant micrite suggests a quiet environment in which transportation of the fauna was minor. Girvanella and minor associated Hedstroemia algae form thick hemispherically shaped coatings on many of the flat fossils. Only a few of these oncoids have been overturned. Large curved fossil fragments of brachiopods and trilobites lie convex upward. In the biomicrites, several horizontal burrows are visible in slightly deformed surrounding sediment. The biomicrites are composed of about 30% micrite and the poorly washed biosparites contain 15% micrite or less. Geopetal structures in the muddy biosparites display micrite infilling which was followed by cementation of the remaining void space. Hummocky stylolites are a minor feature in lithology E2.

The upper unit of lithology E2 (64 m to 66 m from the base of the section) is similar to the poorly washed biosparites of the middle units (discussed above). The major difference is that the matrix of this upper unit is composed of silt and very fine sand pellets instead of micrite.

Paleoenvironmental interpretation. Lithology E2 is inferred to have been deposited subtidally. Girvanella coatings typically form in Middle Ordovician subtidal environments (Moore, 1977). In addition, the rocks contain a diverse biota that appears to be indigenous because of the limited signs of fossil wear. Currents must have been periodically active, however, because curved shells and a few small oncoids are overturned. If the currents had been constant, the Girvanella coatings would not have predominated on just one side of a fossil (Figure 12D, p. 36). Periodic currents would have been capable of removing micrite

not already trapped between fossils, subsequently resulting in a poorly washed biosparite.

Numerous horizontal burrows present in the biomicrites of lithology E2 indicate subtidal deposition. Rhoads (1967) states that sediment feeding burrowers moving laterally produce a horizontal network of burrows as they remove organic material. Horizontal burrows of lithology E2 have deformed the surrounding sediment indicating that the substrate had a low water content and was relatively firm (Rhoads, 1975).

Lithology E3

Thin section analysis. Lithology E3 is the most easily recognized and characteristic lithology of the Eidson Member. It consists of 24 meters (66.2 m to 90.4 m above the base of the section) of thinly laminated mudstone (fossiliferous micrite) interbedded with less abundant thin beds of wackestone (biomicrite) and pelletal grainstones (biopelsparite and poorly washed biopelsparite). Undulose black chert layers 5 cm to 7 cm thick and chert nodules are conspicuously interbedded with these rock units (Figure 13A).

The laminated fossiliferous micrite is composed of straight sponge spicules (about 4%), measuring 0.02 mm wide and 0.6 mm long, coarse silt and very fine carbonate skeletal sand, all in a matrix of micrite, which comprises about 60% of the rock. The carbonate skeletal debris consists of ostracods, trilobites, echinoderms, and bryozoans, which together compose less than 5% of the rock. Undulose biopelsparite

Figure 13. Photographs of lithologies within the Eidson and Hogskin members of the Lincolnshire Formation.

A. Field photograph of black chert nodules within lithology E3 (scale = 10 cm).

B. Photomicrograph of trilobites in thin section within lithology E3, illustrating their excellent preservation, 25X (EF' 33).

C. Field photograph of the cobbly-bedded wackestone and shale in the Hogskin Member, lithology H1 (scale = 10 cm).

D. Field photograph of massive grainstone interbeds separating the cobbly wackestones and shales within the Hogskin Member (staff = 2 m).

E. Photomicrograph of a clay clast exhibiting a calcite microspar halo with decreasing grain size toward the micrite, lithology H1, 30X (EF' 4A).

F. Photomicrograph of echinoderm fragments displaying sutured contacts and an associated squashed oncolite, all within a shale layer, lithology H1, 30X (EF' 18).

G. Photomicrograph of silt-sized dolomite rhombs within a clay lamina. Note their euhedral shapes, lithology H1, 125X (EF' 8).

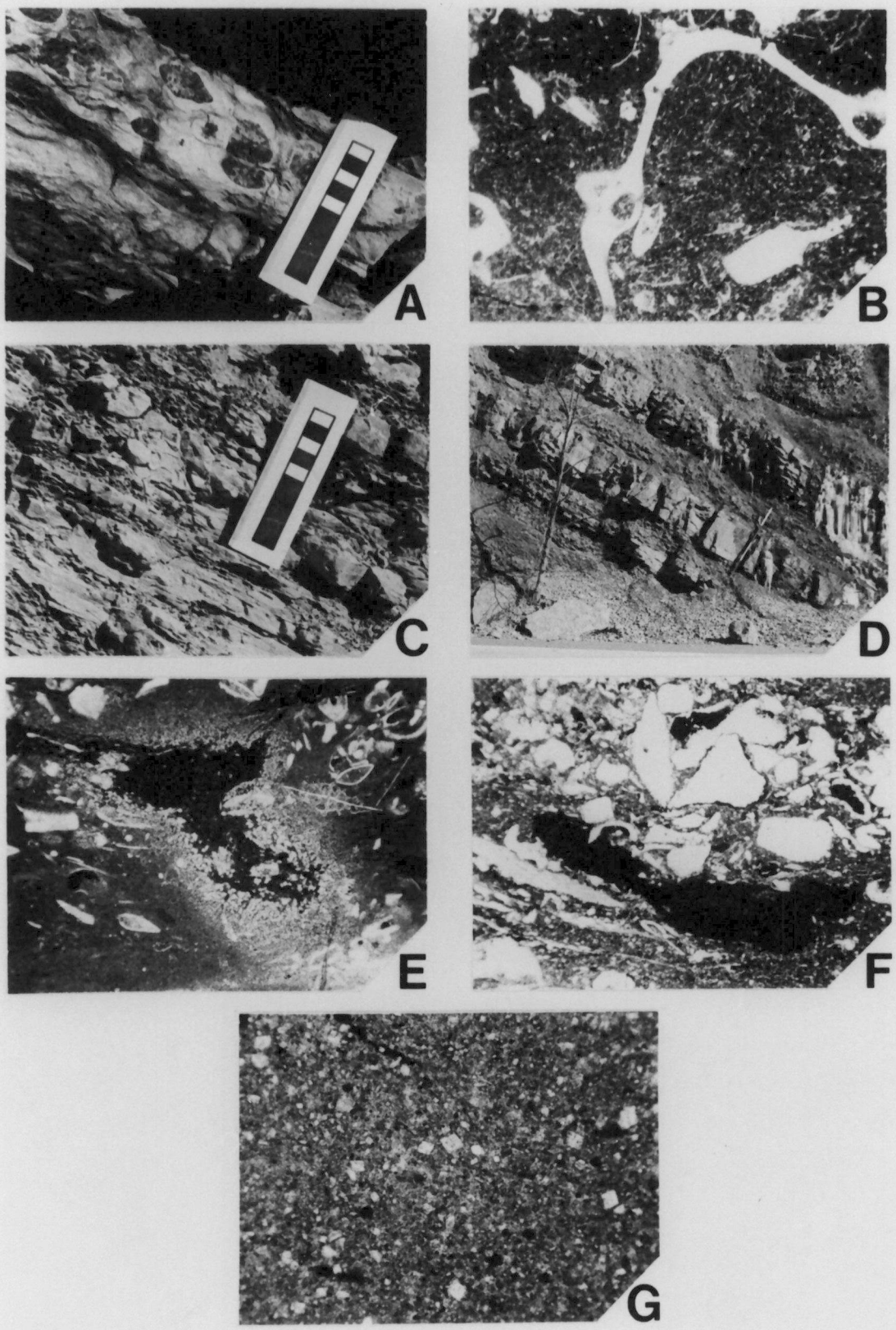


Figure 13

layers and lenses (0.2 mm to 2 mm thick) are interlaminated with the thicker fossiliferous micrites and are frequently disrupted by burrowing activity. Several horizontal burrows are present as vague circular and tubular cross sections. Anastomosing sets of hummocky and irregular stylolites form bands (1 mm to 10 mm thick), trending subparallel to bedding.

The less abundant zone of biomicrite beds consist of echinoderm debris (8%); bryozoan debris (6%); sponge spicules in micrite (5%); trilobite debris (3%, Figure 12B); and brachiopods (< 1%), all in a matrix of 19% micrite and 45% stylocumulate. Stylocumulate is defined by Logan and Semeniuk (1976, p. 13) as "material that passively accumulated as insoluble residue along a pressure solution interface." Fossils collected from this lithology include complete specimens of Rostricellula, Sowerbyites, Isotelus and Calyptaulax (Calliops) the latter exhibiting very delicate ornamentation. The biomicrite is indiscriminately silicified and forms irregular chert nodules that compose roughly 20-40% of the outcrop.

Thin, interbedded biopelsparite beds consist of abraded, well sorted, coarse silt particles and very fine skeletal sand (the constituents similar to those in the biomicrite described above) cemented by spar. Open spaces within the fossil fragments are completely filled with micrite. Clumps of Girvanella are a minor constituent in these beds. One thin section revealed stylocumulate within a chert nodule. This illustrates that pressure solution had occurred before silicification.

Paleoenvironmental interpretation. Lithology E3 was deposited in a subtidal environment, as indicated by the diverse fauna (Figure 9, p. 24) and horizontally oriented deposit-feeder burrows (see Rhoads, 1967). Laminated spicular micrite was deposited in a quiet water environment (60% micrite matrix). Decomposition of the sponges subjected the skeletal spicules to disaggregation by weak currents. Biopelsparite laminae associated with the spicular micrite were probably deposited during storm activity and were subsequently reworked by burrowers, producing irregular and discontinuous layers.

The interbedded zone of thin-bedded biomicrite contains an indigenous fauna, according to the criteria established by Johnson (1960). This fauna is representative of a stable bottom, shallow subtidal community dominated by epifaunal suspension and shallow deposit feeders. Infrequent thin biopelsparite interbeds may represent very large storm deposits or small tidal channel deposits.

V. HOGSKIN MEMBER OF THE LINCOLNSHIRE FORMATION

General Description

The Hogskin Member of the Lincolnshire Formation overlies the Eidson Member and is overlain by the Rockdell Formation. It is well exposed along the east side of the new state Route 25 East, which was completed in 1971 (Figure 1, p. 3). The Hogskin Member is approximately 19 meters thick at Evans Ferry.

The Hogskin Member is generally divisible into 2 lithologies, which alternate vertically with each other. Lithology H1 contains irregular

wavy shale laminae interlaminated with wackestone. Since the wavy shale laminae weather more rapidly than the wackestone layers, lithology H1 forms a characteristically cobbly-bedded appearance (Figure 13C, p. 42). Lithology H2 is a massive bedded, dark brown-gray, fine to coarse grainstone. This rock type resists weathering to form thin (0.4 m to 1 m) ledges between the thicker intervals (1 m to 6 m) of lithology H1 (Figure 13D, p. 42).

Lithology H1

Thin section analysis. Lithology H1 consists of thick intervals (1 m to 6 m) of cobbly bedded wackestone and shale. The nodular wackestone layers and the alternating wavy shale layers average 1 cm to 3 cm in thickness. The majority of the wackestone cobbles consist of echinoderm debris (15%); bryozoan debris (12.3%); brachiopod fragments (2%); ostracod valves (1.7%); trilobite debris (1%); pelecypod debris (< 1%); and gastropod debris (< 1%), all suspended in a matrix of 50% micrite. Approximately 20% of the micrite has been neomorphosed to microspar and pseudospar. Girvanella is present in thin (0.1 mm) sediment coatings (4%) around fossils. Other minor algal constituents include Solenopora type P (see Moore, 1978), Hedstroemia and Nuia. The remainder of the wackestone consists of clay laminae, which grade into horsetail stylolites and associated stylocumulate. Some of the clay contained in the wackestone was deposited as irregular clasts (Figure 13E, p. 42). Many of the faunal elements are articulated and exhibit very minor signs of abrasion.

The allochems range in size from 0.2 mm to 3 mm and about 1 - 2% of them have silicified interiors or pyritized edges. Wackestone nodules containing pellets and fossils that exhibit greater fragmentation (average size is fine sand) are usually associated with burrow networks. Most of the burrows are horizontal, but some are inclined as much as 50° from the bedding plane. Occasionally, micrite containing small pods of biopelsparite is also intercalated with the shale layers in lithology H1.

The shale layers (1 cm to 3 cm thick) are irregular, sometimes discontinuous, and are thicker over depressions in the carbonate bedding surface. Allochems comprise approximately 30% of the shale layers and include, in order of decreasing abundance, brachiopods, echinoderms, trilobites and bryozoans all in a clay matrix. The fossils are oriented with their long axes parallel to the depositional surface, and many have subsequently been broken because of post depositional compaction of the shale. Echinoderm sand occurs suspended (about 1 - 4%) within the clay matrix or as partly dissolved grains (about 5 - 10%) produced by pressure solution within the clay layers (Figure 13F, p. 42). Euhedral, coarse silt, dolomite rhombs (about 1 - 3%) are widely distributed throughout some of the clay layers (Figure 13G, p. 42). These layers frequently grade laterally into anastomosing sets of hummocky stylolites. The wackestone-shale boundaries are characterized by the following types of contacts: (1) an intervening flat shell fragment (sharp contact, Figure 14A); (2) a halo of pseudospar and microspar diminishing in grain size

Figure 14. Photomicrographs of shale laminae within the Hogskin Member (Hl) and associated diagenesis.

A. Photomicrograph of an intervening brachiopod shell separating the wackestone (above) from the shale layer (below), 25X (EF' 12).

B. Photomicrograph of a microspar halo bounding a shale lamina with the microspar decreasing in grain size away from the shale, 25X (EF' 4A).

C. Photomicrograph of an uncompacted oncolite contained in a wackestone cobble, 25X (EF' 18).

D. Photomicrograph of a squashed oncolite contained in the shale layer, indicating compaction, 25X (EF' 18).

E. Photomicrograph of echinoderm fragments in wackestone (top half of photo), which have depressed the underlying shale lamina (bottom half of photo), 30X (EF' 18).

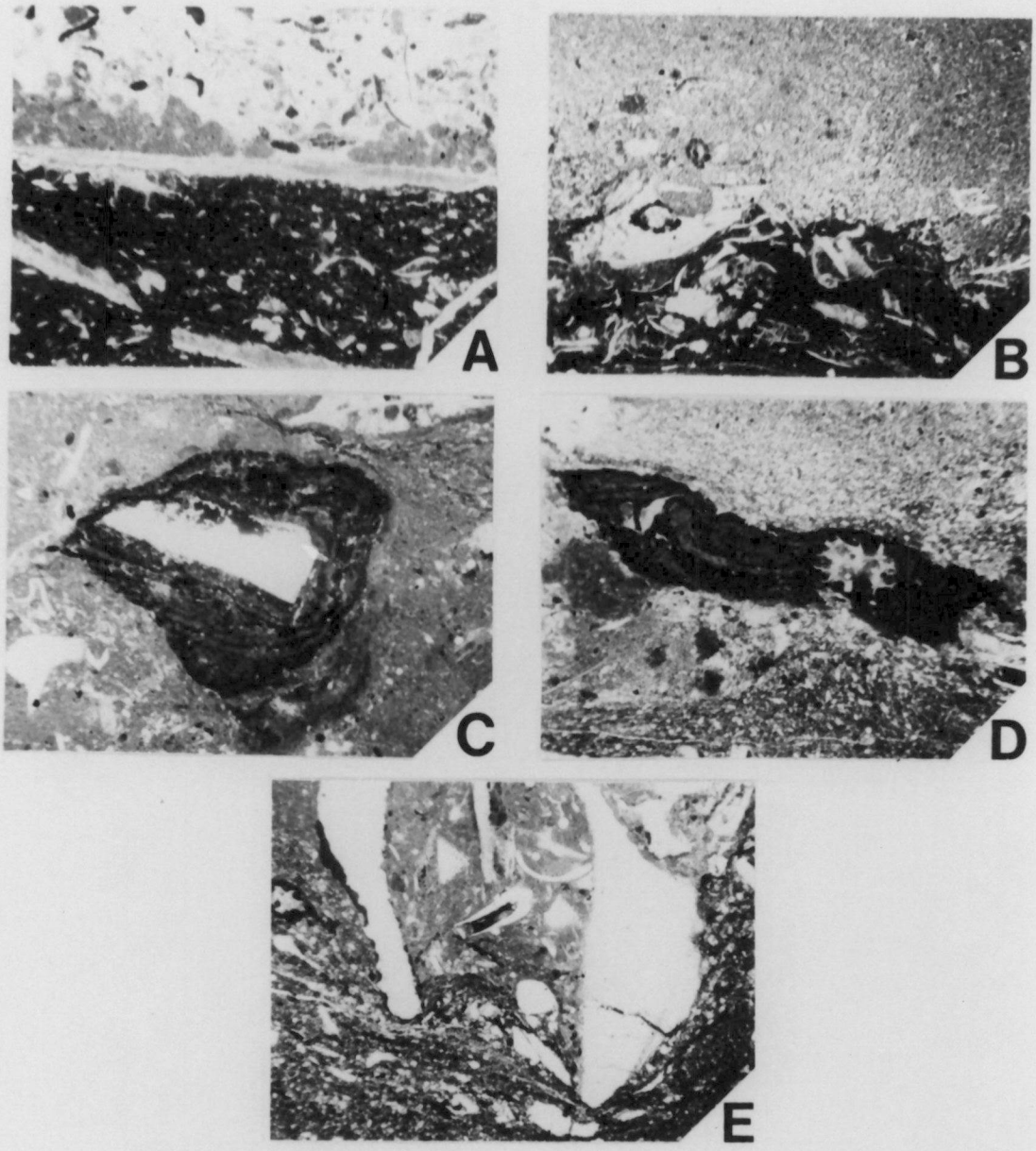


Figure 14

away from the clay (gradational boundary, Figure 14B) and (3) an intervening set of anastomosing hummocky stylolites.

Paleoenvironmental interpretation. Lithology H1 contains a very diverse fauna (Figure 9, p. 24) and flora (Figure 15). Determination of the fossil diversity is based on petrographic analysis which permits identification of fossils only to a gross systematic level. However, Smosna and Warshauer (1978) have shown that petrographic diversity is a good first approximation of simple species diversity. Therefore, I believe that the data presented in Figure 9, p. 24, and Figure 15 are a valid reflection of the biotic diversity within the Hogskin Member. Sanders (1969) proposed that diversity is greatest where physiological stress is least. Consequently, lithology H1 was probably deposited in a stable subtidal area, where conditions were less variable, rather than in stressful intertidal or physically controlled subtidal environments. The high percentage of micrite suggests deposition in relatively quiet water. In addition, pyritized fossil fragments indicate reducing conditions, which may have been caused by decomposition of organic material that settled from suspension. Reducing conditions are most often encountered in subtidal sediments (Logan, 1974).

The biota of lithology H1 appears to be indigenous because shells display only minor breakage and abrasion attributed to transport. Fragmentation of fossils is greatest near burrows, indicating that shell breakage was caused more likely by animals searching the sediment for food rather than by current reworking.

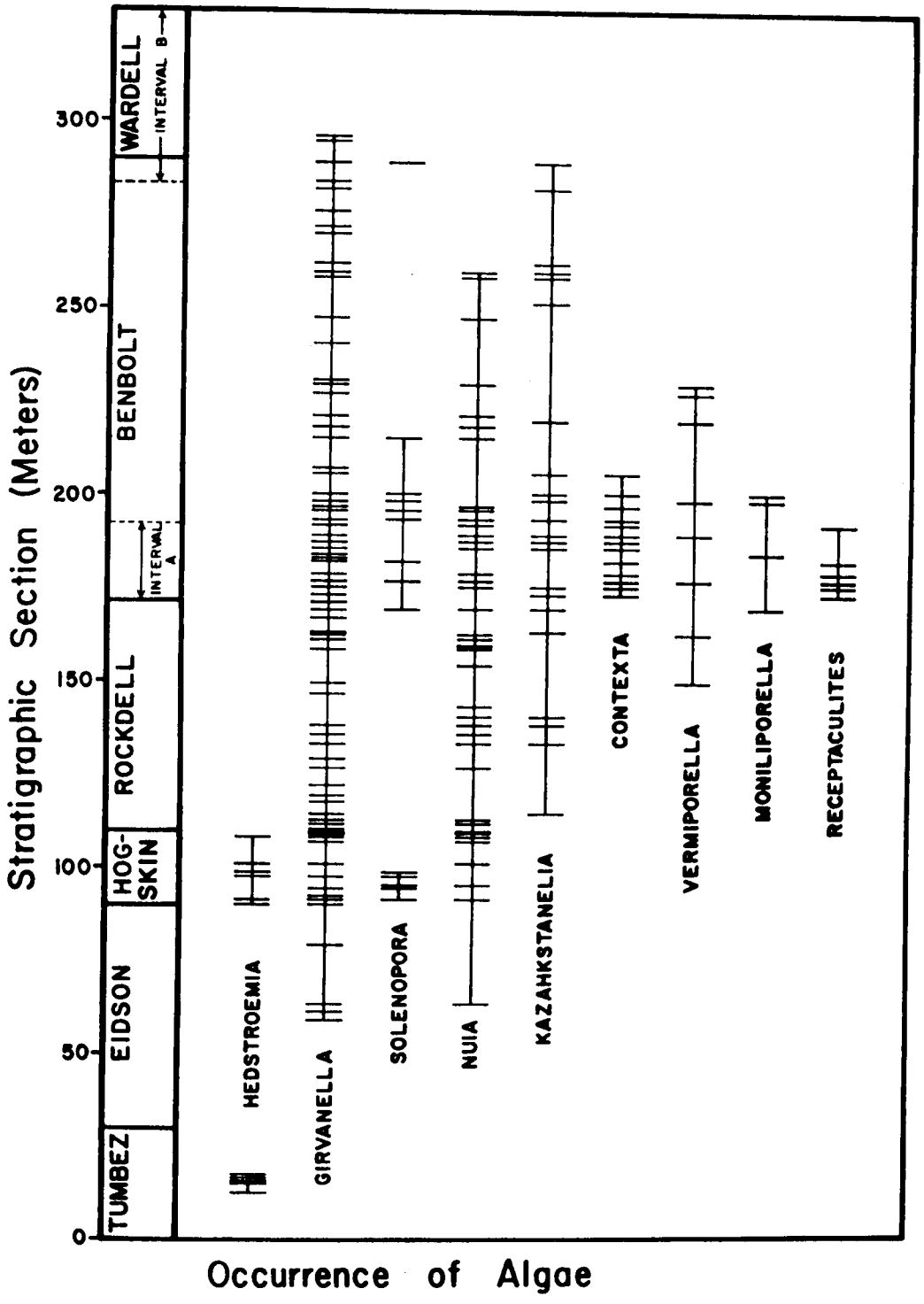


Figure 15. Location of algae in the stratigraphic section at Evans Ferry, Tennessee. Each bar illustrates the occurrence of algae in a particular thin section and is not quantitative.

Occasional clay clasts occurring within the micrite matrix of the wackestones are surrounded by aureoles of microspar, which diminish in grain size away from the clast (Figure 13E, p. 42). Longman (1977) noted a similar halo around clay clasts in the Bromide Formation of south-central Oklahoma. He suggested that Mg ions become attached to the surface of 2 μm calcite grains in micrite as a result of early diagenetic inversion of high-Mg calcite to low-Mg calcite. The clay (may have originally been montmorillonite) acts as a Mg ion pump, drawing Mg from the micrite and allowing it to recrystallize to coarser size. Longman (1977) noted that the ability of the clay to attract Mg ions decreases with distance and thus, the grain size of neomorphosed micrites decreases with distance from the clay clast. This process could serve to explain the presence of aureoles around clay clasts in the wackestone of lithology H1 equally well.

The intercalated shale layers of lithology H1 are indicative of periodic clay deposition. The clay fills minor depressions in the wackestone, but most of the bounding surfaces are obscured by diagenetic alteration (as in the previous discussion). Some oncolites have been squashed during differential compaction of the shale layers following deposition and burial (Figure 14C and D, p. 48). Figure 14E, p. 48, illustrates another feature formed by compaction of the shale. Differential compaction is probably the chief cause of the wavy bedded appearance of the shale layers. Similar postdepositional compaction of clay beds in micrite has been inferred to produce wavy shale partings in the McGregor Member of the Platteville Formation

(Ordovician) of Wisconsin (Byers and Stasko, 1978). Additional evidence for post depositional compaction of the shale is its close association with hummocky stylolites. The stylolites are not present in the wackestone layers. In their study of clays in the Wenlock Limestone, Oldershaw and Scoffin (1966, p. 316) concluded that ". . . clay minerals were instrumental in the mechanism of pressure solution." The process implied in this statement accounts for the abundance of pressure solution features within the clay layers of lithology H1 and their absence in the wackestone layers. Pressure solution is responsible for the formation of reactate (see Logan and Semeniuk, 1976) dolomite, insoluble residues, and partly dissolved echinodermal sand.
The mechanism for the formation of reactate dolomite is not completely understood, but Logan and Semeniuk (1976) postulate that Mg-bearing fluids react with calcite across the pressure solution interface. Possible sources for Mg in lithology H1 are the clays or algae, which concentrate Mg in their vital fluids according to Gebelein and Hoffman (1971).

Lithology H2

Thin section analysis. Lithology H2 is composed of grainstones (biosparite and biopelsparite). The grainstones are variable in composition, but generally consist of echinoderm debris; bryozoan debris; trilobite debris; ostracod valves; gastropod debris; peloids; pelecypod debris; superficial ooids; and brachiopod fragments, in approximate order of decreasing abundance. Minor algal constituents

include Girvanella clumps, fragments of Solenopora type P and Hedstroemia. The modal grain size for all the allochems is 0.7 mm (coarse sand). The allochems are fragmented, subrounded, and moderately to well sorted. A few columnar stylolites (maximum aplitude 2 mm) trend parallel to the bedding plane.

Paleoenvironmental interpretation. Lithology H2 is interbedded with H1 and probably represents high-energy tidal channels or storm layers (i.e., as lag deposits). Strong currents are indicated by the paucity of micrite, the subrounding of fossils, the moderately to well sorted grains, and the presence of superficial ooids. The superficial ooids consist of rounded, medium sand sized fossil fragments or peloids, which have been coated by one or two lamellae (about 0.04 mm thick). The coating is amber in plane-polarized light. It is inferred from the concentrically deposited lamellae that the grain must have been agitated, implying some current activity. The alternation of lithology H2 with H1 may have resulted from the migration of a tidal channel (see Shinn et al., 1969) or alternatively from the periodic activity of strong storm currents (see Ball et al., 1967).

VI. ROCKDELL FORMATION

General Description

The Rockdell Formation overlies the Hogskin Member of the Lincolnshire Formation. It is well exposed along the east and west sides of the new state Route 25 East and is approximately 62 meters thick.

The Rockdell Formation is massive bedded (0.2 m to 2 m thick, Figure 16A) and produces the greatest local relief of the units in the Evans Ferry section. This formation is composed of 2 distinct lithologies. Lithology R1 characterizes the lower 50 meters of the Rockdell Formation. It is massive-bedded, brown-gray, argillaceous packstone, containing abundant anastomosing sets of irregular stylolites. The rocks of lithology R1 have a distinctive H_2S-odor when fractured. Lithology R2 consists of thick-bedded (10 cm), light gray packstone and grainstone and is characteristic of the upper 12 meters of the Rockdell Formation. This lithology also forms a 3 meter interbed in the middle of lithology R1.

Lithology R1

Thin section analysis. Lithology R1 (109.6 m to 159.2 m above the base of the section) consists of argillaceous packstone (biomicrite). The packstone consists of echinoderm debris (15.4%); bryozoan debris (8.2%); sponges and sponge spicules (3%); and ostracod valves (2.7%). The remaining allochems are minor constituents (< 1%) and are, in decreasing order of abundance, trilobites, gastropods, pelecypods, brachiopods and algae. All of these allochems are contained in a matrix of 38% micrite, which has a clotted appearance in the upper 10 meters of this lithology (R1). Clumps of silt pellets occur where they are protected by a large skeletal fragment. Compaction of other unprotected pellets may have produced the clotted micrite texture. The allochems are fragmented, slightly abraded, and range in size from coarse silt to

Figure 16. Photomicrographs and field photograph of the Rockdell Formation (R1).

A. Field photograph illustrating the massive beds of the Rockdell Formation (staff = 2 m).

B. Photomicrograph of a thin section showing a reticulated network of sponge spicules in micrite, 25X (EF' 39).

C. Photomicrograph of the reticulated sponge spicule network of a different sponge, 25X (EF' 28).

D. Photomicrograph of a horizontal burrow exhibiting a deformation halo in the surrounding sediment, 25X (EF' 20).

E. Photomicrograph of columnar stylolites, dissolved fossil fragments and neomorphosed micrite in the Rockdell Formation, 25X (EF' 22).

F. Photomicrograph of euhedral, silt-sized, dolomite rhombs in clay-rich stylocumulate, 125X (EF' 22).

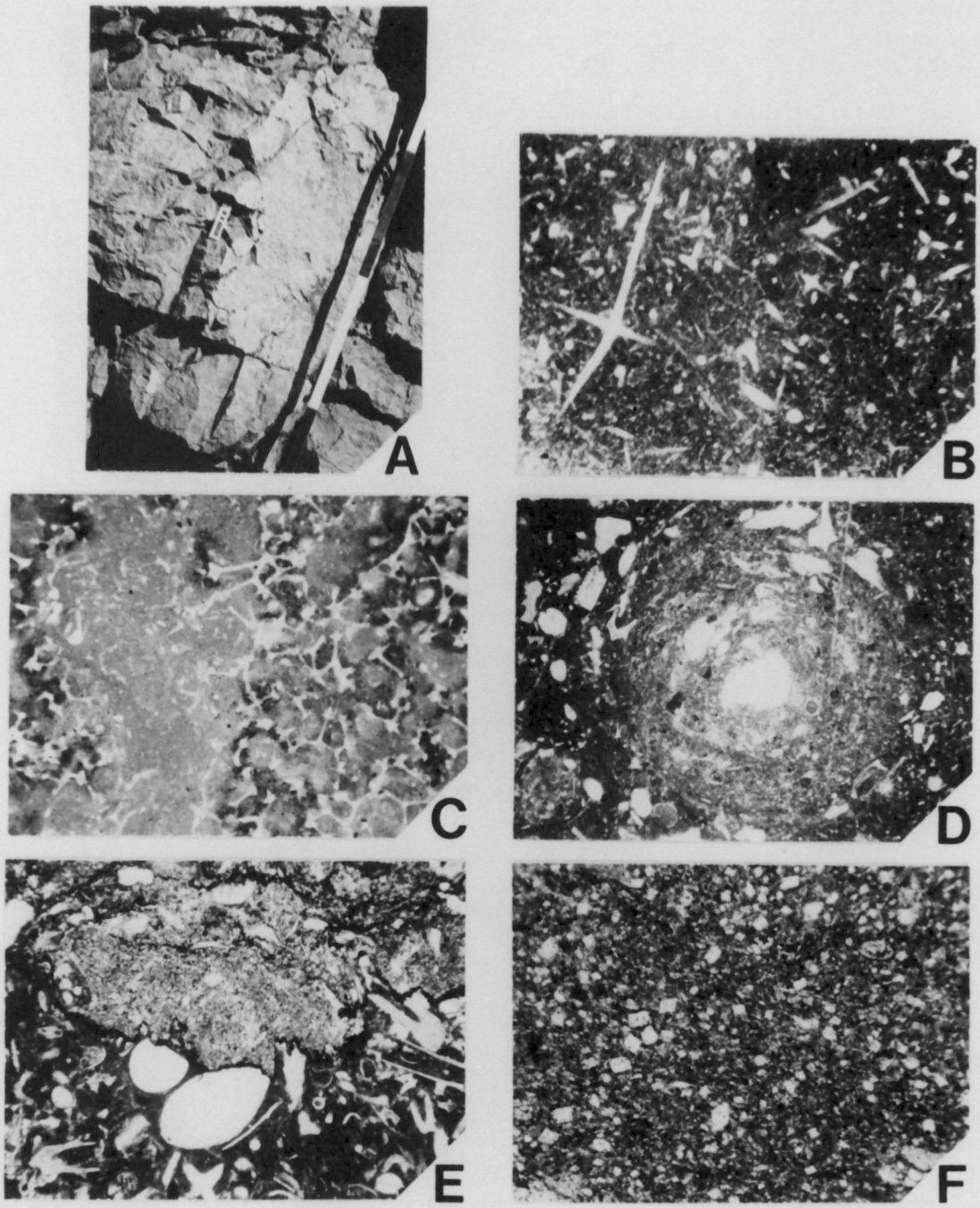


Figure 16

coarse sand. The average grain size is 0.3 mm (medium sand). Sponges are very prominent in the Rockdell Formation (Figure 9, p. 24) and are preserved as spicular networks suspended in micrite (Figure 16B and C) and as loose individual sponge spicules. The dimensions of the largest sponge observed are 10 mm wide by 30 mm high. In general, algae (Girvanella, Nuia and Kazahkstanelia, Figure 15, p. 50) are minor constituents (< 1%) of the Rockdell Formation. Girvanella is the most abundant of the three and occurs as thin coatings on fossil fragments. Girvanella also forms large, loosely bound, irregularly lobate aggregations. However, this latter occurrence of Girvanella is rare and was observed in only one slide, which was point counted and plotted on Figure 17. Therefore, peak 1 on Figure 17 does not represent the actual average abundance of Girvanella, which is much less in lithology R1 than suggested by peak 1.

Horizontal burrows are abundant in lithology R1. As many as 10 burrows per square centimeter were observed in one slide and 4 burrows per square centimeter in several other slides. They are preserved in thin section as biosparite and biomicrite circles and elongated ellipses surrounded by deformation halos (Figure 16D). The significance of these burrows is discussed below.

Anastomosing sets of irregular stylolites are present throughout lithology R1. The stylolites are usually irregular and subparallel to bedding, but they often grade into columnar and peaked types. They are characterized by sutured and partly dissolved grain contacts, neomorphic microspar, euhedral dolomite rhombs and iron oxide stain (Figure 16E and F).

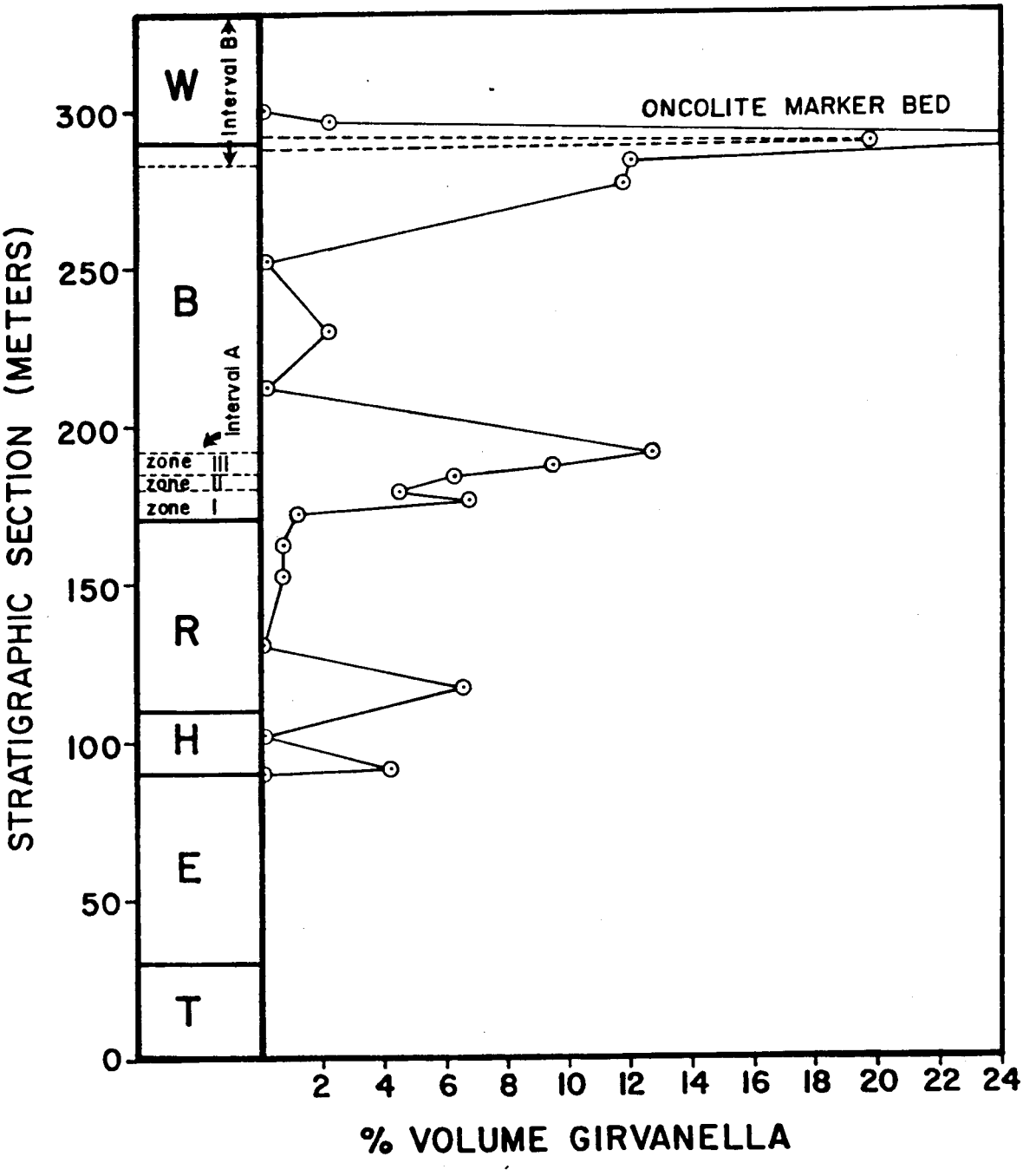


Figure 17. Stratigraphic distribution of the alga Girvanella for Evans Ferry, Tennessee. Volume percent was derived from point count data (see Table A-1, Appendix A).

Paleoenvironmental interpretation. The rocks of lithology R1 are interpreted to have formed in a shallow (at or below wave base) subtidal environment. The echinoderms, bryozoans and sponges display little abrasion and are probably indigenous. The remaining faunal elements were probably transported from a neighboring environment. The presence of loosely aggregated Girvanella tubules and thin Girvanella coatings indicates that current energy was low. The presence of sponges with delicately reticulated sponge spicules is also evidence in support of low current energy. Fragmented fossils in lithology R1 could be products of biological destruction, as described by Ginsburg (1957), rather than physical destruction. In addition, Moore (1977) noted that the occurrence of loosely intertwined Girvanella tubules in Middle Ordovician rocks was probably a function of increased water depth. Therefore, lithology R1 probably represents a deep subtidal environment.

A firm substrate of relatively low water content is inferred for lithology R1 because of the slight deformation halos that surround horizontal burrow structures (see Rhoads, 1975). An abundance of burrows is indicative of high organic content in the sediment and thus a large food supply for deposit feeders. However, semirestricted water circulation and decomposition of organic matter may have caused periodic reducing conditions. These conditions may have led to the strong hydrogen sulfide odor associated with lithology R1. A modern analog for this type of environment is Florida Bay. Ginsburg (1956) and Gorsline (1963) have described Florida Bay as a shallow (less

than 3 meters) triangular area with semirestricted water circulation and a lacelike pattern of shoals separated by deeper water "ponds." Gorsline (1963) observed that high organic content of Florida Bay muds and their impermeability resulted in rapid development of reducing conditions.

Lithology R2

Thin section analysis. Lithology R2 composes the upper 12 meters of the Rockdell Formation. It contains interbedded packstone and grainstone, both of which contain less micrite than is present in lithology R1. An analysis of a representative sample of the grainstone revealed the following constituents: echinoderm debris (29%); bryozoan debris (18.7%); algae (3%); ostracod valves (2.3%); trilobite debris (1.8%); and peloids (1.5%) all cemented by calcite spar (30%). Micrite (8%) present in the grainstone is trapped between and in fossil fragments. In the packstone, micrite occupies half of the void space and appears to have filtered in from above because it forms geopetal structures and is found most frequently above fossil fragments. The allochems are probably not indigenous because they are abraded and fragmented. In addition, they show some size sorting with a modal grain size of 0.3 mm. Some of the fossils exhibit algal borings as shown by their heavily micritized borders.

The algae consist of Contexta, Kazahkstanelia, Girvanella, Nuia, Vermiporella and Moniliporella in approximate order of decreasing abundance (Figure 15, p. 50). Girvanella is present as thin coatings

on fossil fragments and rarely forms lobate oncolites. Contexta and Kazahkstanelia are usually found together and like the other algae (except Girvanella) are probably exotic elements because of their abraded and broken condition.

Horizontal burrows are present (3 per square centimeter) in the lower 4 meters of lithology R2, but are absent from the upper 8 meters. They occur in both packstone and grainstone and are filled with micrite.

Paleoenvironmental interpretation. Lithology R2 and R1 are vertically gradational with each other within an 8 meter interval. In addition, a 3 meter unit of lithology R2 is interbedded with lithology R1. Both lithologies (R1 and R2) have common faunal elements. Consequently, lithology R2 is interpreted to represent an environment of higher energy than that represented by R1, but is thought to have been laterally continuous and gradational with it. Higher current energy is inferred from the lower percentage of micrite matrix and the increased fragmentation and abrasion of fossils. Increased water circulation in the environment of deposition of lithology R2 prevented the reducing conditions responsible for the fetid odor present in the rocks of lithology R1. Calcareous algae contained in lithology R2 exhibit high diversity; however, their abraded condition and micrite-filled cells (other fossils are devoid of micrite) indicate that they are exotic elements from a neighboring environment, possibly a mudbank.

VII. BENBOLT FORMATION

General Description

The contact between the Benbolt Formation and the underlying Rockdell Formation is generally distinctive because of the abundance of shale in the former. The lower Benbolt Formation is exposed on the east and west sides of the new state Route 25 East. The middle and upper portions of the formation are poorly exposed along the valley adjacent to the highway (Figure 1, p. 3). The contact between the Benbolt Formation and the overlying Wardell Formation is delineated by a 40 cm limestone bed containing approximately 50% oncolites (1 cm to 2 cm diameter). I chose the basal contact of the beds as the contact between the 2 formations, thereby including the oncolite bed within the Wardell Formation. The Gratton Limestone, as described by Prouty (1946), is absent at Evans Ferry and so could not be used to separate the Benbolt and Wardell Formations. Rather than combining these two formations (Dryden Formation of Cooper, 1956), it seemed more appropriate to separate these two distinctive lithologies. The oncolite marker bed can be traced laterally at Evans Ferry for at least 275 meters.

The Benbolt Formation is approximately 118 meters thick and can be subdivided into 4 general lithologies on the basis of thin section analysis and field observations of available outcrops. Lithology B1 makes up the basal 30 meters of the Benbolt Formation and consists of cobbly-bedded (similar to Hogskin Member), argillaceous, brown-gray packstone interbedded with shale. The thickness of the shale and

packstone beds is highly variable (1 cm to 15 cm). Lithology B2 directly overlies B1 and consists of 16 meters of massive, cross-bedded, gray grainstone. In the upper 71 meters of the Benbolt Formation, lithologies B3 and B4 are interbedded. This thick interval of the Benbolt Formation is characterized by wavy-bedded wackestone, packstone, and occasional grainstone that are of variable thickness (5 cm to 30 cm). Lithology B3 dominates this 71 meter interval and contains the latter two rock types. Lithology B4 is characterized by algal wackestone, which occurs at the base and middle of the 71 meter interval of the upper Benbolt Formation.

Lithology B1

Thin section analysis. The basal 13 meters of lithology B1 is composed of cobbly-bedded 6 cm thick packstone (biomicrite) cyclically interbedded with 3 cm thick shale layers. The packstone is thinner bedded (3 cm thick) in the last 5 meters of this interval. The upper 17 meters of lithology B1 is composed of 10 cm thick packstones (biomicrite and poorly washed biosparite) beds separated by 1 cm to 2 cm thick shale layers. The biota of lithology B1 consists of: echinoderm debris (18%); bryozoan debris (8.4%); Girvanella (6.8%); trilobite debris (2.3%); ostracod valves (2%); Contexta (1.3%); pelecypods (1.3%); pellets (< 1%); gastropods (< 1%); sponges; and other algae (< 1%) all in a matrix of 30% micrite (half neomorphosed to microspar and pseudospar) and 13% clay. The micrite may have been produced by compaction of fine sand pellets because

the matrix has a clotted texture in most of the slides. Low percentages of pellets are ubiquitous in lithology B1 and low percentages are preserved only when they were sheltered from compaction by large fossil fragments. The pellets are interpreted as fecal in origin because they are uniform in size (0.2 mm) and shape (circular and ellipsoidal). The allochems listed above vary in size from 0.3 mm (medium sand) to 4 mm (granules) and exhibit very minor fragmentation. Lack of abrasion is indicated by preservation of delicate ornamentation on echinoderm plates and trilobite debris. Partly pyritized or blackened fossils are common in lithology B1.

Clay layers and lenses (3-8 mm thick) are interbedded with the packstone. The layers may contain echinoderm debris and minor amounts of other fossils concentrated in pods or laminae, or they may be fossil free. Neomorphic microspar and pseudospar halos similar to those of H1 frequently surround the clay layers. In addition, irregular and hummocky stylolites are often laterally gradational with the clay layers.

Calcareous algae are very diverse in lithology B1, but are minor constituents of the whole biota. Listed in decreasing order of abundance, they are: Receptaculites, Girvanella, Contexta, Nuia, Solenopora (type P and R), Kazahkstanelia, Moniliporella, and Vermiporella (Figure 15, p. 50). Receptaculites (avg. 2.5 cm diameter) was not observed in thin section, but it is an abundant constituent on the weathered outcrop. Girvanella is present (Figure 17, p. 58) as: (1) clumps of micrite and intertwined tubules, (2) thin coatings on fossil fragments and (3) irregularly lobate oncolites. The latter

occurrence of Girvanella forms peak 2 on Figure 17, p. 58, culminating a gradual increase in Girvanella abundance toward the top of lithology B1. Contexta is the only other significantly abundant alga and is frequently recrystallized in part and associated with Kazahkstanelia.

Paleoenvironmental interpretation. Lithology B1 marks a bloom in algal diversity (Figure 15, p. 50); however, the algae are present in minor percentages. The fauna exhibits a similar reduction in abundance concomitant with an increase in diversity (Figure 9, p. 24, 171 m to 200 m). Application of Johnson's (1960) criteria to the biota of lithology B1 implies that they are indigenous. This highly diverse biota is interpreted to represent several intergrading communities in a stable, offshore, subtidal environment. Supporting evidence of this interpretation will be discussed in the following chapter. Frequent environmental disturbances usually lead to communities of low diversity, which might be expected of lithology B1 because of the cyclically interbedded shales. However, since the shale was deposited at regular intervals (cyclic), the environmental perturbations were predictable. Therefore, the biota could achieve high diversity despite the seemingly strong physical stress (Sanders, 1969, has discussed this possibility). This concept is known as pulse stability (Odum, 1971).

The diverse flora is representative of a well-lighted, shallow subtidal environment. Girvanella oncolites are also indicative of shallow depths (Ginsburg, 1960), and their lobate shape implies moderate rather than high current activity.

Lithology R2 grades into B1 within several meters and contains exotic algae indigenous to lithology B1. These facts are a strong indication that these two lithologies represent laterally proximal and interacting environments. The biota and depositional environment of lithology B1 are discussed in greater detail in the following chapter.

Lithology B2

Thin section analysis. Lithology B1 grades upward into B2, which is composed of 16 meters (202 m to 218 m) of massive, cross-bedded grainstone (biosparite). The allochems are: echinoderm debris (29%); bryozoan debris (17.5%); ostracod valves (2.5%); trilobite debris (1.8%); pellets (1.3%); intraclasts (1.3%); brachiopod debris (< 1%); gastropods (< 1%); and sponge fragments all cemented by spar (32%). Micrite is present in low percentages (< 10%) between fossil fragments and may be a product of pellet compaction. The allochems exhibit greater fragmentation (into coarse sand) and abrasion than in lithology B1. Algal bores in echinoderm debris and trilobite fragments are indicated by the presence of numerous micrite envelopes. Broken and abraded Contexta and Kazahkstanelia fragments are negligible constituents of the biota in lithology B2. Girvanella is rarely present as lobate oncolites.

Paleoenvironmental interpretation. Lithology B2 is so distinctive that it has been mapped separately as Member "a" of the Benbolt Formation by Harris and Mixon (1970). Small scale (5 cm in height)

bidirectional trough cross-beds are visible on some outcrop surfaces (Figure 18A), which implies deposition by tidal currents. Increased percentages of echinoderm and bryozoan debris from lithology B1 to B2 (Figure 9, p. 24) is accompanied by increased fossil abrasion and decreased particle size, regarded as transportational effects. These observations lead to the inference that lithology B2 represents a tidal channel or tidal skeletal sand bar deposit. This deposit is gradational with the rock units above (B3) and below (B1).

Lithology B3

Thin section analysis. The upper 71 meters of the Benbolt Formation (218 meters from the base of the section to 289 meters) is characterized by a repetitive sequence of thick units (0.5 m to 2 m) composed of thin-bedded (5 cm to 30 cm) borderline wackestone - packstone (biomicrite) interbedded with occasional grainstone (bioparite) and algal wackestone separated by thick (0.5 m to 7 m) covered intervals. The rock types within the covered intervals could not be positively determined, but they are thought to represent weathered clay shale units. Unusual thin bedded (5 cm to 10 cm) algal wackestones occurred in two locations within lithology B3 and are discussed separately in the next section (lithology B4). The allochemical content of lithology B3 remains basically the same throughout, but abundances are highly variable. The allochems include echinoderm debris (6% - 19%); bryozoan debris (6% - 16.5%); brachiopod valves (< 1% - 12.8%); Girvanella (2.5% - 11.8%); pelecypod valves (1% - 7.5%); trilobite

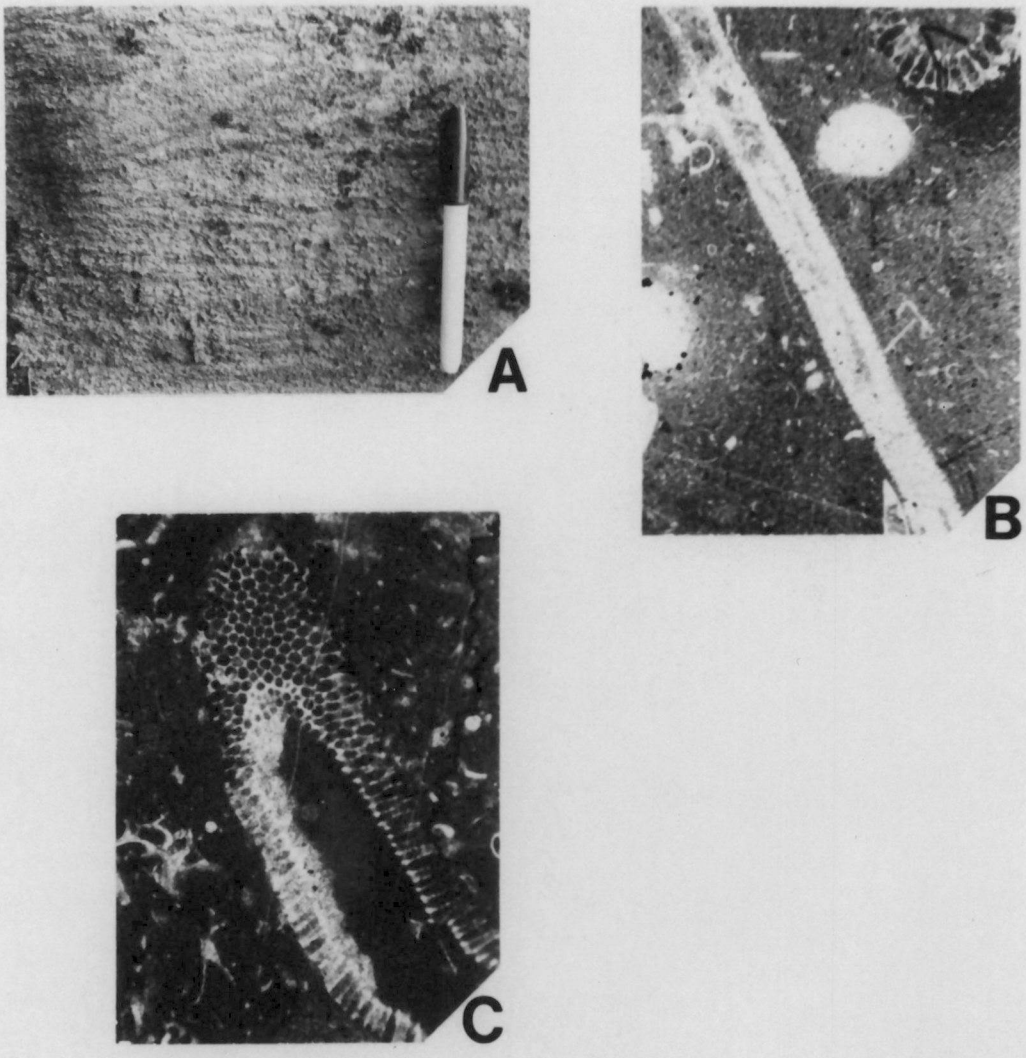


Figure 18. Field photograph and photomicrographs of the middle and upper Benbolt Formation.

A. Field photograph displaying the dominant set of gently dipping small scale trough cross-beds in the Benbolt Formation (B2). Cross-bed sets in the reverse direction were not photographed (pen = 13.5 centimeters).

B. Photomicrograph (EF' 71) of the alga Vermiporella in probable life position. Kazahkstanelia is in the top right of the photograph in a matrix of micrite. 25X.

C. Photomicrograph (EF' 80) of the alga Kazahkstanelia in probable life position in a matrix of micrite. 25X.

debris (< 1% - 3.3%); ostracod valves (< 1% - 2.8%); pellets (0 - 11%); and intraclasts (0 - 1.5%). The wackestone-packstone has a matrix of approximately 42% micrite, of which 30% has been neomorphosed to microspar. Based on the median size of the contained allochems, the rocks of lithology B3 are generally divisible into two broad categories, each of which has distinctive characteristics. In one category, the allochems are coarse to very coarse sand (0.6 mm to 1.6 mm) and in the other, the allochems are fine to medium sand (0.12 mm to 0.3 mm). The fossils composing allochems of the first group exhibit minor fragmentation and abrasion, while those in the latter group are highly fragmented and abraded, and are frequently bored by algae. Intraclasts are associated with the latter group.

Thin Girvanella coatings (superficial oncolites) and clumps are erratically distributed throughout the rocks of lithology B3. Girvanella oncolites, however, are restricted to the upper Benbolt Formation (Figure 17, p. 58, 276 meters - 289 meters). Other calcareous algae occur in low abundances and appear to be limited to specific zones (Vermiporella at 230 meters and Kazahkstanelia at 260 meters). These zones of algal occurrence loosely correspond to the presence of lithology B4 (219 and 252 meters) and consist of broken and abraded fragments (discussed below).

Clay layers, lenses and clasts are ubiquitous in lithology B3. They are characterized by neomorphic microspar aureoles and rare euhedral dolomite rhombs. Many layers grade laterally into irregular stylolites. Fossil allochems are minor constituents within the thin (2 mm) clay layers.

A marked change occurs in the faunal abundance of lithology B3 at 250 meters from the base of the section. Brachiopods and pelecypods gradually increase in abundance (Figure 9, p. 24), whereas echinoderms decline sharply in abundance and maintain a low percentage upward to the top of the measured section. Silicified brachiopods are numerous on weathered surfaces of slabs in the upper 10 meters of lithology B3, while pelecypods are only visible in thin section. Brachiopods become the dominant faunal element near the top of the Benbolt Formation. Girvanella oncolites display a similar upward increasing trend in abundance and ultimately make up 50% of the rock at the base of the Wardell Formation (Figure 17, p. 58). In addition to the biota, terrigenous quartz silt appears at 280 meters and persists in minor percentages throughout most of the Wardell Formation (Figure 11, p. 32). The deposition of quartz silt is probably representative of encroaching terrigenous sediments from the southeast (see Shanmugam and Walker, 1978). Consequently, the faunal modifications toward the top of the Benbolt Formation are probably a response to stronger currents (increased oncolite abundance) and increased terrigenous influx (introduction of quartz silt). The upper 6 meters of the Benbolt Formation is the interval which contains one of the biotas on which the second chapter of this report concentrates and the interval is discussed in greater detail in that chapter.

Paleoenvironmental interpretation. The bedding exposures of lithology B3 are separated by approximately 7 meters or less of soil throughout the lower 60 meters. Therefore, inferences concerning

the environment of deposition must be viewed with this fact in mind. It is quite possible that the lack of outcrop in these thin, somewhat regularly spaced intervals is indicative of terrigenous shale that has been severely weathered and destroyed.

Lithology B3 represents a mosaic of similar yet subtly different environments of deposition. Lithology B4 is interbedded with B3 adding to the environmental complexity. The loose correspondence of Kazahkstanelia and Vermiporella algal fragments in packstones of lithology B3 to the occurrence of the algal wackestones of lithology B4 suggests laterally intergradational rather than mutually exclusive paleoenvironments. The algal fragments of lithology B3 were probably derived from the in situ algal mudmounds of lithology B4 (discussed in the next section).

In addition to these few algal fragments, the wackestone-packstones contain a diverse assortment of allochems. These allochems are either fragmented and abraded (rock type A) or exhibit few signs of abrasion and moderate fragmentation (rock type B). This grain size divergence may be a reflection of: (1) intensified physical activity, producing rock type A; or (2) intensified biological destruction, producing rock type A. In this context, it is interesting to note that algal boring of fossil fragments is frequent in rock type A and uncommon in rock type B.

These various interbedded rock types imply a depositional environment characterized by mudmounds (algal wackestones, discussed in next section) surrounded by deeper water "ponds" or channels. These interbank areas would be expected to contain both indigenous

and exotic biotic elements (the latter derived from adjacent mudbanks). The rock record of lithology B3 is similarly constructed.

Lithology B4

Thin section analysis. Vermiporella and Kazahkstanelia wackestones comprise lithology B4. This lithology was sampled at 219 meters and 252 meters from the base of the section. The lower bed is composed of Vermiporella (7%) and minor Kazahkstanelia (1%), while the upper bed is composed of Kazahkstanelia (7.5%) and minor Tetradium (1%). Faunal elements common to both upper and lower beds and each composing less than 3% (by volume) of the rock are: gastropods, bryozoans, echinoderms and trilobites, in order of decreasing abundance. The algae and associated fauna display no signs of abrasion and few of the fossil shells are broken. The allochems are enclosed in a matrix of 76% micrite, of which 30% has been neomorphosed to microspar. Clay lenses (surrounded by neomorphic microspar) compose the remainder (5%) of the rock. Numerous horizontal burrows with vague outlines occur in the micrite, indicating that the original sediment had a high water content (see Walker, 1974).

Paleoenvironmental interpretation. Lithology B4 is interpreted to represent wave-baffled mudbanks. Calcareous algae associated with ramose bryozoans, echinoderms and Tetradium probably acted as a baffle to currents, allowing fine sediment (micrite and organic particles) to be trapped and stabilized between the various erect forms. Upon death and repeated current impact the upright biota fell over and

were preserved in the micrite matrix. In rare occurrences, Vermiporella and Kazahkstanelia are found standing in probable life position (Figure 18B and C, p. 68). Trilobites and burrowing deposit feeders (numerous horizontal burrows) must have fed on the organic debris trapped with the micrite. The sediment had a high water content because the horizontal burrowers didn't deform the surrounding sediment. Gastropods, probably feeding on the algae, were one of the most abundant constituents in the baffled mudbank environment. Davies (1970a) in his study of a modern mudbank, postulated that calcareous algae, bryozoans and crinoids may have served as current baffles and sediment stabilizers similar to the role of seagrasses in mudbanks since the Cretaceous.

VIII. WARDELL FORMATION

General Description

The Wardell Formation is separated from the Benbolt Formation by a distinctive basal Girvanella oncolite (maximum 1 cm diameter) bed, which is about 40 cm thick. This marker bed was easily recognized at 3 different outcrops in the Evans Ferry area that spanned 275 meters. Use of this marker bed elsewhere remains questionable, since this investigator did not try to trace the bed beyond the general study area. The Wardell Formation is 41 meters thick at Evans Ferry and is succeeded by the Bowen Formation.

For organizational purposes the Wardell Formation will be discussed as 3 separate, but intergrading, lithologies. The first lithology (W1)

consists of thin-bedded (4 cm to 15 cm thick) blue-gray wackestone and packstone interbedded with calcareous shale laminae (basal 10 meters of Wardell Formation). The overlying lithology (W2, 13 m thick) is characterized by interbedded dolomitic mudstone (micrite) and calcareous shale laminae. The third lithology (W3, 9 m thick) characterizes the upper Wardell Formation. It consists of mud-cracked, brown-gray, calcareous shale and mudstone laminae. The latter two lithologies (W2 and W3) are interbedded in the upper 20 meters of the Wardell Formation; however, the mud-cracked rocks (W3) dominate the upper 9 meters.

Lithology W1

Thin section analysis. Lithology W1 makes up the lower 10 m of the Wardell Formation and consists of 3 cm to 4 cm thick wackestone (predominant) and packstone (biomicrite and poorly washed biosparite) beds with intercalations of dolomitic calcareous shale laminae (1 cm thick). The allochems contained in the wackestone and shale layers are echinoderm debris (17%); bryozoan debris (11%); brachiopod fragments (7%); trilobite debris (3.5%); gastropod debris (2%); ostracod valves (2%); and pelecypod debris (< 1%) all in a matrix of 20% micrite and 26% clay. These allochems vary in size from silt to coarse sand and are highly fragmented. Five percent of them have partly silicified interiors and about 10% of the allochems have pyritized outlines. The dolomitic calcareous shale laminae comprise from 20% to 35% of the rock and consist of silt sized euhedal dolomite rhombs (composing up to 15% of the laminae) and the sand-sized allochems listed above. The

shale is dark orange-brown, wavy, irregular, and varies in thickness from 2 mm to 1 cm. They form both gradational and sharp boundaries with the wackestone layers. Pressure solution features such as truncation of fossils are associated with some of the shale laminae (Figure 19A). Compaction of the shale laminae is indicated by flattened oncolites contained within the clay layers, whereas surrounding wackestone beds contain circular oncolites (Figure 19B).

In situ Tetradium cellulosum colonies are located within the basal 2 meters of lithology W1. The colonies are dome-shaped (avg. dimensions are 25 cm × 15cm × 4cm) and are intercalated with oncolitic wackestone-packstone (Figure 19C). The individual vertical corallites in the Tetradium colonies are usually replaced by drusy calcite spar (Figure 19D) and only rarely exhibit internal septae. The interstitial sediment is micrite with occasionally intermixed sand-sized pellet and fossil debris. The latter is sometimes concentrated in patches. The lower 5 meters of lithology W1, which includes the oncolite marker bed (44%), contains approximately 15% Girvanella oncolites (Figure 17, p. 58, peak 3). According to the classification scheme of Logan et al. (1964), these are described as concentrically stacked spheroids. Other minor algal constituents are Solenopora type R (see Moore, 1978) and Kazahkstanelia. Poorly washed biosparite beds are more common in the lower 5 meter interval. In the upper 5 meters of lithology W1, algae are absent.

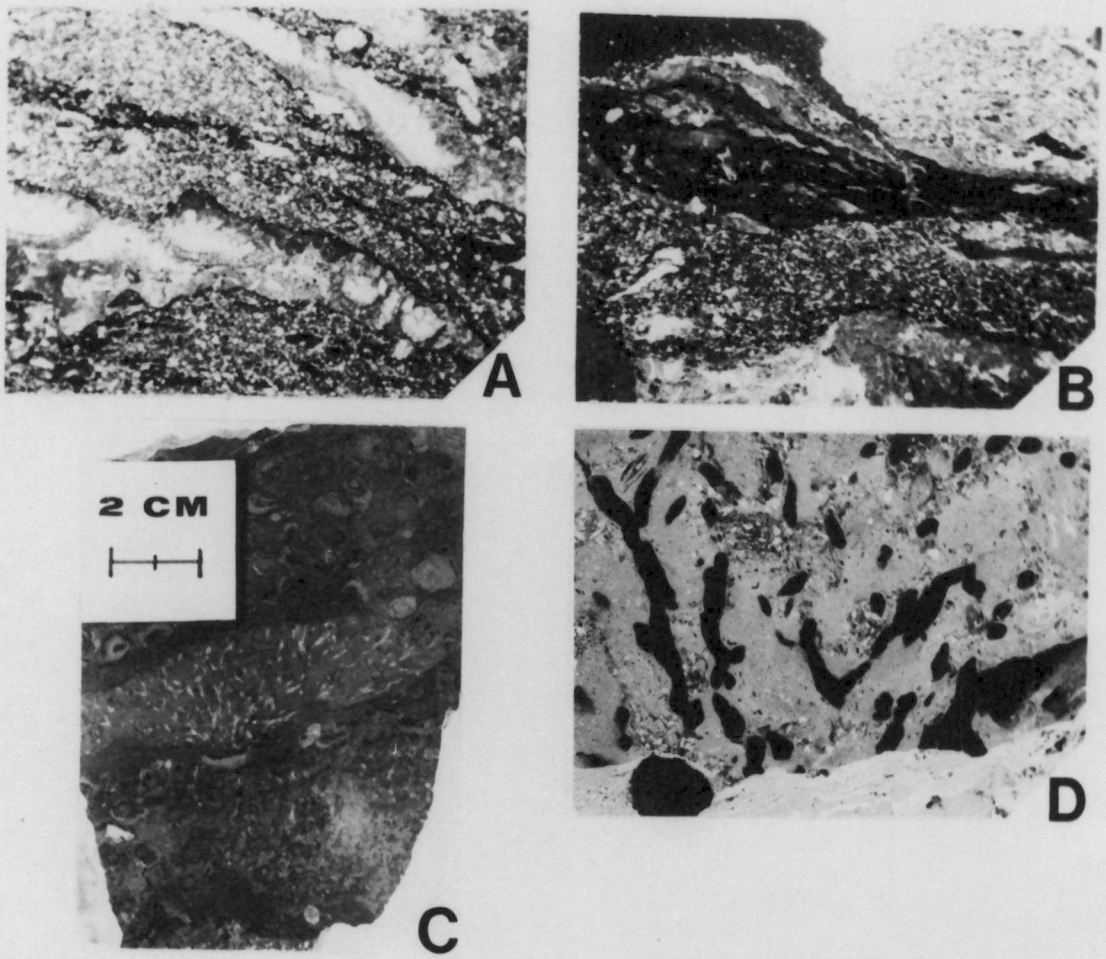


Figure 19. Photomicrographs and hand specimen of the lower Wardell Formation.

A. Photomicrograph (EF' 90) of an almost completely dissolved wackestone layer bounded by clay rich stylocumulate. 25X.

B. Photomicrograph (EF' 90) of a squashed oncolite contained within a clay layer. 25X.

C. Hand sample exhibiting close association of Girvanella oncolites to Tetradium colonies (EF' 90).

D. Negative print of a thin section (EF' 90) that illustrates spar filled (black) upright corallia of a Tetradium colony with interstitial micrite and clay. 3X.

Paleoenvironmental interpretation. Lithology W1 represents two distinct subtidal environments. Both are represented by diverse silt and sand-sized faunal fragments. The lower 5 meters of lithology W1 and of the Wardell Formation is characterized by large Girvanella oncolites and in situ Tetradium cellulosum colonies. Oncolites are indicative of a submerged area of shoaling water sufficiently turbulent to permit relatively constant motion of the spheroid (Logan, 1961). The small dome-shaped Tetradium colonies are sparsely distributed within a rock interval 2 meters thick that extends laterally for 275 meters. They were associated with conditions of agitated water (as implied by the associated oncolites); therefore, the corallia may have acted as a current baffle that trapped interstitial micrite and sandy allochems (see Walker, 1972). A modern example could be the current baffling and sediment-trapping abilities of the marine grass Thalassia Testudinum (Scoffin, 1970). Current activity may also be inferred from the presence of poorly washed bioparites (micrite partially removed by currents) in this lower 5 meter interval of lithology W1.

The upper 5 meters of lithology W1, which does not contain algae (Figure 15, p. 50), makes up the second environment. The disappearance of skeletonized algae was probably the result of shoaling waters, with harsher and more restricted environmental conditions. The fauna also disappears at the top of lithology W1 (Figure 9, p. 24). Current activity was probably less prevalent during deposition of the upper interval because current indicators (e.g., oncolites, Tetradium colonies and poorly washed biosparites) are no longer present.

The shale layers compose one third of the rock and are intercalated with wackestone as very irregular wavy layers. The shale layers have been compacted, which may have caused their irregular undulatory appearance. The euhedral dolomite rhombs are probably a secondary product resulting from pressure solution of the shale (see discussion of the clay laminae in the Hogskin Member). Truncated fossil fragments and partly dissolved wackestone layers (Figure 20A) are further testimony to the fact that pressure solution has operated within the shale layers.

Lithology W2

Thin section analysis. Lithology W2 succeeds W1 and is approximately 21 meters thick. It is characterized by 3 types of laminae, which in order of decreasing abundance are: (1) dolomitic calcareous shale laminae (0.08 mm to 3 mm thick); (2) lenticular pelsparite laminae (0.06 mm to 1.8 mm thick); and (3) dolomitic micrite laminae (0.2 mm to 1.5 mm thick). These layers are interlaminated with each other; however, no definite pattern is discernible. Fine irregular fenestrae (0.05 mm to 0.45 mm thick) and tubular fenestrae (0.4 mm wide) occur together and are minor constituents of lithology W2.

The dolomitic calcareous shale laminae and the dolomitic micrite laminae are wavy and continuous. They comprise 38% and 29% of the rock, respectively. Silt-sized euhedral dolomite rhombs make up 60% (by volume) of the calcareous shale laminae (Figure 20A) while clay (35%) and micrite (5%) compose the remainder. In the micrite laminae,

Figure 20. Photomicrographs of thin sections within the middle and upper Wardell Formation.

A. Photomicrograph of a dolomite rhomb-rich calcareous shale lamina bounded by pelsparite laminae, lithology W2, 100X (EF' 94).

B. Photomicrograph of horizontal burrows in a neomorphosed micrite lamina, lithology W2, 25X (EF' 97).

C. Negative print of an acetate peel showing a "bubble" (center of photo) in calcareous shale laminae exhibiting slightly thickened laminations (dark bands) at the arch of the bubble and slight thinning at the troughs, lithology W2, 3X (26-5).

D. Photomicrograph of lenticular pelsparite laminae interlaminated with calcareous shale, lithology W2, 25X (EF' 93).

E. Field photograph of mudcrack polygons in lithology W3 of the Wardell Formation (scale = 10 cm).

F. Photomicrograph of micrite intraclasts in bowed area, probably caused by desiccation. Dark bands are calcareous shale laminae. Light areas represent the spar filled fenestral fabric, lithology W3, 25X (EF' 95).

G. Negative print of a thin section showing laminoid fenestral fabric disrupted by deep vertical burrows. Fenestrae are black on this negative print, lithology W3, 3X (EF' 95).

H. Hand sample displaying abundant vertical burrows and laminoid fenestral fabric, lithology W3.

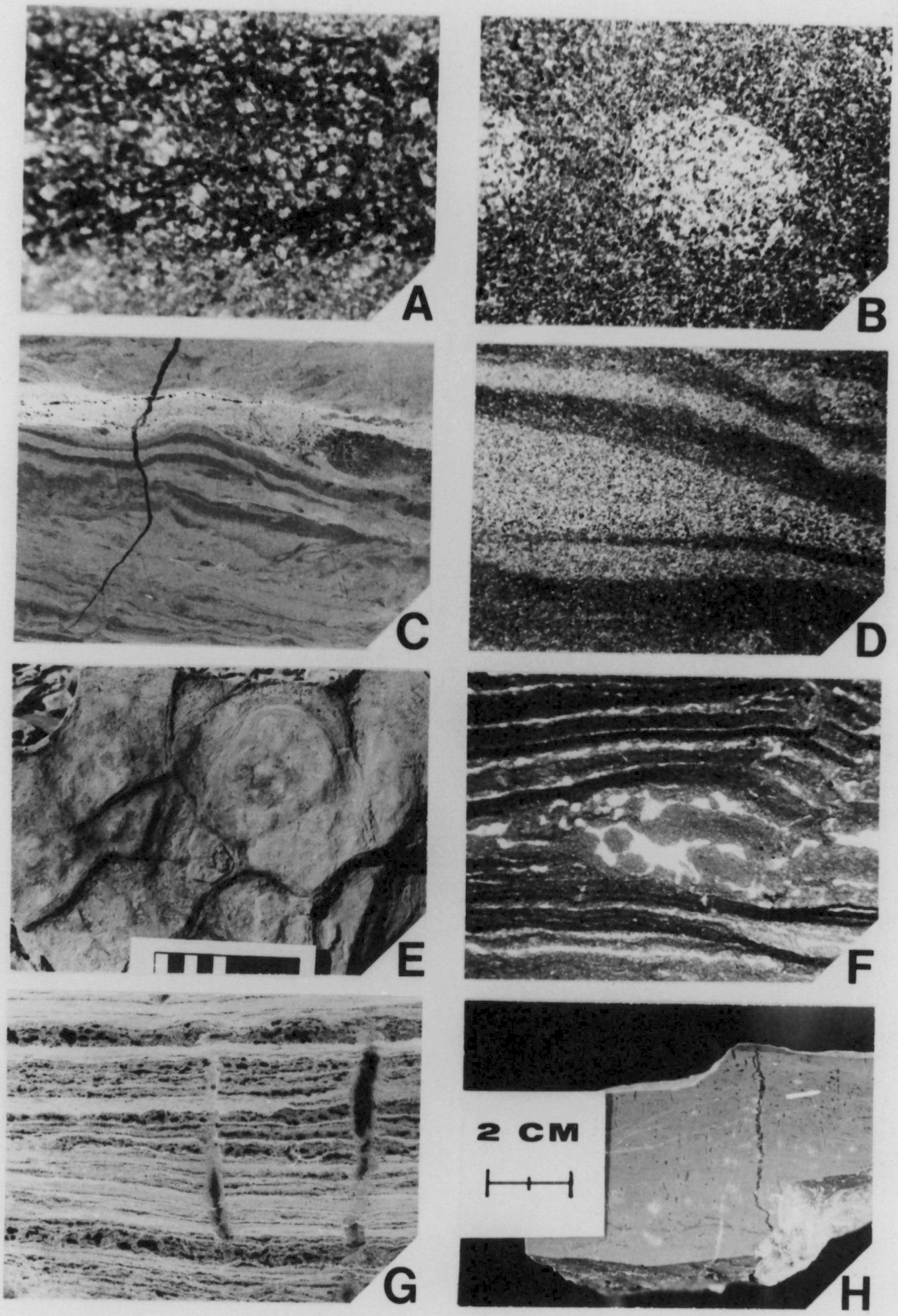


Figure 20

dolomite rhombs are much less abundant (about 5%) and are sometimes absent. Vertical burrows disrupt both types of laminae to depths of up to 8 mm. Horizontally oriented burrows are also present (Figure 20B) in approximately equal abundance. The micrite and calcareous shale laminae are sometimes bowed to form bubbles or domes (5 mm long). The laminations are thicker at the arch of the dome and thinner at the troughs (Figure 20C), which is not indicative of deposition by currents.

The lenticular pelsparite laminae (Figure 20D) make up 32% of the rock, are discontinuous, and appear to have filled irregularities in the surface of the underlying sediment. These laminae are composed of silt pellets (0.01 mm to 0.05 mm), quartz silt (2%), calcite spar cement and indistinct dolomite rhombs. Only occasionally can fossil skeletal debris be distinguished from the cement. Burrows disrupt the pelsparite laminae and are frequently filled by pelsparite. Horizontally oriented or inclined tabular micrite intraclasts are rare constituents within the pelsparite laminae.

One sample contains two layers of partially imbricated ostracod valves and trilobite debris in a micrite matrix separated by 2 cm of "normal" horizontal laminations. The shell debris is fragmented and sand-sized. This sample also contains scattered silt and sand-sized echinoderm debris (< 2%).

Paleoenvironmental interpretation. Lithology W2 has several features indicative of cryptalgal laminates (see Aitken, 1967): (1) bubbles on the scale of several millimeters in length; (2) occasional fenestral

structures; and (3) laminae not explainable by sediment settling (i.e., sediment thicker on highs). Cryptalgal laminations are the product of smooth, blue-green algal mats. Davies (1970b) has described primary structures formed in algal-laminated sediments in the Gladstone Embayment of Shark Bay, Australia, that possess characters similar to those above.

The shell layers observed in one sample are probably records of storm deposits. In the recent sediments of the Gladstone Embayment, Davies (1970b) noted similar intercalations of shelly layers between algal laminae.

The paucity of laminoid and irregular fenestrae in lithology W2 concomitant with the absence of other desiccation structures, suggests that the cryptalgal structures were formed in the outer (offshore) intertidal environment. Equivalent numbers of horizontal and vertical burrows indicates that the sediment was still manageable for some deposit feeding burrowers. Therefore, lithology W2 was probably deposited in the outer intertidal to shallow subtidal environment, where desiccation of algal mats is an unusual event. Similarly, lithology W2 may be interpreted to represent intertidal (algal) flats surrounding subtidal ponds as described on Andros Island, Bahamas, by Shinn et al. (1969).

The dolomite rhombs associated with the calcareous shale and micrite laminae are interpreted to be a secondary product. The dolomite probably formed by a process similar to that outlined by Gebelein and Hoffman (1973). They proved experimentally that blue-green algae

concentrate Mg in their sheaths and could produce sufficient Mg to form dolomite layers 1 mm thick. The calcareous shale and micrite laminae of lithology W2 are, therefore, interpreted as algally formed laminae, while the interlaminated pelsparite probably represents current-deposited particulate sediment. Abundance of the dolomite rhombs in the calcareous shale laminae versus the micrite laminae is not understood, but it may be related to the presence of clay.

Lithology W3

Thin section analysis. Lithology W3 is predominant in the upper 9 meters of the Wardell Formation, although lithology W2 is interbedded near its base. Lithology W3 is mudcracked, laminated dismicrite and pelletal micrite with very thin, alternating laminae of clay-rich micrite. Desiccation produced mudcracks in the form of large undisturbed polygons of micrite that are about 6 cm across (Figure 20E, p. 80). At the edges of the mudcracked polygons, roughly the upper 1 cm of sediment is upwarped. Fenestrae similar to Logan's (1970) fine laminoid type, range from 0.03 mm to 0.7 mm in thickness and occur in pelletal micrite and micrite layers (0.04 mm to 1.4 mm thick), which are separated by dark brown clay-rich micrite laminae (0.02 mm to 0.6 mm thick). In general, the micrite and pelletal micrite laminae are broken into flat and bowed chips (0.2 mm to 5 mm long) that still lie parallel to the depositional surface. Vertical and horizontal cracks formed between the micrite and pelletal micrite chips are filled with spar cement (Figure 20G, p. 80) and, thus, form the laminoid fenestral fabric.

Occasionally, the micrite chips are warped upward to form pods or bubbles (1 mm to 2 mm long, Figure 20F, p. 80). The micrite and clay-rich micrite laminae tend to be slightly thicker on the arches of the pods. The alternating clay-rich micrite laminae are continuous, and smooth to slightly crenulate in appearance.

Tubular fenestrae (Figure 20H, p. 80) occurring in lithology W3 display several features indicative of vertically burrowing fauna, these are: (1) alignment normal to the laminae; (2) disruption of laminae; (3) vertical penetration of 1 cm to 3 cm; (4) diameter of 0.4 mm; and (5) infilling of micrite, silt pellets and spar cement.

Paleoenvironmental interpretation. The laminations described above are inferred to be cryptalgal laminites because they exhibit the following features (see Aitken, 1967): (1) pods or bubbles (1 mm to 2 mm); (2) desiccation cracks; (3) fenestral fabric; (4) micrite laminae broken into small chips; and (5) sediment laminae not explainable by current deposition (micrite thicker on highs). These cryptalgal structures are smooth and do not display large structural modifications. Analogous algal-laminated sediments have been observed by Davies (1970b) and Logan et al. (1974) in the recent sediments of Shark Bay, Australia. These recent algal-laminated sediments were formed by smooth algal mats located in a protected (i.e., an embayment) intertidal environment (Davies, 1970b). Logan et al. (1974) observed that fine laminoid fenestral fabric (analogous to the fenestrae of lithology W3) are also formed by smooth algal mats

and occur mainly in the middle to upper intertidal zones. In addition, lithology W3 contains vertically oriented burrows, which are more common in intertidal environments (see Rhoads, 1967). These observations and the presence of large, well developed mudcracks implies that lithology W3 was probably deposited in a high intertidal to supratidal environment.

IX. SUMMARY

The Evans Ferry section from the post-Knox unconformity to the Wardell Formation represents a transgressive sequence followed by a regressive sequence. The basal Tumbez Formation and the lower Eidson Member were deposited in a low intertidal environment. The upper Eidson Member, the Hogskin Member, and the Rockdell and Benbolt formations were deposited in subtidal environments with varying depths, water turbulence and sediment supply. A return to intertidal conditions is represented by the Wardell Formation. Desiccation features occurring at the top of the Wardell Formation (i.e., the top of the Evans Ferry section) suggest a high intertidal to supratidal environment of deposition.

CHAPTER III

PALEOECOLOGY OF INTERVAL A (PORTERFIELDIAN AGE) AND INTERVAL B (WILDERNESSIAN AGE)

I. INTRODUCTION

Chapter III presents the data and inferences drawn from an analysis of the biotic content of 2 selected fossiliferous intervals within the Evans Ferry section. Interval A (Figure 1, p. 3) comprises the basal 21 meters of the Benbolt Formation (171.3 m to 192.3 m from the base of the section). Based on the ratio of packstone to shale in this interval, three distinct changes in lithology can be observed. Interval B (Figure 1, p. 3) comprises the upper 6 meters of the Benbolt Formation and all of the Wardell Formation (282.9 m to 330.1 m above the base of the section).

On the average, fossiliferous slabs and individual specimens for intervals A and B were collected at spacings no greater than 0.35 meters. The lower 9 meters of interval A yielded numerous individual fossils and weathered slabs, which facilitated taxonomic identification. Partially weathered fossiliferous slabs and a few individual fossils were all that could be obtained from the remaining 12 meters of interval A. The main differences between these contrasting outcrops are the degree of weathering and the rock type, with weathering believed to be the most influential factor. The lower 9 meters of interval A has been subjected to intense weathering compared with the fresher,

vertical exposure of the upper 12 meters. Interval B yielded an abundance of weathered fossiliferous slabs, but only rarely were individual fossils collectable.

Following collection and identification, the fossil material was grouped into 1.5 meter intervals for the purposes of synthesis and illustration. Lists of genera and species for each of the sample intervals are presented in Appendix C. The sample intervals are labeled by a field unit number and alphabetically-ordered letters designating upwardly successive collection intervals. Most of the biota were identified from the surface of fossiliferous slabs or as individual specimens except for bryozoans and algae, which were identified from thin sections and acetate peels.

Fossil identifications were conducted at various taxonomic levels depending upon the accessibility of information in the literature, the availability of assistance from an expert on a particular taxon and the preservation of the specimen. General references used in the systematic treatment of taxa are the Treatise on Invertebrate Paleontology (parts G, H, and O). Trilobites, pelmatozoan echinoderms and algae were identified to the generic and specific levels. Brachiopods and algae were identified by the author using Cooper (1956) and Moore (1978), respectively, as sources. Confirmation of some brachiopod taxa was provided by R. E. McLaughlin. Trilobites were identified through a collaborative effort between the author and M. R. Maitland (using Cooper, 1953 and Butts, 1940 as sources). Pelmatozoan echinoderms were identified with the aid of T. W. Broadhead

using Brower and Venus (1974), Parsley and Mintz (1975), Bassler (1950), and Paul (1972) as sources.

Bryozoan identifications were accomplished with the help of F. K. McKinney, and from the literature (Ferrigno, 1973; Karklins, 1969). These identifications were limited to familial and generic levels because of the time-consuming quantitative data necessary for species determinations. Those bryozoans listed in the table by family generally include only a single genus and are distinct from the other taxa listed at the generic level. Gastropods and cephalopods were differentiated as A, B, C, . . . etc. and are described in Tables B-1 and B-2, Appendix B. This procedure was necessary because of the poor quality of the specimens and the lack of sufficient information in the literature concerning these two faunal groups. Each taxon (e.g., gastropod A) probably represents a single species of one genus. Pelecypods and ostracods were only visible in thin section and, consequently, are treated in broad terms at the class level only.

This study did not determine quantitative abundance or biovolume percentages for each of the species identified because of the great amount of time involved in such a procedure. However, a gross ranking of taxa was attempted from visual estimation of fossiliferous slabs, thin sections, acetate peels and the rock outcrop. Consequently, many of the species may be ranked in one of the following three categories, listed in order of decreasing abundance: (1) dominant (D), (2) common (C) and (3) rare (R). A dominant species is numerically or volumetrically (visually estimated) the most abundant biotic element

in the unit of interest. Common species occur frequently in several, but not all, fossiliferous slabs, thin sections, or acetate peels from the unit of interest. Rare species are those represented by a few (1-5) indigenous individuals contained in several slabs, but collectively compose a minor proportion of the biovolume in the unit of interest.

The biotas of interval A exhibit very gradual vertical changes in taxonomic composition. No short term successional sequences were observed (such as those described by Walker and Alberstadt, 1975). However, at this fossil locality three distinct lithologic changes are shown. The first 9 meters are composed of 4 cm thick, cobbly beds of packstone regularly interbedded with 2 cm beds of shale. The following 4.5 meters exhibits a two-fold increase of shale in 4 cm thick interbeds and an equal reduction of packstone beds (2 cm thick). The final 7.5 meters is composed of 10 cm thick wavy beds of packstone with 2 cm thick shale intercalations. Thus the limestone to shale ratio changes from 2:1 in the lower part to 1:2 in the middle and 5:1 in the upper part of interval A.

The fossil species grouped according to the sample intervals are included in Tables C-1 to C-32, Appendix C. The fossil assemblages contained in the sample intervals are discussed in relation to the specific lithologic zone (noted above) in which each occurs. It can be seen that the diversity exhibited by the biotas of interval A is very high as is characteristic of low stress or stable environments (Sanders, 1968) and significantly greater than that shown by the biotas of interval B. The indication of low environmental stress coupled with

the absence of sedimentary structures, which indicate shallow, turbulent conditions, suggest deposition of interval A in a level bottom, offshore subtidal environment. In addition, the gradual increase in the abundance of Girvanella oncolites, an indicator of shoal water (Benedict and Walker, 1978), suggests gradually shallowing water during interval A deposition. In summary, interval A is interpreted as representing a gently shallowing, stable, subtidal environment. Additional evidence of the depositional environments represented in this interval was presented in Chapter II.

Interval B contains a biota displaying a constant change in composition in response to rapidly shoaling waters as evidenced by a regular decrease in species diversity (see Sanders, 1968) and the appearance of desiccation features (e.g., mudcracks) toward the top of this interval. The distribution of brachiopods reflects this change most dramatically and, consequently, prominent members of this group have been used to subdivide the fossil assemblages into paleocommunities. Five communities were recognized: (1) Hesperorthis community; (2) Strophomena-Hesperorthis community; (3) a brachiopod-free, Tetradium-Girvanella oncolite community; (4) Chaulistomella-Strophomena community; and (5) Strophomena-Rostricellula community. These paleocommunities exhibit a regular decrease in species diversity upward through interval B and are succeeded by cryptalgal laminites and mudcracks. Interval B is interpreted as representing an environmental spectrum from the shallow, but nearshore, subtidal environment to the high intertidal-supratidal environment. Chapter II contains detailed

evidence of the depositional environments represented by this interval. Further analyses of the biotas and corresponding lithologic zones in the 2 fossil intervals are given.

II. INTERVAL A

General Description

Interval A comprises a sequence of 21.0 meters of rock at the base of the Benbolt Formation (171.3 meters to 192.3 meters above the base of the section). This interval is divisible into three lithologic zones (Figure 21A) according to the packstone to shale ratio (pk:sh) in each. Listed in ascending order, these are: (I) 9 meter zone with a 2:1 ratio; (II) 4.5 meter zone with a 1:2 ratio; and (III) 7.5 meter zone with a variable ratio. Fossil assemblages within these zones exhibit high species diversity, but short-term successional events (see Walker and Alberstadt, 1975), or recurring taxonomic assemblages are not apparent. The biota did show some compositional changes from one lithologic zone to another; however, changes in fossil composition within each zone were broad and gradual. Consequently, interval A could not be subdivided into paleocommunities.

Trophic group and substrate niche ternary diagrams (similar to those described by Scott, 1976 and 1978) were constructed in order to compare the structure of the associated fossil assemblages. Each 1.5 meter sample interval in interval A is plotted as a point on these ternary diagrams. As will be shown, lithologic zone II contains fossil assemblages with ecological structures distinct from the other two zones.

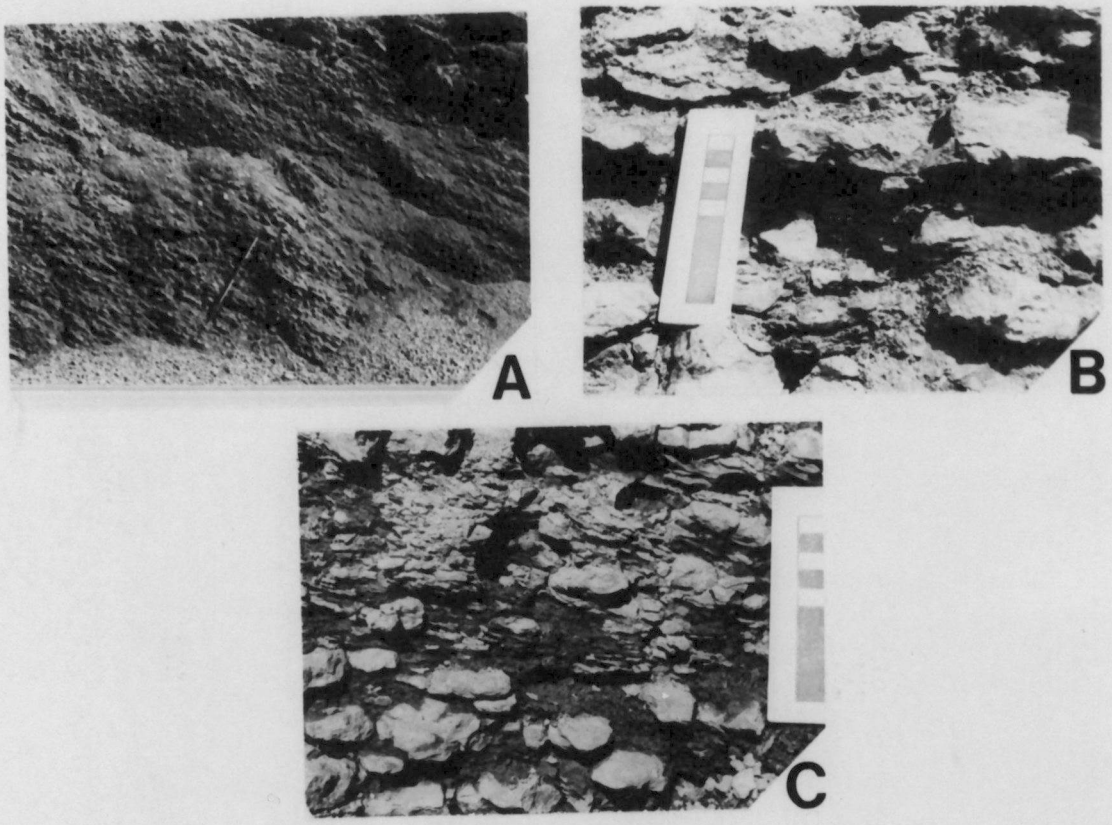


Figure 21. Field photographs of interval A in the Benbolt Formation.

A. Photograph displaying the three lithologic zones of interval A in the Benbolt Formation (staff = two meters).

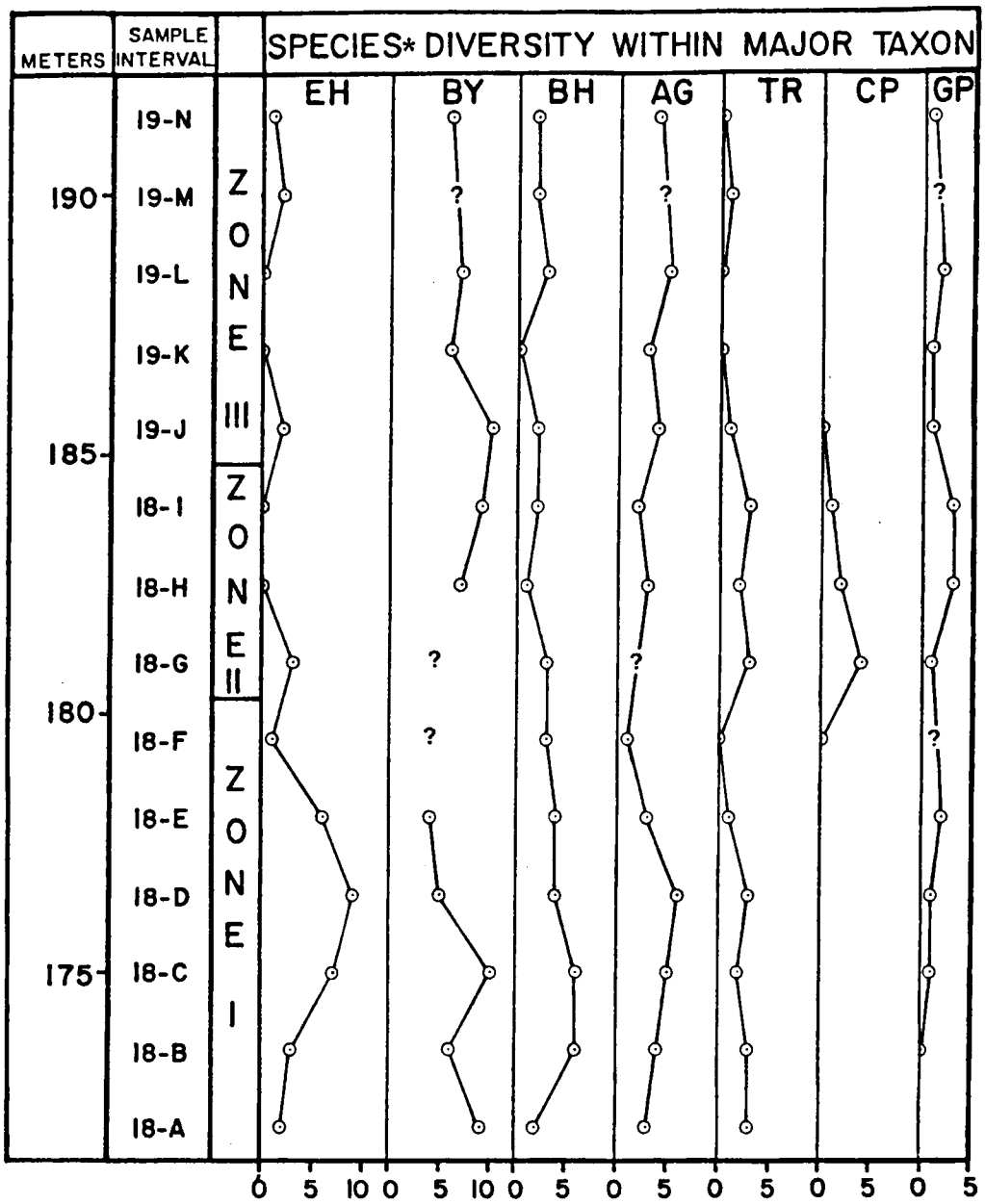
B. Photograph of wavy packstone beds separated by shale (zone I). Pk:Sh=2.1 (scale = 10 centimeters).

C. Photograph of packstone cobbles and interbedded shale (zone II). Pk:Sh = 1:2 (scale = 10 centimeters).

Characteristics of each of the three lithologic zones in interval A, providing evidence on which environmental conclusions have been based, are described in detail below.

Lithologic Zone I

General description. Lithologic zone I is 9 meters thick (171.3 m to 180.3 m above the base of the section) and is characterized by nodular and wavy packstone beds separated by shale (Figure 21B). The packstones contain taxonomically diverse fossil assemblages (Figure 22), while the shale contains few if any fossils. The fossil assemblages appear to represent very gradual changes in environmental conditions because no sharp breaks in fossil distribution can be observed. The species diversity for fossil assemblages in this zone is the highest for any interval covered in this study. A basic concern is the distinction of true species diversity versus artificial species diversity derived from transported faunal and floral elements. The abundance of micrite matrix suggests a quiet-water environment with a largely indigenous biota. In addition, the biota of zone I, although not in growth position, do not exhibit transportational effects. Remains were probably disturbed by vagile fauna in search of food (see Ginsburg, 1957) or by weak or periodic currents. The following is a list of evidence, based on criteria established by Johnson (1960), in support of this assumption: (1) articulation of many of the brachiopod valves; (2) presence of widely variable brachiopod shell



*Many taxa are identified to the generic level, but are believed to be represented by a single species.

Figure 22. Stratigraphic distribution of species diversity within each major taxon for interval A, Evans Ferry, Tennessee.

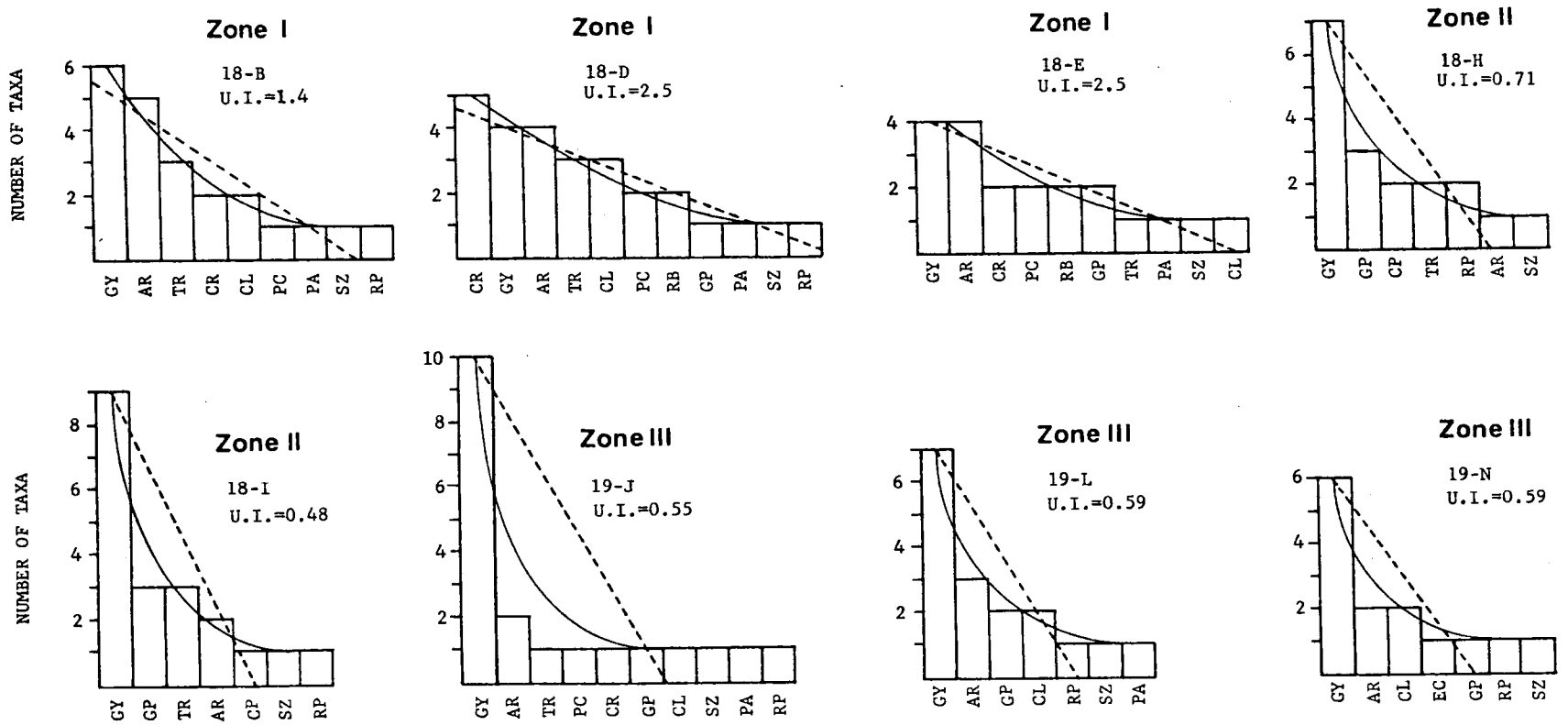
sizes (no selective sorting); (3) preservation of detailed ornamentation on most fossil exteriors; (4) preservation of several adjoining pelmatozoan echinoderm plates and long columnal segments; (5) preservation of pelmatozoan holdfasts in "rooted" position; and (6) variable orientation of shells in relation to the bedding plane (not all parallel to bedding). Since these fossil assemblages do not exhibit signs of transportation and there are no sharp breaks or changes in fossil composition, they probably represent contiguous and intergrading benthic communities. The intergradational character of the fossil assemblages of lithologic zone I suggests that environmental conditions were also gradational (see Johnson, 1973).

Species diversity. The high species diversity of the biota contained in zone I is the most outstanding and diagnostic feature of interval A. Sanders (1968) discussed the concept that species diversity is higher in stable and more predictable environments. Other authors have noted the same pattern and state further that offshore regions are most likely to contain high species diversities because physical conditions are more constant and uniform (Margalef, 1968; Bretsky and Lorenz, 1969; Johnson, 1973). Therefore, the fossil assemblages of lithologic zone I are interpreted as representing communities of a stable offshore subtidal environment.

One peculiar feature of the zone is the occurrence of shale intercalations that seemingly had no effect on the high diversities

attained by the marine benthic communities. Predictability is the key to understanding this phenomenon. Sanders (1969) and Bretsky and Lorenz (1969) discussed the possibility that predictable oscillations of low magnitude and long duration would still enable communities to reach high diversities. This concept is similar to Odum's (1971) pulse stability, which maintains an ecosystem at an intermediate stage of development. The sedimentologic record for zone I displays regular spacing and thickness of shale, which suggests predictable low scale disturbances in the environment of deposition, assuming that the depositional rate was constant. Consequently, the intergrading benthic communities of lithologic zone I were adapted to the regular fluctuations of sediment (shale) and may have benefited (in species diversity) from the additional heterogeneity of the sediment and periodic water turbulence.

Uniformity index. A technique was devised to analyze the species diversity patterns that occur in the fossil assemblages for intervals A and B. This illustrative technique is independent of numbers of individuals within each species. It has been suggested by Scott (1976) that the total number of species is probably better preserved than the relative or absolute abundances of individuals. A series of histograms were constructed so that the most species-diverse taxonomic class (e.g., Gymnolaemata) is on the left and the least species diverse class is on the right for any given sample interval (Figure 23). Therefore, a



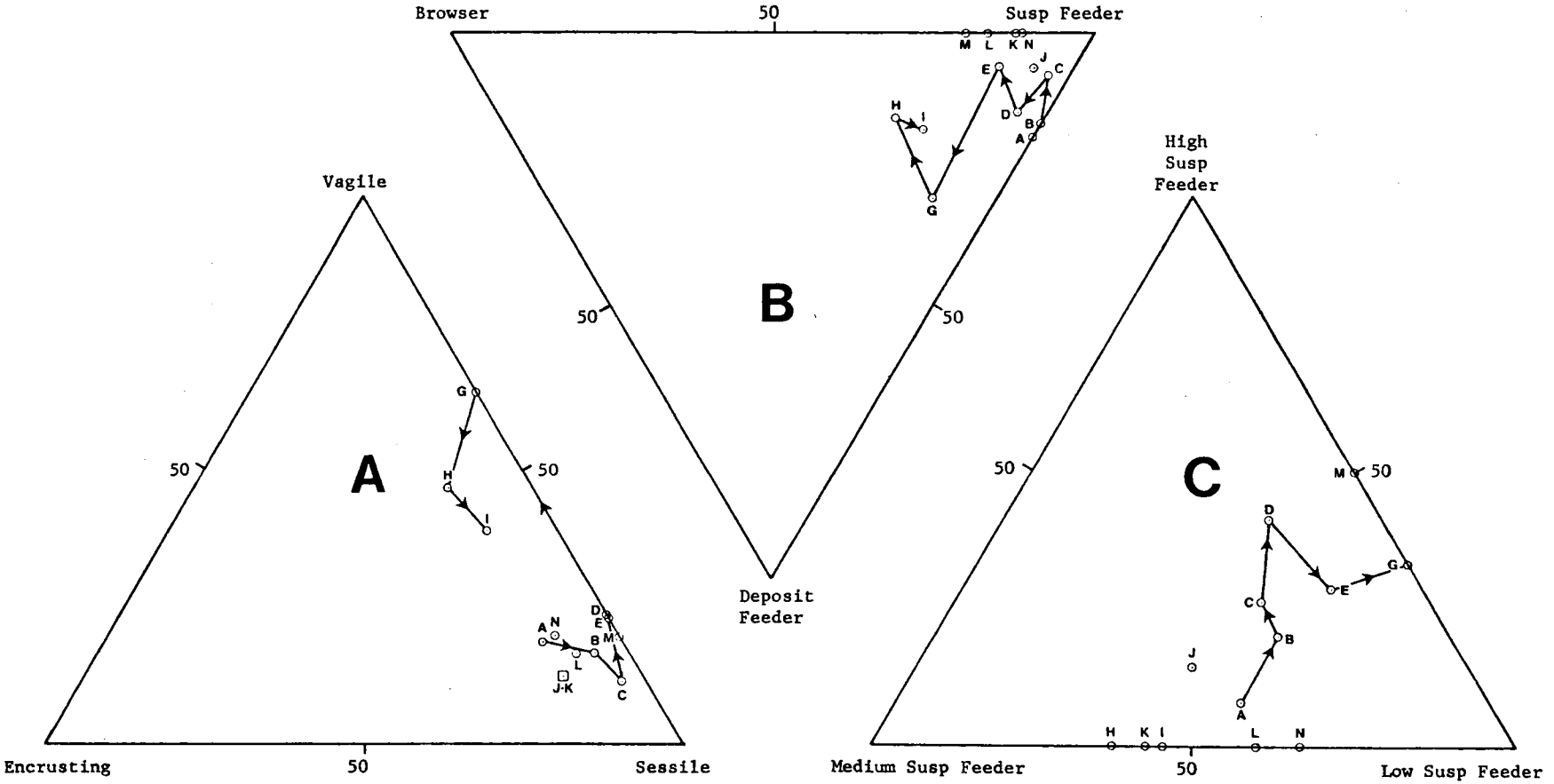
AR=Articulata, CP=Cephalopoda, CL=Chlorophyceae, CR=Crinoidea, EC=Eocrinoidea, GP=Gastropoda, GY=Gymnolaemata, PC=Paracrinoidea, PA=Problematical algae, RP=Rhodophyceae, RB=Rhombifera, SZ=Schizophyceae, TR=Trilobita.

Figure 23. Series of histograms illustrating species diversity within classes for selected sample intervals within interval A. The superimposed curves represent the uniformity index (U.I.) of which the numerical value was obtained from the slope of the dashed line (representing the average slope of the curve). Each histogram is constructed so that the most diverse class is listed on the left and the least diverse on the right.

curve drawn through the midpoints of the bars on each histogram in Figure 23 will produce a series of curves of varying steepness and shape depending on species variety within each class. For example, curves with steep slopes illustrate large disparities between numbers of species within classes. Stated differently, the slope of the curve reflects the apportionment of species among each class for a given sample interval. A "best fit" straight line was superimposed on the curves such that as many midpoints plot above the line than as below it, in order to calculate an absolute value based on the slope. The reciprocal of the slope value will be referred to as the uniformity index by the author and will be used throughout this chapter. Less accurate absolute indices are expected for those curves that strongly deviate from a straight line. In summary, a high uniformity index indicates a curve with a gentle slope, representing monotonically decreasing numbers of species for each adjacent fossil class. The fossil assemblages present within lithologic zone I with a uniformity index ranging from 1.4 to 2.5 (very low slopes; see Figure 23, parts 18-B, 18-D and 18-E) provide an example of high uniformity indices. The species diversity in any one class does not dominate over the diversity in the adjacent fossil classes in the example given above. Whether this is a definite characteristic of stable subtidal environments comparable to the lack of dominant numbers of individuals within any one species, as noted by others, remains to be proved by much further investigation. The uniformity indices of other zones are discussed below.

Analysis of autecologic parameters. Several autecologic parameters for individual species that occur within the fossil assemblages of intervals A and B are listed in Table B-3, Appendix B. The parameters for each species were inferred either from a presumed relationship to extant species in the same or related higher taxon or on the basis of close morphological similarity. These autecologic parameters were used in a trophic and substrate niche analysis (refer to Scott, 1976; 1978) in order to determine if the fossil assemblages contained in the sample intervals display any significant structure or zonation. Figure 24, parts A and B, illustrate that the fossil assemblages within lithologic zone I (A, B, C, D and E) are dominantly attached epifaunal suspension feeders with minor percentages of vagile deposit feeders and browsers. Sample interval F is omitted from the plots because few samples were available for this interval. However, the available fossiliferous slabs from that interval contain faunal elements, which are similar to those in sample interval E, suggesting a similar depositional environment. The only noticeable change between sample intervals is a short-lived increase in high level suspension feeders upward in the section (arrows on Figure 24, part C). Consequently, the trophic group and substrate niche diagrams exhibit subtly different suspension feeding fossil assemblages, which probably represent gently intergrading level-bottom marine communities.

The predominance of epifaunal suspension feeders suggests good water circulation, substratum stability, and food resources favorable for their growth. Agitated water is inferred from the diversity of



Susp= Suspension.

Figure 24. Classification of trophic categories (A and C) and mobility relationships (B) for species occurring in interval A. The letters represent 1.5 meter sample intervals listed in Table B-2, Appendix B. A trend between several vertically successive sample intervals is illustrated by arrows.

suspension feeder species, which require renewal of suspended nutrients and removal of waste products. The presence of several Girvanella oncolites further suggests some water movement (see Logan et al., 1964). Water circulation was probably periodic as evidenced by the cyclic deposition of packstones and shales. Deposition of the mud probably disturbed the level bottom communities locally. Subsequent spat falls from members of the surrounding communities could then repopulate the disturbed area from all sides.

The substrate was composed of soft carbonate mud as illustrated by the pelmatozoan echinoderm holdfast structures "rooted" in the sediment. A few horizontal burrows present exhibit a vague concentric arrangement of shells around the burrow, indicating that the sediment was somewhat plastic rather than "soupy." Bryozoans and brachiopods were probably attached to fallen remains of hard-shelled fauna; however, no in situ preservation was observed.

Stenohaline fauna predominated in lithologic zone I (Figure 25, A, B, C, D and E) suggesting "normal" marine salinities. This is inferred from the fact that the closest living relatives of these suspension feeders are found in normal marine environments today.

Lithologic Zone II

General description. Lithologic zone II is a 4.5 meter (180.3 m to 184.8 m above the base of the section) fossiliferous rock sequence containing nodular packstones alternating with shale. The packstone/shale

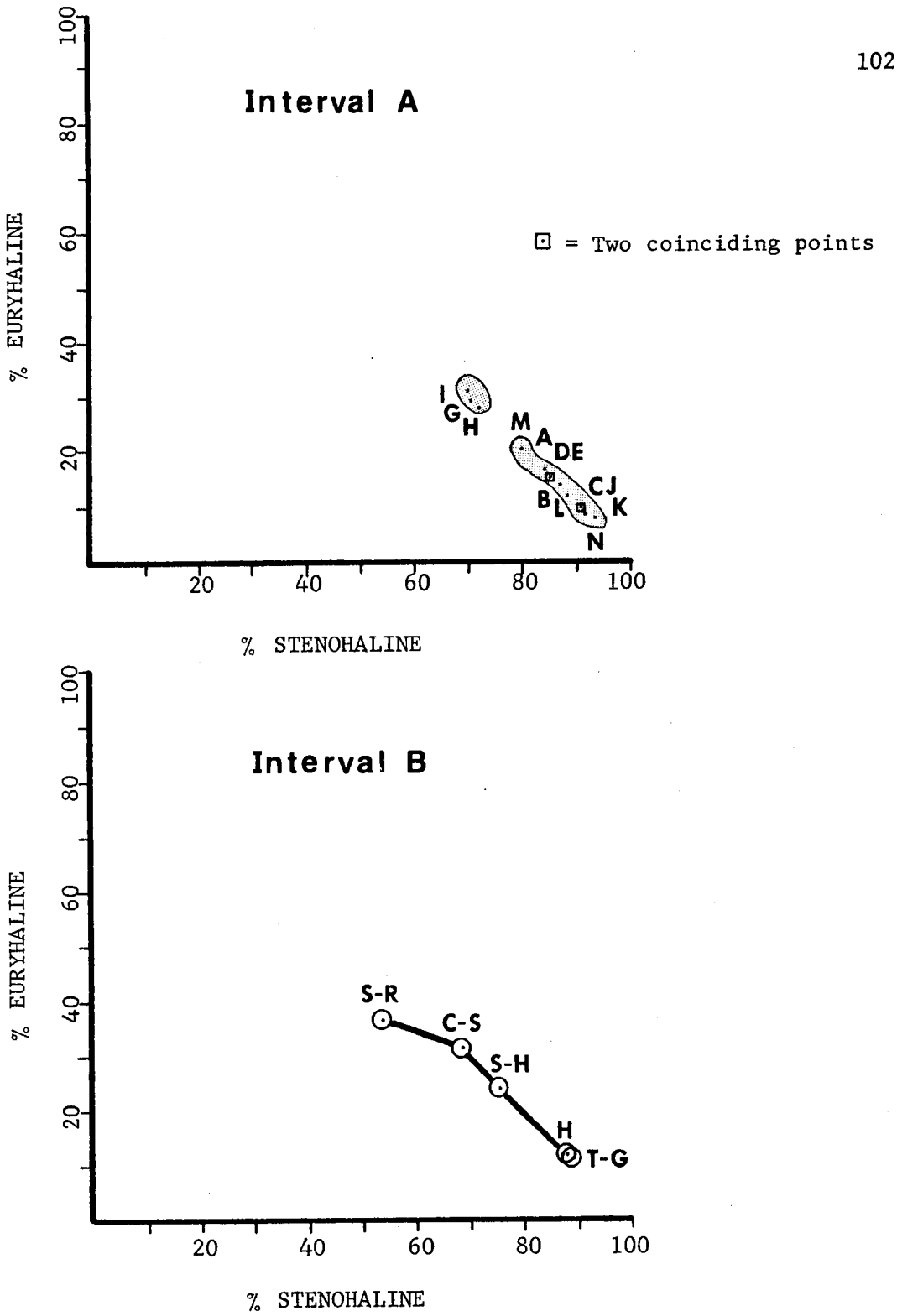


Figure 25. Percent euryhaline species versus percent stenohaline species for the biota of intervals A and B. The letters for interval A represent sample intervals and those for interval B represent paleocommunities.

ratio is approximately 1:2 (Figure 21C, p. 92). The outcrop used for collecting zone II is a vertical face, which is not weathered to a high degree as compared to the sloping outcrop used for zone I. Therefore, preservational bias or differences caused by the degree of exposure might be expected to influence the comparative composition of the fossil assemblages in the two lithologic zones, creating possible sources of error. In addition, the bryozoan and algal species for sample interval G could not be determined because thin sections were not available; however, complete information was obtained for sample intervals H and I of zone II. Fossils collected in these sample intervals displayed very few signs of wear and are interpreted to represent a model II type assemblage (Johnson, 1960). These are the only sample intervals in which cephalopods are preserved intact. Species diversity for fossil assemblages contained in lithologic zone II is much lower than for zone I (Figure 22, p. 94), suggesting less stability or predictability in the environment of deposition. Perhaps the instability was related to the more frequent influx of mud as indicated by the lower packstone/shale ratio in this zone.

Species diversity and the uniformity index. Although low species diversities are recorded for fossil assemblages in lithologic zone II, they are not as low as those displayed by fossil assemblages in interval B. A more unpredictable nearshore environment of deposition for interval B has been deduced from lithologic evidence. The reduction in species diversity from lithologic zone I to zone II

was probably caused by increased environmental perturbations. The influx of lime mud and clay appears to be the major environmental disturbance and is recorded in the rock record by beds of limy shale that are twice the thickness of the packstone nodules. Even though these shale beds represent regular (even spaced) and probably predictable sedimentation in the environment of deposition, their magnitude (thickness) was too great for the establishment of high species diversity. However, since the environmental disturbances were regular, benthic communities were able to attain intermediate species diversity (see Odum, 1971, p. 268) as compared to the very low diversity in the unpredictable nearshore environment of interval B.

The uniformity indices for the fossil assemblages of lithologic zone II are low (Figure 23, p. 97, 18-H and 18-I). The curves are very steep for sample intervals 18-H and 18-I because the species diversity of the bryozoan class, Gymnolaemata, is much higher than for the next most diverse class. Figure 24, p. 100, illustrates the reduction and disappearance of attached suspension-feeding species concomitant with an increase in vagile, deposit-feeding, browsing, and predatory species in the fossil assemblages of lithologic zone II. Increased deposition of fine sediment (as shown by the thicker shale beds in zone II) subjected suspension feeders to longer periods of muddy water. Consequently, fewer species were able to withstand the rigors of the environment. Reduction of algal species may have been related to the same disturbance. Longer periods of turbid water would reduce the amount of light reaching the benthic algae. Thus, fewer species of algae could tolerate such conditions.

Analysis of autecologic parameters. Ternary diagrams of trophic groups and substrate niches (see Scott, 1976) for the fossil assemblages of interval A (Figure 24, p. 100) display a distinct zonation of the sample intervals contained in lithologic zone II (G, H and I). Those sample intervals contain fossil assemblages dominated by vagile deposit feeders and browsers and include, also, predator cephalopods not plotted on the ternary diagram. These sample intervals compose a field on the ternary diagrams distinctly separate from the sample intervals of both zone I and zone III. The position of this field is taken as a reflection of the increased influx of fine sediment during the deposition of lithologic zone II. An increase of deposit feeders and a decline of suspension feeders is expected in fine-grained substrates. The percentage of organic detritus should increase with decreasing grain size because of its low specific gravity. Consequently, the food resource is usually greater for deposit feeders in fine grained sediments. The converse is true for suspension feeders (see Walker, 1974). Suspension feeders would be affected adversely during periods of muddy water and lower food resources.

In a plot of stenohaline species versus euryhaline species (Figure 25, p. 102), the sample intervals of lithologic zone II comprise a separate field characterized by fossil assemblages with slightly greater salinity tolerances than for the fossil species of the other two zones.

Lithologic Zone III

General description. Lithologic zone III consists of 7.5 meters (184.8 m to 192.3 m above the base of the section) of alternating packstone and shale of variable thicknesses. The zone begins with a packstone/shale ratio of 5:1 and gradually changes to a 2:1 ratio toward the final 2 meters. The thick-bedded (5-15 cm) packstones yielded very few individual fossils. Most of the fossil species were identified from the surfaces of slabs and from thin sections. Few trilobite and pelmatozoan echinoderm body fossils were found, yet point count data indicate that both are present in percentages equal to or greater than in the previous two lithologic zones. Consequently, in less exposed and weathered lithologic zone III sample collecting bias may be large. Species of bryozoans, algae and gastropods were identified from thin sections, so that for these species there is less bias introduced as a result of the degree of weathering (thin section not available for sample interval M). The few collectable fossils exhibit few signs of abrasion or fragmentation. They are probably representative of a model II assemblage (Johnson, 1960). Girvanella forms oncolites and thin algal coatings around many of the fossils in lithologic zone III (about 9 volume percent Girvanella). Oncolites suggest shoal water (Benedict and Walker, 1978).

Species diversity and the uniformity index. Species diversity of the class Gymnolaemata (bryozoans) decreases upward in the section (Figure 23, p. 97; 19-J, 19-L, and 19-N) likely in response to an increase in the amount of sediment comprising the interbedded shale. Bryozoan diversity is greatest for 10 cm packstone beds separated by 2 cm of shale and least in 4 cm packstone beds separated by 2 cm of shale. Thus, as the frequency of shale intercalations increases, the bryozoan diversity decreases. Deposition of fine sediment (clay) creates turbid water conditions, probably inhibiting the food gathering ability of these suspension feeders. The uniformity index is correspondingly low (steep slope) for the fossil assemblages in the same intervals of lithologic zone III. The marked disparity in species diversity between the two most diverse classes may be largely due to the limited number of collectable specimens of the second most diverse group (articulate brachiopods). Most of the species in the last three histograms (Figure 23, p. 97) have been identified from thin sections.

Analysis of autecologic parameters. The graphs representing trophic groups and substate niches display the dominance of attached medium to low level suspension feeders in lithologic zone III (Figure 24, p. 100, J, K, L, M and N). It is possible that these plots may reflect bias introduced by thin section identifications of the bryozoans, algae and gastropods versus those taxa identified on slabs and as individual specimens. A similar possibility exists

for the graph of salinity tolerance (Figure 25, p. 102), which shows the predominance of stenohaline species.

Discussion of Interval A

In summary, interval A represents a stable, offshore, level bottom, subtidal environment as evidenced by: (1) high species diversity within many fossil classes (Figure 22, p. 94); and (2) a lack of any intertidally-formed structures such as mudcracks, abundant intraclasts, cryptalgal laminites or vertical burrows. Species diversity is greatest for zone I, low for zone II and moderately low for zone III (Figure 26). Increased periods of turbid water probably caused species reduction in zone II (Figure 26), while species reduction in zone III (Figure 26) may be a reflection of preservational bias (less exposure to weathering may have affected collectable fossils). Zone I represents stable subtidal conditions with very gentle environmental gradients, inferred from the subtly different, species-diverse, and intergrading fossil assemblages.

Girvanella is present in all three lithologic zones of interval A as algal coatings, hemispherically stacked oncolites, and concentric oncolites (see Logan et al., 1964 for descriptive terms). The volume percent and the size (2 mm to 4 mm) of the oncolites increases upward in the section (zone I to zone III, Figure 17, p. 58). In lithologic zone III, the Girvanella oncolites are largest and most abundant, composing about 12 volume percent of the rock. Modern oncolites occur in agitated shoal water (Ginsburg, 1960 and Logan et al., 1964)

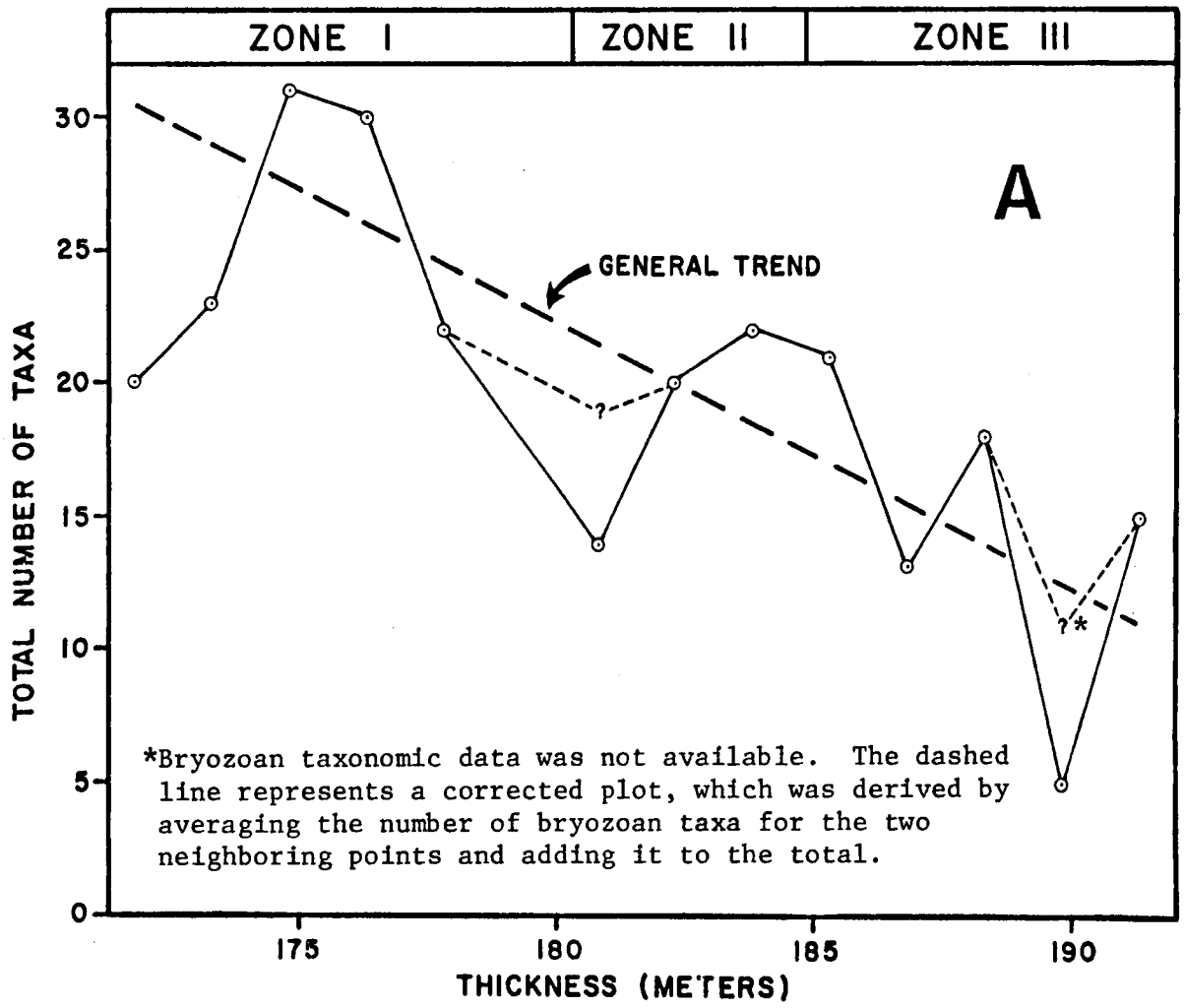


Figure 26. Total species diversity for interval A toward the top of the Evans Ferry section. Using Walther's Law, this vertical rock sequence is interpreted to represent horizontally continuous environments. Interval A represents a slight shoaling event (left to right) in the offshore subtidal environment.

and Girvanella oncolites have been used as a shoal water indicator (Benedict and Walker, 1978).

In summary, interval A from bottom to top represents a gently shallowing, offshore, stable, subtidal environment with widespread and intergradational communities lacking sharp boundaries.

III. INTERVAL B

General Description

Interval B comprises a sequence of 47.2 meters of rock of which the lower 26.4 meters is fossiliferous, while the remainder is composed of an interbedded sequence of alternating (sometimes dolomitic) mudstone laminae and calcareous shale laminae. Mudcracks in the calcareous shale and mudstone laminae occur more frequently toward the top of interval B (i.e., the top of the Wardell Formation). The lower 26.4 meters of interval B is of great interest because it contains an abundant biota, which exhibits a distinct and rapid change in composition toward the middle of interval B. Brachiopods display the most dramatic change in composition because they are usually the numerically dominant members of the fossil assemblages. Consequently, it is possible to group the assemblages into paleocommunities based on the distribution of the brachiopods. Community is used here in the sense of Johnson (1964, p. 109), "the assemblage of organisms inhabiting a specified space." The communities, listed in order of appearance from the base of interval B to the middle, are: (1) Hesperorthis community; (2) Strophomena-Hesperorthis community; (3) a brachiopod-free

Tetradium-Girvanella community; (4) Chaulistomella-Strophomena community; and (5) Strophomena-Rostricellula community. The biotic constituents of these paleocommunities were determined from species lists compiled from collections within successive 1.5 meter intervals (see Tables C-15 to C-32, Appendix C). These 1.5 meter sample intervals have been labeled by letters of the alphabet for each successive lithologic unit described in the field (e.g., 24-B, 24-C, 25-A, . . . etc.). Each of these paleocommunities is discussed separately and interval B is reviewed as a whole in the paragraphs below.

Hesperorthis Community

The Hesperorthis community occurs in wackestone beds (4 cm to 6 cm thick) situated in the lower 3 meters of interval B (282.9 m to 286 m above the base of the section). The biotic constituents of this community and their estimated abundances are listed in Table 1. Hesperorthis sp. cf. tricenaria (Appendix C, Plate C-3) is the dominant member of the community followed by such common faunal elements as Nicholsonella sp., Hallopora sp., Hemiphragma sp. and Pachydictya sp. (Appendix C, Plates C-1 and C-2). Hesperorthis is present as articulated and disarticulated specimens exhibiting well preserved shell ornamentation and varying shell sizes. Using the criteria suggested by Johnson (1960), Hesperorthis is an indigenous element of a Model II (intermediate exposure and transportation) type fossil assemblage. The remaining members of the community display similar features characteristic of indigenous

Table I. Composition and estimated abundances of the Hesperorthis community.

Trace Fossils	Bryozoans	Brachiopods	Trilobites	Echinoderms	Algae
Unidentified burrowing deposit feeder(s) (R)	Nicholsonella sp. (C) Hallopora sp. (C) Hemiphragma sp. (C) Pachydictya sp. (C) Escharopora sp. (R) Amplexopora sp. (R) Phylloporonid (R) Helopora sp.(R) Coeloclema sp. (R)	Hesperorthis sp.cf. tricenaria (D) Strophomena sp. (R) Camerella sp. cf. plicata (R)	Bumastus sp. (R) Illaenus sp. (R)	Cyclocystoid (R)	Kazahkstanelia (R) Girvanella (R)

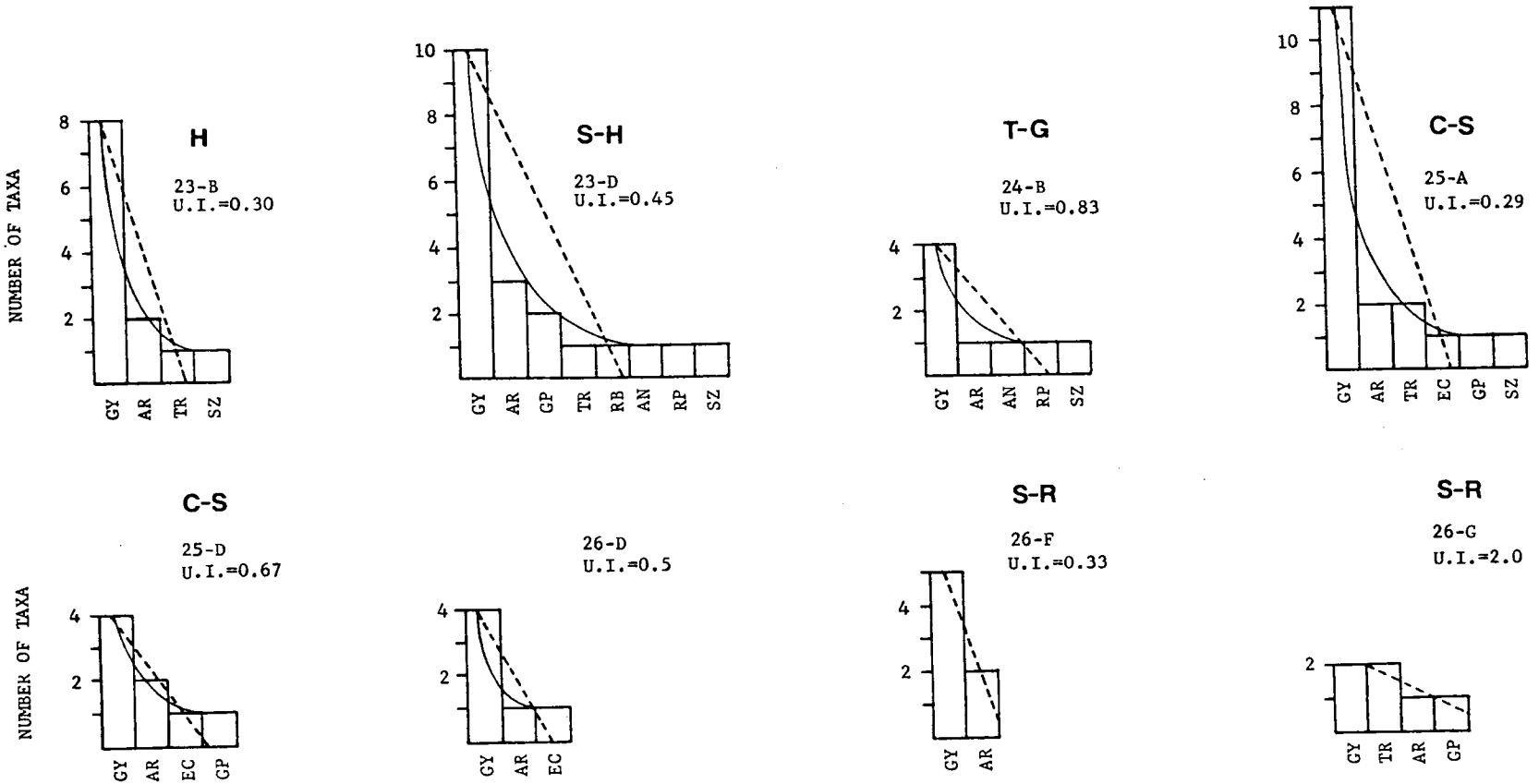
D = dominant, C = common, R = rare.

biota. Transported faunal elements are difficult to identify from acetate peels alone. Consequently, it is conceivable that a few (probably no more than one or two) of the rare (R) bryozoans could have been transported. In addition to the taxa listed in Table 1, many horizontal burrows are present. These burrows exhibit deformation halos in the surrounding micrite and clay-rich matrix, which is indicative of a soft, but not "soupy" substrate (see Walker, 1974; Rhoads, 1975).

Although the articulate brachiopods dominate this community, the gymnolaemate bryozoans are taxonomically more diverse as illustrated in Figure 27, interval 23-B. However, the overall diversity of the Hesperorthis community is rather low, especially when compared to the assemblages from interval A (refer to Figure 23, p. 97). Sample interval 23-B (Figure 27) has a low uniformity index.

Strophomena-Hesperorthis Community

The Strophomena-Hesperorthis community is intergradational between the underlying Hesperorthis community (observed in rocks with a high percentage of matrix) and the overlying Tetradium-Girvanella oncolite community (observed in rocks with a low percentage of matrix). Consequently, the Strophomena-Hesperorthis community contains faunal elements common to both the underlying and overlying communities. The biotic constituents of the Strophomena-Hesperorthis community are contained within a 3 meter-thick rock interval (286 meters to 289 meters above the base of the section) and are listed in Table 2.



AN=Anthozoa, AR=Articulata, EC=Eocrinoidea, GP=Gastropoda, GY=Gymnolaemata, RP=Rhodophyceae, RB=Rhombifera, SZ=Schizophyceae, TR=Trilobita.

Figure 27. Series of histograms illustrating species diversity within classes for selected sample intervals within interval B. The superimposed curves represent the uniformity index (U.I.) of which the numerical value was obtained from the slope of the dashed line (representing the average slope of the curve). Each histogram is constructed so that the most diverse class is listed on the left and the least diverse on the right.

Table 2. Composition and estimated abundances for the Strophomena-Hesperorthis community.

Coral	Bryozoans	Brachiopods	Trilobites	Echinoderms	Algae	Gastropods
Tetradium cellulosum (R)	Nicholsonella sp. (C) Diplotrypa sp. (C) Escharopora sp. (R) Amplexopora sp. (R) Pachydictya sp. (R) Helopora sp. (R) Constellaria sp. (R) Hallopora sp. (R) Hemiphragma sp. (R) Ottoseetaxis sp. (R)	Strophomena inspeciosa (D) Hesperorthis sp.cf. tricenaria (C) Plectocamara sp. cf. erecta (R)	Bumastus sp. (R) Calyptaulax (Calliops) (R)	Coronocystis angulatus (R)	Solenopora type R (R) Girvanella (C)	Gastropod C (C) Gastropod D (R) Gastropod E (R)

D = dominant, C = common, R = rare.

Strophomena inspeciosa (Appendix C, Plate C-4) dominates most of the wackestone slabs, while Hesperorthis sp. cf. tricenaria is subordinate or absent. These fossils are present as articulated and disarticulated valves exhibiting delicate costation. Strophomena and Hesperorthis valves are usually found convex-upward, implying that they were overturned by currents or by progressive excavation of the underlying sediment. Current activity is responsible for an increased percentage of Girvanella oncolites. Currents are also indicated by the occurrence of biosparite patches within the wackestone, and the presence of broken pieces of transported Tetradium corallia. In addition, currents have probably contributed to the high bryozoan species diversity (Figure 27, p. 114, 23-D) by introducing exotic faunal elements from neighboring communities or by increasing the water exchange rate, the latter providing additional suspended food resources. The uniformity index (Figure 27, p. 114, 23-D) for the Strophomena-Hesperorthis community is subsequently lower than that for the neighboring communities even though the diversity (varietal aspect) of the community is higher.

An interbed containing a small domal Tetradium colony and spheroidal Girvanella oncolites occurs near the base of the 3 meter Strophomena-Hesperorthis sequence. The Tetradium colony overlies an oncolitic Strophomena rich packstone separated by a 1 cm shale intercalation. This interbed illustrates the variable environmental conditions present during the deposition of the Strophomena-Hesperorthis beds. The Strophomena-Hesperorthis community grades into the Tetradium-Girvanella oncolite community vertically over one meter.

The presence of biotic elements from neighboring communities, which are shared with the Strophomena-Hesperorthis community, strongly suggests that the Strophomena-Hesperorthis community represents an ecotone. According to Odum (1971), the number of species is often greater in an ecotone than in the communities flanking it because it contains biotic elements from all three. This is true of the Strophomena-Hesperorthis community as illustrated by histograms 23-B (Hesperorthis community), 23-D (Strophomena-Hesperorthis community) and 24-B (Tetradium-Girvanella oncolite community) on Figure 27, p. 114. Hesperorthis and Tetradium are each members of a flanking community and the ecotonal community, while Strophomena inspeciosa is primarily indigenous to the ecotone. Consequently, Strophomena inspeciosa would be considered an "edge" species as described by Odum (1971).

Tetradium-Girvanella Oncolite Community

Girvanella oncolites and small domal in situ Tetradium colonies (avg. dimensions = 25 cm × 15 cm × 4 cm) are the dominant members of the brachiopod-free Tetradium-Girvanella oncolite community. The fossil assemblages that compose this paleocommunity occur in a 5 meter-thick zone starting from the oncolite marker bed (Figure 17, p. 58, peak 3) at the base of the Wardell Formation (289.2 meters from the base of the section). The biotic constituents of this community are listed in Table 3. Solenopora type R (Appendix C, Plate C-9) is associated with Girvanella (Appendix C, Plate C-9) either as the core of oncolites or as an integral part of the concentric coatings. Concentrically stacked

Girvanella oncolites indicate that the environment of deposition for the Tetradium-Girvanella oncolite community must have been characterized by turbulent, shoal water. The occurrence of Tetradium elsewhere in the geologic record supports this inference (see Walker, 1972, p. 2509). The in situ Tetradium colonies probably acted as a wave baffle, trapping fine-grained sediment among individual corallia (refer to the discussion in Chapter I, p. 77). The dome-shaped Tetradium colonies are distributed in small patches, but broken, mud-filled individual corallia can be found throughout the oncolitic packstone (poorly washed biosparite) characteristic of this 5 meter rock sequence. Several Tetradium colonies found fallen to one side (corallites horizontal or oblique to bedding) were encrusted by successively-layered sheets of Constellaria sp. (Appendix C, Plate C-2) followed by Nicholsonella sp., the latter being the most abundant. The remaining bryozoans and gastropod D were observed in acetate peels. The latter fossils did not exhibit external abrasion characteristic of other, exotic faunal elements.

Table 3. Composition and estimated abundances for the Tetradium-Girvanella oncolite community.

Anthozoans	Bryozoans	Algae	Gastropods
Tetradium cellulosum (D)	Nicholsonella sp.(C) Constellaria sp. (C) Hallopora sp. (R) Pachydictya sp. (R) Escharopora sp. (R)	Girvanella (D) Solenopora type R (C)	Gastropod D (C)

D = dominant, C = common, R = rare.

The Tetradium-Girvanella oncolite community exhibits anomalously low diversity between surrounding communities of higher diversity (Figure 27, p. 114, unit 24). The reduction of species diversity was probably related to harsher environmental conditions (i.e., agitated, shoaling water). Several authors have correlated harsh environmental conditions with low species diversity as in the immature community of Margalef (1968) and the physically controlled community of Sanders (1969). The uniformity index for the Tetradium-Girvanella oncolite community is significantly higher than for the surrounding communities (Figure 27, p. 114, 24-B) because the agitated water conditions inhibited bryozoan species diversity.

Chaulistomella-Strophomena Community

The Chaulistomella-Strophomena assemblages occur in a 6.5 meter sequence (294.0 meters to 300.5 meters from the base of the section) of thin-bedded (5 cm to 8 cm thick), shaly wackestones. Thin beds (2 cm to 3 cm thick) of laminated micrite are interbedded with these wackestones in the upper 2 meters of this sequence. The biotic constituents of the Chaulistomella-Strophomena community are listed in Table 4. Chaulistomella inaequistriata (Appendix C, Plate C-4) and Strophomena medialis (Appendix C, Plate C-4) occur in approximately equal proportions and are the dominant members of the community. These brachiopods display several criteria established by Johnson (1960) for recognizing an indigenous Model II assemblage. These are: (1) articulated and disarticulated valves; (2) valves of variable size

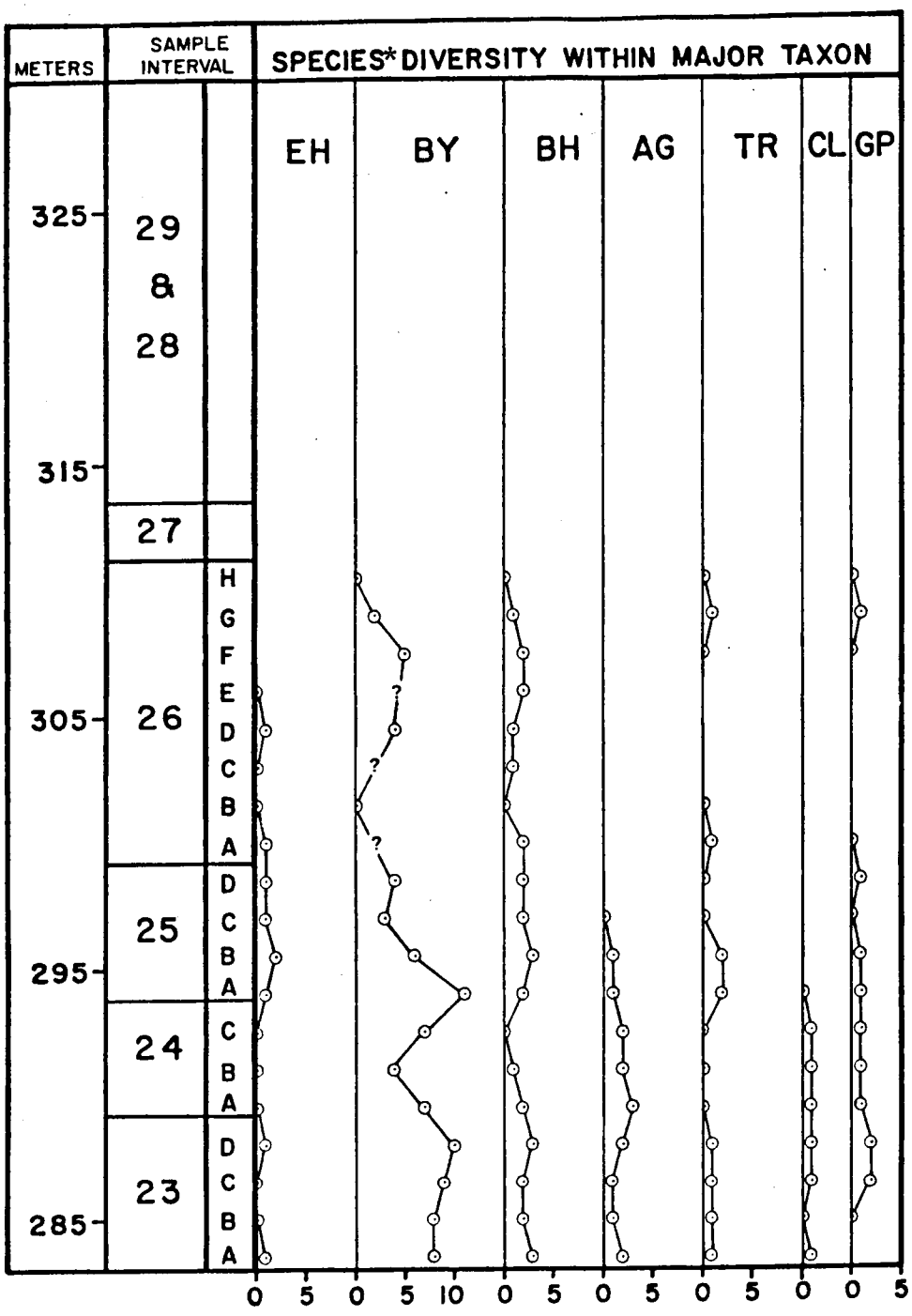
Table 4. Composition and estimated abundances for the Chaulistomella-Strophomena community.

Trace Fossils	Bryozoans	Brachiopods	Trilobites	Echinoderms	Gastropods
Unidentified burrowing deposit feeder(s) (R)	Hemiphragma sp. (C) Helopora sp. (C) Escharopora sp. (R) Pachydictya sp. (R) Hallopora sp. (R) Phylloporinid (R)	Chaulistomella inaequistriata (D) Strophomena medialis (D) Plectocamara sp. cf. erecta (R)	Nanillaenus sp. (R) Calyptaulax sp. (R) Illaenus sp. (R)	Batherocystis appressa (D) Coronocystis angulatus (R)	Gastropod D (R) Gastropod C (R)

D = dominant, C = common, R = rare.

(juvenile and adult); (3) well preserved shell costation; (4) valves horizontal to the bedding plane; and (5) moderate fossil densities. Many of the other faunal elements listed (Table 4) are present on the same brachiopod-dominated slabs, especially plates of Batherocystis appressa (Appendix C, Plate C-7) and partially fragmented branches of ramose Helopora sp., Escharopora sp. and Hemiphragma sp. colonies (Appendix C, Plates C-1 and C-2). A few brachiopod-free slabs intercalated with those containing the brachiopod assemblages contain intact, fragile colonies of ramose Hemiphragma and Helopora. Sudden deposition with rapid burial of the colonies may have occurred. The top 2 meters of this 6.5 meter rock sequence is characterized by interbedded, laminated micrites. These micrites dominate the succeeding 6 meters of rock (299.0 meters to 305 meters from the base of the section) between the Chaulistomella-Strophomena assemblages and the Strophomena-Rostricellula assemblages. The micrites are characterized by (1) alternating micrite and shaly micrite laminae, (2) vertical burrows and (3) occasional cryptalgal laminites. The latter are inferred from bowed shaly micrite laminae, which form domal structures several millimeters long. The laminations are thicker at the arch of the domes and thinner in the troughs. Recent algally-laminated sediments are primarily restricted to the intertidal environment (refer to Logan et al., 1964). Thus, the laminated micrites appear to represent interfingering, intertidally-deposited sediments.

The species diversity of the Chaulistomella-Strophomena community decreases upward in the section as the interbeds of intertidally-deposited sediments become more abundant (Figure 28, unit 25).



*Many taxa are identified to the generic level, but are believed to be representative of only a single species.

Figure 28. Stratigraphic distribution of the varietal aspect of species diversity within each major taxon for interval B, Evans Ferry, Tennessee.

Applying the stability-time hypothesis of Sanders (1969), which states that benthic species diversity will decrease along a stress gradient (encroaching intertidal conditions), this trend is predictable. The uniformity index increases upward in the 6.5 meter brachiopod-dominated rock sequence, probably in response to fluctuating physical conditions (Figure 27, p. 114, 25-A and 25-D). A low uniformity index is recorded at sample interval 25-A because of high species diversity within the bryozoans. Environmental conditions appear to have been stable during the deposition of wackestone beds in this interval (25-A, no lithologic change). In sample interval 25-D (3 meters above 25-A), the bryozoan species diversity decreased because of changing environmental conditions (implied by the micrite interbeds); subsequently, the uniformity index was raised between the few classes remaining (Figure 27, p. 114). Some classes disappear in the lower half of unit 26 (299 meters to 305 meters from the base of the section). Those that are present, occur in rare interbeds of wackestone bounded by increasingly abundant, cryptallgally-laminated and vertically furrowed micrites. Sample interval 26-D demonstrates a uniformity index (Figure 27, p. 114) representative of a few of these wackestone beds.

Strophomena-Rostricellula Community

The Strophomena-Rostricellula community is the most poorly preserved community of the 5 that have been recognized. It is represented by faunal assemblages that occur in a 4.5 meter interval (305 m to 309.5 m above the base of the section) lying above the

beds containing the Chaulistomella-Strophomena assemblages. Assemblages composing the Strophomena-Rostricellula community are contained in shaly wackestone beds (5 cm to 10 cm thick) interbedded with laminated shaly micrites (2 cm to 3 cm thick). The laminated shaly micrites dominate the remaining 20.6 meters of interval B (i.e., 309.5 m to 330.1 m above the base of the section). The biotic constituents of the Strophomena-Rostricellula community are listed in Table 5. Amplexopora sp. (Appendix C, Plate C-1) is the dominant member of the community and occurs in the form of robust, intact ramose branches buried in shaly micrite. Strophomena medialis and Rostricellula ovata (Appendix C, Plate C-3) are usually disarticulated, but the valves are whole and delicate costation is preserved. Apparently, these two brachiopods were not involved in any short-term successional events such as described by Walker and Parker (1975). Several Calyptaulax pygidia (Appendix C, Plate C-6; unabraded) an unidentified glabellar region from a different trilobite genus, scattered ostracod valves and a high-spired gastropod (gastropod; Appendix C, Plate C-5) were found on the uppermost fossiliferous slab in this 4.5 meter interval. These faunal elements are all euryhaline and thus best fitted to withstand the encroaching intertidal environmental conditions.

Table 5. Composition and estimated abundances for the Strophomena-Rostricellula community.

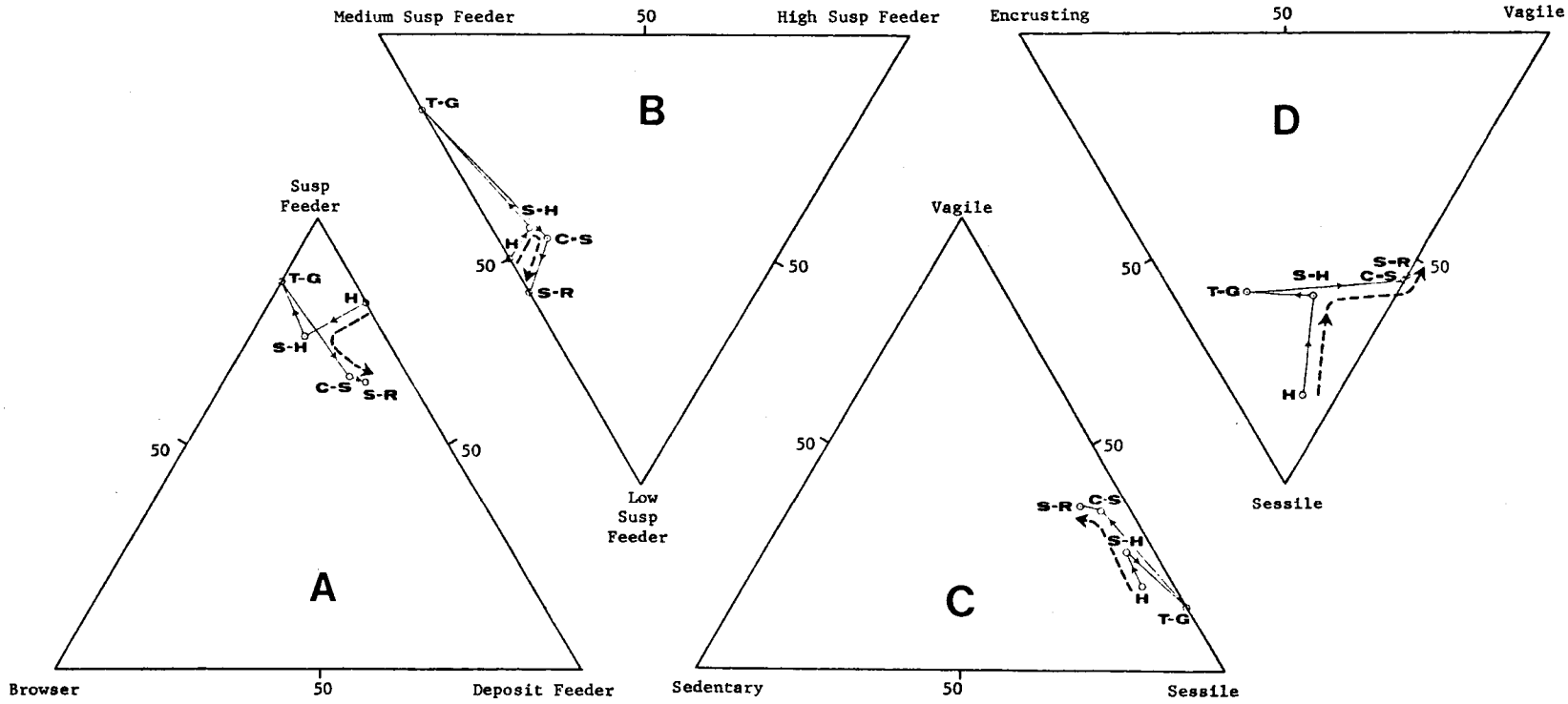
Bryozoans	Brachiopods	Trilobites	Ostracods	Gastropods
Amplexopora sp. (D) Escharopora sp. (R) Phylloporinid (R) Helopora sp. (R) Pachydictya sp. (R)	Strophomena medialis (C) Rostricellula ovata (C)	Calyptaulax sp. (C) "Unidentified trilobite" (R)	Ostracod A (C)	Gastropod F (R)

D = dominant, C = common, R = rare.

The species diversity of the Strophomena-Rostricellula community is the lowest for the 5 communities identified in interval B (Figures 27 and 28, pp. 114 and 122, 26-F and 26-G). This decline in species diversity is expected because of the unpredictable environmental conditions characteristic of proximal intertidal areas (see Sanders, 1968; Bretsky and Lorenz, 1969).

Analysis of Autecologic Parameters for Interval B

Analysis of trophic groups, salinity tolerance, and mobility relationships of the species contained in the 5 paleocommunities in interval B reveals some interesting trends. Figure 29, part A, is a plot of suspension feeders, deposit feeders, and browsers. The paleocommunities display a distinct trend from suspension feeders to deposit feeders with decreasing distance from shore (upward in section, dashed line, Figure 29). The decline of suspension feeders may be related to increased bottom turbulence above the very fine-grained (micrite and clay) substrate. Currents would be expected to disturb the bottom sediments more easily in shoal water. Scavenging and burrowing deposit feeders may also have stirred the bottom muds more frequently. The suspension feeders are restricted to medium (7 cm to 14 cm) and low (1 cm to 6 cm) level varieties (Figure 29, part B). The Tetradium-Girvanella oncolite community does not follow the trend set by the other communities in the succession. The number of suspension feeders versus deposit feeders increases rather than decreases principally because of the increased water turbulence, which probably



H=Hesperorthis, S-H=Strophomena-Hesperorthis, T-G=Tetradium-Girvanella, C-S=Chaulistomella-Strophomena, S-R=Strophomena-Rostricellula and Susp=Suspension.

Figure 29. Classification of trophic categories (A and B) and mobility relationships (C and D) for species occurring in interval B. The small arrows illustrate the actual succession of paleocommunities upward in the section and the larger dashed arrow shows the major trend in community development upward in the section.

provided additional nutrients for suspension feeders and helped remove waste products.

Figure 29, parts C and D, are essentially the same except one apex has been varied from encrusting to sedentary. Both plots reveal a pattern of increasing mobility toward the shore. Increased mobility would enable a member of the vagile benthos to manage shifting bottom muds (due to increasing turbidity), or to move from locally harsh conditions characteristic of nearshore areas (brought about by an abrupt change in salinity or a rapid influx of terrigenous clay and silt). The Tetradium-Girvanella community deviates from the trend displayed by the other communities. Sessile suspension feeders were better adapted to the increased water turbulence inferred for the paleodepositional environment of this community.

The last parameter examined is salinity tolerance. Figure 25, p. 102, illustrates the gradual trend toward increasing dominance of euryhaline faunal elements as the shore is approached. Salinities are more variable in intertidal areas compared with the subtidal environment because of periodic evaporation and fresh water runoff. Consequently, a change in the fauna and flora favoring euryhaline forms is expected. The Tetradium-Girvanella community would seem to disrupt the orderly progression of decreasing stenohaline biota. Perhaps continual water movement (evidenced by spheroidal oncolites) maintained normal marine salinities.

It is interesting to note that the position of the Strophomena-Hesperorthis community on each of the ternary diagrams is intermediate

between the Hesperorthis community and the Tetradium-Girvanella oncolite community. This coincides with the interpretation that the Strophomena-Hesperorthis community represents an ecotonal community. Since it contains members of each of the adjacent communities, an intermediate position on plots of autecologic parameters is predictable. As noted earlier, the greater species diversity in this community, than in either of the communities bounding it, is characteristic of an ecotone. Thus, two lines of evidence support the conclusion.

Discussion of Interval B

Interval B represents an offshore to onshore regressive sequence of five benthic marine communities. Listed in decreasing distance from shore, these are: (1) Hesperorthis community; (2) Strophomena-Hesperorthis community; (3) Tetradium-Girvanella oncolite community; (4) Chaulistomella-Strophomena community; and (5) Strophomena-Rostricellula community. The species diversity for each of these communities gradually decreased with decreasing distance from shore (Figure 30). Ziegler, Cocks and Bambach (1968) noted a similar trend for 5 benthic communities in the Lower Silurian rocks in the Welsh Borderland and Wales. Decreasing species diversity toward shore can be related to increasingly harsher physical conditions and environmental unpredictability (Sanders, 1968). Physical conditions present in the intertidal environment (i.e., fluctuating salinities, desiccation, wide temperature ranges, and increased wave turbulence) constitute severe physiological stress for most organisms. Consequently,

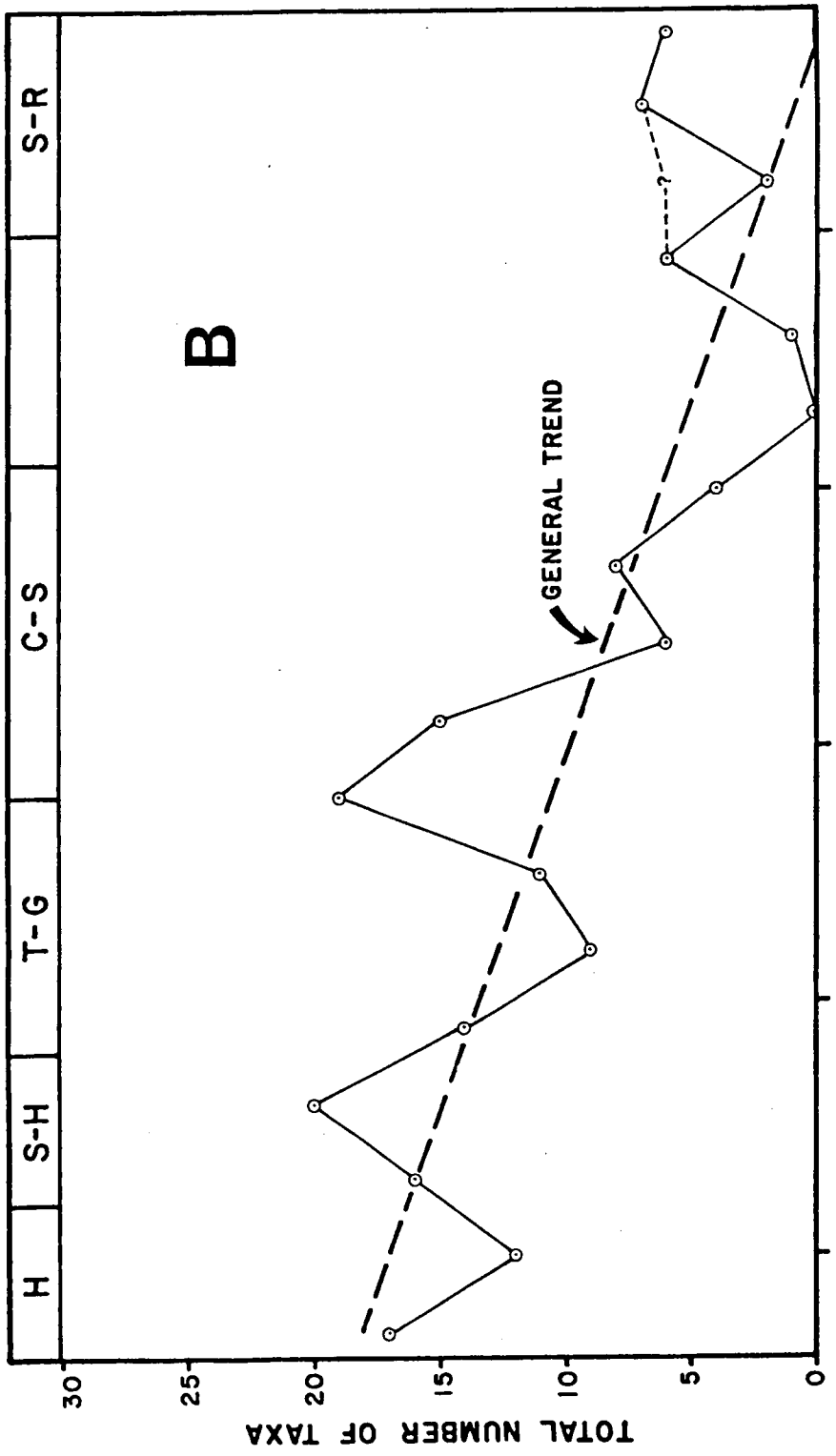


Figure 30. Total species diversity for interval B toward the top of the Evans Ferry section. Using Walther's Law, this vertical rock sequence is interpreted to represent horizontally continuous environments. Interval B represents an offshore to onshore environmental progression (left to right). Compare with similar plot for interval A in Figure 26, p. 109.

only a few species are adapted to survive under these conditions, whereas, many more species can flourish in the less harsh, offshore environmental setting.

The Tetradium-Girvanella oncolite community marks an anomalously sharp break in the gradual decline of species diversity toward the shore (Figure 29, p. 126, and Figure 30, 289 m to 294 m). This drop in species diversity is attributed to an increase in turbulence, which is inferred from the presence of abundant spheroidal oncolites (Figure 17, p. 58). Oncolites increase and decrease in abundance throughout the rock interval containing the Tetradium-Girvanella oncolite community. Thus, they reflect fluctuating physical conditions (primarily, current activity) present during the time of deposition.

Individual sample intervals (e.g., 23-A, 23-B, . . . etc.) within interval B are characterized by one class with a high species diversity and the remaining classes with markedly low species diversity. The result is a low uniformity index or a curve with a very steep slope (Figure 27, p. 114). These curves strongly deviate from a monotonic decrease in species diversity within classes (straight-line relationship). Sample interval 26-G (representing assemblages closest to the shore) has a high uniformity index, similar to those indexes for interval A, zone I. The high uniformity index (low slope) is a reflection of the reduced dominance of species diversity within the most diverse class as harsher environmental conditions are encountered. Distinction between the high uniformity index (in a nearshore subtidal environment as above) and those indices shown in interval A, zone I

(offshore subtidal) is an easy one to make because of the great disparity in species diversity between the two areas.

IV. SUMMARY AND CONCLUSIONS

At Evans Ferry, Tennessee, the Middle Ordovician rocks from the post-Knox unconformity to the top of the Wardell Formation display an environmental spectrum from a supratidal-intertidal environment to a stable offshore subtidal environment and back to the former. The Tumbez Formation represents a supratidal-high intertidal environment at its base (T1) and a low intertidal algal flat environment (T3 and T4) at its top. Algal flats were maintained throughout the depositional history of the lower Eidson Member (E1), but were succeeded by shallow subtidal conditions in the middle to upper units (E2 and E3). Stable, quiet, subtidal conditions are inferred for the deposition of the Hogskin Member (H1) because of an increase in faunal and floral diversity (see Sanders, 1968). Storm deposits or possibly tidal channels (H2) occasionally interrupted this depositional sequence. The succeeding rock units of the Rockdell Formation were deposited in a subtidal environment characterized by semirestricted water circulation (R1). The latter is inferred from a high percentage of micrite matrix, a strong hydrogen sulfide odor released upon fracturing of the rock (suggestive of reducing conditions) and an absence of current-induced sedimentary features.

The upper units of the Rockdell Formation (R2) are gradational with the lower units of the Benbolt Formation (B1). These two lithologies

(R2 and B1) represent proximal and interacting stable subtidal environments characterized by rhythmically intermittent shale deposition and decreasing water depth (inferred from an increase in oncolites at the top of B1). A tidal skeletal sand bar exhibiting bidirectional trough cross beds and abraded allochems (B2) succeeds lithology B1. The remainder of the Benbolt Formation represents algal mud mounds (B4) and deeper subtidal intermound areas (B3). A return to shallow nearshore depositional environments occurs at the base of the Wardell Formation (W1), which exhibits abundant oncolites (shallow water indicator) and low biotic diversities. Succeeding rock units (W2) display cryptalgal structures, vertical burrows, and a few ostracods suggesting a low intertidal environment containing smooth algal mats. The remainder of the Wardell Formation (W3) displays mudcracks of shaly micrite interbedded with cryptalgal laminites. These features imply a high intertidal-supratidal environment of deposition analogous to Recent intertidal algal flats. In summary, the Evans Ferry section from bottom to top, represents a transgressive phase (Tumbez Formation, Eidson and Hogskin members of the Lincolnshire Formation, Rockdell Formation, and Benbolt Formation) followed by a regressive phase (Wardell Formation).

Two fossiliferous intervals (A and B) were selected for paleoecological analysis using the ecostratigraphic framework, just described, as a reference. Interval A of the Porterfield stage represents a stable, gently shallowing, offshore subtidal environment, while interval B of the Wilderness stage represents an environmental

spectrum from the shallow nearshore subtidal environment to the high intertidal-supratidal environment. Intervals A and B are separated by a stratigraphic thickness of 90.6 meters probably representing no more than 1-3 million years. This time interval is sufficiently short so that the overall effects of evolution on community composition are much less significant than environmental change. Therefore, the paleoecologic differences in the biotas within intervals A and B can be viewed from the standpoint of environmental changes.

A comparison of Figures 26 and 30, pp. 109 and 129, reveals a marked decline in species diversity from interval A to B. In addition, species diversity within each interval declines from bottom to top. In view of the paleoenvironmental interpretations presented in Chapters I and II, the disparity between species diversity is a reflection of low stress environmental conditions (interval A) versus high stress environmental conditions (interval B). Similar observations have been made in other fossil and Recent community studies (see Bretsky and Lorenz, 1970).

The uniformity index (Figures 23 and 27, pp. 97 and 114) provides a means of displaying the varying species diversities as gentle slope (high uniformity index) for the lower portion of interval A and steep slopes (very low uniformity index) for interval B. A very high uniformity index (monotonically decreasing numbers of species within fossil classes) may be characteristic of very stable subtidal environments, while low indices may reflect unstable environmental conditions. If these parallels are valid, a useful tool in analyzing assemblages may have been introduced in this study.

An analysis of trophic categories for each interval (Figure 24, p. 100, parts B, C; and Figure 29, p. 126, parts A, B) reveals a predominance of suspension feeders. Interval A, however, contains many more high level suspension feeders in comparison to their near absence in interval B. Two explanations for this trend may be offered: either (1) the subtidal environment of interval A had a greater suspended food resource; or (2) high level suspension feeders could not withstand the fluctuating environmental conditions of interval B.

The suspension feeders are dominantly sessile, therefore, accommodation of a sessile habit characterizes the prevalent substrate niche in each interval (Figure 24, p. 100, part A; and Figure 29, p. 126, parts C, D). However, in zone II (G, H and I) of interval A and in interval B, similar substrate niche trends are exhibited. Each one displays a trend toward increasing mobility upward in the section, which is probably related to two factors: (1) a lack of suspended nutrients and (2) rapid deposition of sediment. Increased deposition of shale in zone II favors mobile faunas able to escape burial. Changing salinities and periodic episodes of rapid sedimentation in interval B result in a similar situation favoring vagile faunas. In addition, the vagile fauna is predominantly composed of deposit feeders benefiting from the organic matter associated with the deposition of fine grained sediments. Zone III in interval A returned to the dominance of sessile suspension feeders once the deposition of mud was reduced.

A graph of salinity tolerances for each interval (Figure 25, p. 102) illustrates an interesting point. The faunas of interval A are basically stenohaline and do not reveal any significant trends. However, the paleocommunities of interval B form a distinct trend (excluding the aberrant Tetradium-Girvanella community) toward increasing salinity tolerance upward in the section. This sequence depicts increasingly harsh environmental conditions (due to sudden changes in salinity) encountered as the shoreline is approached. The stenohaline biota of interval A was not subjected to fluctuating salinities in the low stress stable subtidal environment represented in that interval.

In summary, interval A represents intergrading benthic communities subject to minor physical oscillations (gentle environmental gradients), while interval B represents several communities exhibiting distinct compositional changes in direct response to increasingly harsh physical conditions as the shoreline shifted (regressed) seaward.

REFERENCES CITED

REFERENCES CITED

Aitken, J. D., 1967, Classification and environmental significance of cryptalgal limestones and dolomites, with illustrations from the Cambrian and Ordovician of southwestern Alberta: Jour. Sed. Petrology, v. 37, pp. 1163-1178.

Ball, M. M., E. A. Shinn, and K. W. Stockman, 1967, Geologic effects of hurricane Donna in South Florida: Jour. Geol., v. 75, pp. 583-597.

Bassler, R. S., 1950, Paleontology: new genera of American Middle Ordovician "Cystoidea": Jour. Washington Acad. Sci., v. 40, pp. 273-277.

Bathurst, R. G. C., 1966, Boring algae, micrite envelopes and lithification of Molluscan biosparites: Geol. Jour., v. 5, pp. 15-32.

_____, 1967, Subtidal gelatinous mat, sand stabilizer and food, Great Bahama Bank: Jour. Geol., v. 75, pp. 736-738.

Benedict, G. L., and K. R. Walker, 1978, Paleobathymeric analysis in Paleozoic sequences and its geodynamic significance: Am. Jour. Sci., v. 278, pp. 579-607.

Bergstrom, S. M., 1971a, Conodont biostratigraphy of the Middle and Upper Ordovician of Europe and eastern North America: in W. C. Sweet and S. M. Bergstrom, eds., Symposium on conodont biostratigraphy, Geol. Soc. Am., Mem. 127, pp. 83-161.

_____, 1971b, Correlation of the North Atlantic Middle and Upper Ordovician conodont zonation with the graptolite succession: in Colloque Ordovician-Silurien, Brest. Bur. Rech. Geol. Min., Mem. 73, pp. 177-187.

_____, 1973, Biostratigraphy and facies relations in the lower Middle Ordovician of easternmost Tennessee: Am. Jour. Sci., v. 273-A, pp. 261-293.

Bretsky, P. W., and D. M. Lorenz, 1969, Adaptive response to environmental stability: a unifying concept in Paleoecology: Proc. N. Am. Paleontological Convention, pp. 522-550.

Brower, J. C., and J. Venus, 1974, Middle Ordovician Crinoids from southwestern Virginia and eastern Tennessee: Bull. Am. Paleontology, v. 66, no. 283, 125 pp.

Butts, C., 1940, Geology of the Appalachian Valley in Virginia: Virginia Geological Survey, Bull. 52, pt. 1, 568 pp.

Byers, C. W., and L. E. Stasko, 1978, Trace fossils and sedimentologic interpretation—McGregor Member of Platteville Formation (Ordovician) of Wisconsin: Jour. Sed. Petrology, v. 48, pp. 1303-1310.

Carnes, J. B., 1975, Conodont biostratigraphy in the Lower Middle Ordovician of the western Appalachian thrust-belts in northeastern Tennessee: Ohio State University, unpub. Ph.D. dissertation, 291 pp.

Cooper, B. N., 1945, Industrial limetones and dolomites in Virginia: Clinch Valley district: Virginia Geol. Surv. Bull., v. 66, pp. 42-68, 133, 137.

_____, 1953, Trilobites from the lower Champlainian formations of the Appalachian Valley: Geol. Soc., Am., Mem. 55, 69 pp.

_____, 1956, Chazyan and related brachiopods: Smithsonian Inst. Misc. Coll., pts. 1 and 2, 1245 pp.

Cooper, B. N., and C. E. Prouty, 1943, Stratigraphy of the Lower Middle Ordovician of Tazewell County, Virginia: Bull. Geol. Soc. America, v. 54, pp. 819-886.

Davies, G. R., 1970a, Carbonate bank sedimentation, eastern Shark Bay, Western Australia: in Logan, B. W., ed., Carbonate sedimentation and environments, Shark Bay, Western Australia, Am. Assoc. Petroleum Geologists, Mem. 13, pp. 85-168.

_____, 1970b, Algal-laminated sediments, Gladstone embayment, Shark Bay, Western Australia: in Logan, B. W., ed., Carbonate sedimentation and environments, Shark Bay, Western Australia, Am. Assoc. Petroleum Geologists, Mem. 13, pp. 169-205.

Deffeyes, K. S., F. J. Lucia, and P. K. Weyl, 1965, Dolomitization of Recent and Plio-Pleistocene sediments by marine evaporite waters on Bonaire, Netherlands Antilles: in Pray, L. C., and R. C. Murray, eds., Dolomitization and limestone diagenesis: a Symposium, Soc. Econ. Paleontologists Mineralogists, Spec. Publ., 13, pp. 71-88.

Folk, R. L., 1962, Spectral subdivision of limestone types: in Ham, W. E., ed., Classification of carbonate rocks, Am. Assoc. Petroleum Geologists, Mem. 1, pp. 62-84.

Ferrigno, K. F., 1973, Paleoecology of the reefs of the Holston Limestone: Univ. of Tennessee, unpub. Ph.D. dissertation, 142 pp.

Friedman, G. M., 1971, Micritic envelopes of carbonate grains are not exclusively of photosynthetic algal origin: Sedimentology, v. 16, pp. 89-96.

Gebelein, C. D., and P. Hoffman, 1973, Algal origin of dolomite laminations in stromatolitic limestone: Jour. Sed. Petrology, v. 43, pp. 603-613.

Ginsburg, R. N., 1956, Environmental relationships of grain size and constituent particles in some South Florida carbonate sediments: Bull. Am. Assoc. Petroleum Geologists, v. 40, pp. 2384-2427.

_____, 1957, Early diagenesis and lithification of shallow-water carbonate sediments in South Florida: in Regional aspects of carbonate deposition, Soc. Econ. Paleontologists Mineralogists, Spec. Publ. 5, Tulsa, Oklahoma, pp. 80-99.

_____, 1960, Ancient analogues of Recent stromatolites: XXI International Geol. Cong., pt. 22, pp. 26-35.

Ginsburg, R. N., and L. A. Hardie, 1975, Tidal and storm deposits, northwestern Andros Island, Bahamas: in Ginsburg, R. N., ed., Tidal deposits, a casebook of Recent and fossil counterparts, New York, Springer-Verlag, pp. 201-208.

Gorsline, D. S., 1963, Environments of carbonate deposition: Florida bay and Florida straits: in Bass, R., and S. Sharps, eds., Shelf carbonates of the Paradox Basin, Four Corners Geol. Soc., Fourth Field Conf. Sym., pp. 130-143.

Grover, G., and J. F. Read, 1978, Fenestral and associated vadose diagenetic fabrics of tidal flat carbonates, Middle Ordovician New Market Limestone, southwestern Virginia: Jour. Sed. Petrology, v. 48, pp. 453-473.

Harris, L. D., and R. B. Mixon, 1970, Geologic map of the Howard Quarter Quadrangle, northeastern Tennessee: U. S. Geol. Surv., Map GQ-842, 1:24,000.

Illing, L. V., A. J. Wells, and J. C. M. Taylor, 1965, Penecontemporary dolomite in the Persian Gulf: in Pray, L. C., and R. C. Murray, eds., Dolomitization and limestone diagenesis: a Symposium, Soc. Econ. Paleonotolotists Mineralogists, Spec. Publ., 13, pp. 89-111.

Johnson, R. G., 1960, Models and methods for analysis of the mode of formation of fossil assemblages: Bull. Geol. Soc. Am., v. 71, pp. 1075-1086.

_____, 1973, Conceptual models of benthic marine communities: in Schopf, T. J. M., ed., Models of paleobiology, Freeman, Cooper and Company, San Francisco, pp. 148-459.

Karklins, O. L., 1969, The cryptostome Bryzoa from the Middle Ordovician Decorah Shale, Minnesota: Univ. Minnesota Spec. Pub., no. 6, 121 pp.

Logan, B. W., 1961, Cryptozoan and associate stromatolites from the Recent, Shark Bay, Western Australia: Jour. Geol., v. 69, pp. 517-533.

_____, 1974, Inventory of diagenesis in Holocene-Recent carbonate sediments, Shark Bay, Western Australia: in Logan, B. W., ed., Evolution and diagenesis of Quaternary carbonate sequences, Shark Bay, Western Australia, Am. Assoc. Petroleum Geologists, Mem. 22, pp. 195-249.

Logan, B. W., R. Rezak, and R. N. Ginsburg, 1964, Classification and environmental significance of algal stromatolites: Jour. Geol., v. 72, pp. 68-83.

Logan, B. W., P. Hoffman, and C. D. Gebelein, 1974, Algal mats, cryptalgal fabrics, and structures, Hamelin Pool, Western Australia: in Logan, B. W., ed., Evolution and diagenesis of Quaternary carbonate sequences, Shark Bay, Western Australia, Am. Assoc. Petroleum Geologists, Mem. 22, pp. 140-194.

Logan, B. W., and V. Semeniuk, 1976, Dynamic metamorphism: processes and products in Devonian carbonate rocks, Canning Basin, Western Australia: Geological Society of Australia, Inc., Spec. Publ., no. 6, 138 pp.

Longman, M. W., 1977, Factors controlling the formation of microspar in the Bromide Formation: Jour. Sed. Petrology, v. 47, pp. 347-350.

McLaughlin, R. E., 1973, Observations on the biostratigraphy and stratigraphy of Knox County, Tennessee, and vicinity: in Geology of Knox County, Tennessee, Tenn. Div. Geol. Bull. 70, pp. 25-62.

Moore, N. K., 1977, Distribution of the benthic algal flora in Middle Ordovician carbonate environmental units of the southern Appalachians: in Ruppel, S. C., and K. R. Walker, eds., The ecostratigraphy of the Middle Ordovician of the southern Appalachians (Kentucky, Tennessee, and Virginia) U.S.A., Knoxville, Univ. Tennessee, Dept. Geol. Sci., Studies in Geology 77-1, pp. 18-29.

_____, 1978, Taxonomy and paleoenvironmental distribution of the benthic algal flora from Middle Ordovician carbonate rocks of East Tennessee: Univ. of Tennessee, unpub. Ph.D. dissertation,

Moore, R. C., ed., 1953, Treatise on invertebrate paleontology, part G, Bryozoa: Geol. Soc. Am., 253 pp.

_____, 1959, Treatise on invertebrate paleontology, part O, Arthropoda 1: Geol. Soc. Am., 560 pp.

_____, 1965, Treatise on invertebrate paleontology, part H, Brachiopoda 1 and 2: Geol. Soc. Am., 927 pp.

Neumann, A. C., C. D. Gebelein, and T. P. Scoffin, 1970, The composition, structure and erodability of subtidal mats, Abaco, Bahamas: Jour. Sed. Petrology, v. 40, pp. 274-297.

Odum, E. P., 1971, Fundamentals of ecology: W. B. Saunders Company, Philadelphia, 574 pp.

Oldershaw, A. E., and T. P. Scoffin, 1966, The source of ferroan and nonferroan calcite cements in the Halkin and Wenlock Limestones: Geol. Jour., v. 5, pp. 309-320.

Parsley, R. L., and L. W. Mintz, 1975, North American Paracrinoidea: (Ordovician: Paracrinozoa, new Echinodermata): Bull. Am. Paleontology, v. 68, no. 288, 115 pp.

Paul, C. R. C., 1972, Cheirocystella antiqua gen. et. sp. nov. from the Lower Ordovician of western Utah, and its bearing on the evolution of the Cheirocrinidae (Rhombifera: Glyptocystitida): Brigham Young Univ., Geol. Studies, v. 19, pt. 1, pp. 15-63.

Powers, M. C., 1953, A new roundness scale for sedimentary particles: Jour. Sed. Petrology, v. 23, pp. 117-119.

Prouty, C. E., 1946, Lower Middle Ordovician of southwest Virginia and northeast Tennessee: Bull. Am. Assoc. Petroleum Geologists, v. 30, pp. 1140-1191.

Rhoads, D. C., 1967, Biogenic reworking of intertidal and subtidal sediments in Barnstable Harbor and Buzzards Bay: Mass. Jour. Geol., v. 75, pp. 461-475.

_____, 1975, The paleoecological and environmental significance of trace fossils: in Frey, R. W., ed., The study of trace fossils, New York, Springer Verlag, pp. 147-160.

Rodgers, J., 1953, Geologic map of East Tennessee with explanatory text: Tenn. Dept. Conserv. Div. Geol. Bull. 58, pt. 2, pp. 64-99.

Rodgers, J., and D. R. Kent, 1948, Stratigraphic section at Lee Valley, Hawkins County, Tennessee: Tenn. Div. Geol., Bull. 55, 47 pp.

Sanders, H. L., 1968, Marine benthic diversity: a comparative study, Am. Naturalist, v. 102, pp. 243-282.

_____, 1969, Benthic marine diversity and the stability-time hypothesis: Brookhaven Symposium in Biology, v. 22, pp. 71-81.

Scoffin, T. P., 1970, The trapping and binding of subtidal carbonate sediments by marine vegetation in Bimini Lagoon, Bahamas: Jour. Sed. Petrology, v. 40, pp. 249-273.

Scott, R. W., 1974, Bay and shoreface benthic communities in the Lower Cretaceous: Lethaia, v. 7, pp. 315-330.

_____, 1976, Trophic classification of benthic communities: in Scott, R. W., and R. R. West, eds., Structure and classification of paleocommunities, Dowden, Hutchinson and Ross, Stroudsburg, PA, pp. 24-66.

_____, 1978, Approaches to trophic analysis of paleocommunities: Lethaia, v. 11, pp. 1-14.

Shanmugam, G., and K. R. Walker, 1978, Tectonic significance of distal turbidites in the Middle Ordovician Blockhouse and Lower Sevier Formations in East Tennessee: Am. Jour. Sci., v. 278, pp. 551-578.

Shaw, F. C., 1974, Simpson Group (Middle Ordovician) trilobites of Oklahoma: Paleontol. Soc., Mem. 6, 54 pp.

Shinn, E. A., 1968a, Practical significance of birdseye structures in carbonate rocks: Jour. Sed. Petrology, v. 38, pp. 215-223.

_____, 1968b, Burrowing in Recent carbonate sediments of Florida and Bahamas: Jour. Paleontology, v. 42, pp. 879-894.

Shinn, E. A., R. M. Lloyd, and R. N. Ginsburg, 1969, Anatomy of a modern carbonate tidal-flat, Andros Island, Bahamas: Jour. Sed. Petrology, v. 39, pp. 1202-1228.

Smosna, R., and S. Warshauer, 1978, Fossil diversity in thin section: Jour. Sed. Petrology, v. 48, pp. 331-336.

Swinchatt, J. P., 1965, Significance of constituent composition, texture, and skeletal breakdown in some Recent carbonate sediments: Jour. Sed. Petrology, v. 35, pp. 71-90.

Walker, K. R., 1972, Community ecology of the Middle Ordovician Black River Group of New York State: Geol. Soc. Am Bull., v. 83, pp. 2499-2524.

_____, 1974, Mud substrata: in Principles of benthic community analysis (notes for a short course) by Ziegler, A. M., and others, Division of Marine Geology and Geophysics, Rosenstiel School of Marine and Atmosphere Science, Univ. of Miami, pp. 5.1-5.11.

_____, 1977, A brief introduction to the ecostratigraphy of the Middle Ordovician of Tennessee: in Ruppel, S. C., and K. R. Walker, eds., The ecostratigraphy of the Middle Ordovician of the southern Appalachians (Kentucky, Tennessee, and Virginia) U.S.A., Knoxville, Univ. Tennessee, Dept. Geol. Sci., Studies in Geology 77-1, pp. 12-17.

Walker, K. R., and L. P. Alberstadt, 1973, A new facies hypothesis concerning the Middle Ordovician of the southern Appalachians (abst.): Geol. Soc. Am., Southeast Ann. Meeting, (Program with abst.), pp. 447-448.

_____, 1975, Ecological succession as an aspect of structure in fossil communities: Paleobiology, v. 1, pp. 238-257.

Ziegler, A. M., L. R. M. Cocks, and R. K. Bambach, 1968, The composition and structure of Lower Silurian marine communities: Lethaia, v. 1, pp. 1-27.

APPENDICES

APPENDIX A

Table A-1. Constituent particle analyses (rock volume percent) for selected thin sections.

Sample no.	Micrite	Microspar	Spar	Intraclasts	Peloids	Brachiopod fragments	Gastropods	Ostracod valves	Trilobite debris	Pelecypod debris	Echinoderm debris	Bryzoan debris	Algae	Onocolites	Sponge debris	Other fossils	Clay laminae	Detrial quartz	Other minerals
EF 3	64.8	8.8	18.3	5.0	0.0	0.0	0.0	0.0	0.0	0.0	0.0	0.0	0.0	0.0	0.0	0.0	0.0	0.0	3.1
EF 17	5.0	7.5	37.9	6.3	19.2	0.0	0.0	1.9	0.4	0.0	12.7	0.0	4.1	0.0	0.0	5.0	0.0	0.0	0.0
EF 22	31.3	2.8	32.0	0.0	1.5	0.0	0.0	0.0	0.0	0.0	2.3	0.0	0.0	0.0	0.0	0.8	18.8	3.5	6.8
EF 31	20.3	7.8	28.5	0.0	6.2	0.0	0.0	1.3	0.0	0.0	7.5	26.0	1.2	1.2	0.0	0.0	0.0	0.0	0.0
EF 33	18.8	1.8	0.7	0.0	0.2	0.5	0.0	0.0	3.0	0.0	7.5	5.8	0.0	0.0	5.2	4.5	45.5	0.0	6.5
EF 40	42.3	5.7	14.5	0.0	12.0	0.0	0.0	1.0	0.0	0.0	1.3	0.0	0.0	0.0	0.5	2.7	5.0	0.0	15.0
EF' 4-A	30.5	11.0	9.3	0.0	0.0	2.0	0.0	1.7	1.0	0.8	15.0	12.2	4.3	0.0	0.0	2.2	10.0	0.0	0.0
EF'10	26.5	9.0	29.5	0.0	3.3	0.5	0.0	1.0	0.0	0.0	5.7	1.5	0.0	0.0	6.8	3.2	13.0	0.0	0.0
EF'22	31.5	13.4	8.3	0.0	1.5	0.2	0.0	2.0	0.0	0.0	13.9	2.4	6.5	0.0	0.0	7.3	12.9	0.0	0.0
EF'28	18.3	9.6	9.3	0.0	1.0	1.5	0.0	3.0	1.3	0.5	15.7	8.4	0.0	0.0	4.3	5.3	21.6	0.0	0.0

Table A-1 (continued)

Sample no.	Micrite	Microspar	Spar	Intraclasts	Peloids	Brachiopod fragments	Gastropods	Ostracod valves	Trilobite debris	Pelecypod debris	Echinoderm debris	Bryzoan debris	Algae	Oncolites	Sponge debris	Other fossils	Clay laminae	Detrital quartz	Other minerals
EF' 37	18.0	9.5	13.8	0.0	0.2	1.0	0.8	3.0	0.2	0.3	16.5	13.8	1.0	0.0	1.7	3.5	16.7	0.0	0.0
EF' 45	5.3	2.5	30.2	1.5	1.5	0.3	0.0	2.2	1.8	0.0	29.0	18.7	3.0	0.0	0.0	1.0	3.0	0.0	0.0
EF' 50	20.0	18.5	22.5	0.5	0.5	0.3	1.0	0.2	2.5	2.0	11.3	7.0	6.2	0.0	0.0	0.8	6.7	0.0	0.0
EF' 52	8.5	6.3	29.7	0.0	1.8	0.2	0.3	2.0	2.2	0.3	15.5	10.2	4.5	3.5	0.0	1.5	13.5	0.0	0.0
EF' 53	10.2	10.7	12.7	0.0	0.0	0.0	0.3	3.0	2.7	2.0	17.7	7.5	3.2	1.5	0.0	3.5	24.9	0.0	0.0
EF' 54-A	11.8	13.0	10.0	0.0	0.0	0.5	0.0	0.7	2.5	1.0	21.3	11.5	7.7	2.5	1.0	1.3	15.2	0.0	0.0
EF' 56	3.8	20.2	12.0	0.5	0.5	0.3	0.0	2.7	2.3	0.5	25.0	5.7	6.5	3.8	0.0	2.7	13.5	0.0	0.0
EF' 58	19.5	10.5	13.5	0.3	0.2	0.3	0.0	3.0	1.5	1.7	17.0	8.8	3.5	10.0	0.0	3.2	5.8	0.0	1.2
EF' 68	4.8	6.0	31.5	1.2	1.3	0.7	0.5	2.5	1.8	0.2	28.8	17.5	0.2	0.0	0.0	1.5	1.5	0.0	0.0
EF' 76	13.3	28.7	7.0	0.5	0.0	0.8	0.0	1.7	3.3	1.0	19.0	6.0	2.5	0.0	0.0	4.2	12.0	0.0	0.0

Table A-1 (continued)

Sample no.	Micrite	Microspar	Spar	Intraclasts	Peloids	Brachiopod fragments	Gastropods	Ostracod valves	Trilobite debris	Pelecypod debris	Echinoderm debris	Bryzoan debris	Algae	Oncolites	Sponge debris	Other fossils	Clay laminae	Detrital quartz	Other minerals
EF'80	45.3	24.7	5.3	0.0	0.0	0.0	1.0	0.7	0.5	2.3	2.0	2.2	7.8	0.0	0.0	3.5	4.7	0.0	0.0
EF'87	10.8	11.0	13.5	1.5	11.0	4.2	0.0	2.8	0.5	7.5	5.0	16.5	2.7	9.0	0.0	2.3	1.7	0.0	0.0
EF'89	5.8	33.7	4.0	0.0	0.0	12.8	0.0	0.2	2.5	1.5	6.5	7.5	8.5	3.5	0.0	2.5	6.5	4.5	0.0
EF'90	6.0	12.0	1.8	0.0	0.0	2.0	0.0	0.7	0.8	0.5	2.5	3.2	5.3	38.5	0.0	2.2	21.5	3.0	0.0
EF'92	11.0	11.0	0.8	0.0	0.0	7.2	1.8	1.7	3.5	0.0	17.0	10.8	3.2	0.0	0.0	4.3	25.7	2.0	0.0
EF'93	21.2	26.6	0.6	0.0	5.0	0.0	0.0	0.1	0.0	0.0	0.0	0.0	0.0	0.0	0.0	0.0	29.6	1.6	15.3
EF'94	37.2	16.6	0.0	0.0	11.3	0.0	0.0	0.0	0.0	0.0	0.0	0.0	0.0	0.0	0.0	0.0	9.4	3.4	22.2
EF'95	14.4	23.1	16.6	0.0	1.9	0.0	0.0	0.0	0.0	0.0	0.0	0.0	0.0	0.0	0.0	0.0	34.4	3.1	6.6
EF'96	13.7	8.4	13.1	0.0	19.7	0.0	0.0	1.3	0.0	0.0	0.0	0.0	0.0	0.0	0.0	0.0	9.4	6.6	27.8
EF'98	33.1	15.3	13.8	0.0	0.6	0.0	0.0	0.0	0.0	0.0	0.0	0.0	0.0	0.0	0.0	0.3	28.8	2.5	5.6

APPENDIX B

Table B-1. Descriptions of gastropods found in intervals A and B.

GASTROPODS	DESCRIPTIONS
(1) Gastropod A	conispiral, 4 or 5 whorls, holostomatous, several shoulders, dextral. Hand sample.
(2) Gastropod B	conispiral, 3 or 4 whorls, holostomatous, smooth (no shoulders), dextral. Hand sample.
(3) Gastropod C	planispiral, smooth. Thin section.
(4) Gastropod D	small ($\leq$ 1mm), low spired, smooth (no shoulders), 2 to 3 whorls. Thin section.
(5) Gastropod E	small (1-2mm), low spired, shoulders, 3 to 4 whorls.
(6) Gastropod F	large (2cm high), high spired, small apical angle, 5 to 6 whorls. Hand sample.
(7) Gastropod G	medium (2-3mm high), high spired, 4 or 5 whorls, smooth. Thin section.

Table B-2. Descriptions of cephalopods found in interval A.

CEPHALOPODS	DESCRIPTIONS
(1) Endoceroid	eurysiphonate (marginal), depressed cross section, gently tapering phragmacone, straight suture—widely spaced.
(2) Cephalopod A	stenosiphonate (marginal), phragmacone slightly constricted, body chamber flattened, subconical, expanded anteriorly, saddles on flanks and 1 lobe each on dorsal and ventral side, depressed cross section, closely spaced sutures.
(3) Cephalopod B	stenosiphonate (marginal), depressed cross section, gently tapering phragmacone—slightly flexed, straight—closely spaced sutures.
(4) Cephalopod C	siphuncle marginal, expanded connecting rings, compressed cross section, strongly tapering phragmacone, straight—widely spaced sutures.
(5) Cephalopod D	stenosiphonate (submarginal), depressed cross section, strongly tapering phragmacone, lateral lobes and dorsal and ventral saddles, widely spaced sutures.

Table B-3. Autecologic parameters of the taxa present in intervals A and B of the Benbolt and Wardell Formations, respectively, at Evans Ferry, Tennessee (autecologic parameters and chart format after Walker, 1972). A major feature or occurrence is denoted by an X and an 0 denotes a secondary feature or occurrence. The species are listed in alphabetical order within each major fossil group.

	Community					Salinity Tolerance		Relation to Bottom				Mobility Relationships Within the Benthos						Mode of Food Acquisition						
								Benthic				Epifaunal				Inf.		Filter Feeder						
	Supratidal-High Intertidal	Middle-Low Intertidal	Wave Baffle	Shallow Subtidal (nearshore)	Stable Subtidal (offshore)	Euryhaline	Stenohaline	Epifaunal	Infaunal	Nectobenthic	Nectonic	Encrusting	Attached	Sessile	Vagile	Sessile	Vagile	High(15-30cm)	Med.(7-14cm)	Low (1-6 cm)	Deposit Feeder Scavenger	Browser	Predator (active)	Benthic Primary Producer
Allosaccus prolixus					X	X		X					X						X					
Tetradium cellulosum			X				X	X					X						X					
Amplexopora sp.				X			X	X					X						X					
Astreptodictya sp.					X		X	X					X						X					
Batostoma sp.				0	X		X	X				0	X						X					
Bythopora sp.				X	0		X	X					X							X				
Coeloclema sp.					X		X	X				X								X				
Constellaria sp.				X	0		X	X				X								X				
Diplotrypa sp.				X			X	X					X							X				
Hallopora sp.				X	0		X	X					X						X					
Helopora sp.				X	0		X	X					X							X				
Hemiphragma sp.				X	X		X	X					X						X					
Homotrypa sp.					X		X	X					X						X					
Leptotrypa sp.					X		X	X				X							X					
Nicholsonella sp.				X	0		X	X				X	0						X					
Ottoseetaxis sp.				0	X		X	X					X						X					
Pachydictya sp.				0	X		X	X					X						X					
Phylloporinid				X	0		X	X					X							X				
Stictopora sp.				X			X	X					X						X					
Camerella sp. cf. plicata				X			X	X					X							X				

Table B-3 (continued)

	Community					Salinity Tolerance		Relation to Bottom				Mobility Relationships Within the Benthos						Mode of Food Acquisition							
								Benthic				Epifaunal				Inf.		Filter Feeder							
	Supratidal-High Intertidal	Middle-Low Intertidal	Wave Baffle	Shallow Subtidal (nearshore)	Stable Subtidal (offshore)	Euryhaline	Stenohaline	Epifaunal	Infaunal	Nectobenthic	Nectonic	Encrusting	Attached	Sessile	Vagile	Sessile	Vagile	High(15-30cm)	Med.(7-14cm)	Low (1-6 cm)	Deposit Feeder Scavenger	Browser	Predator (active)	Benthic Primary Producer
Chaulistomella inaequistriata				X			X	X					X							X				
Cyrtonotella sp.					X		X	X					X							X				
Dactylogonia sp.					X		X	X					X							X				
Glyptorthis rara					X		X	X					X							X				
Glyptorthis uniformis					X		X	X					X							X				
Hesperorthis sp. cf. tricenaria				X			X	X					X							X				
Lingulella sp.					X		X	X					X							X				
Macrocoelia sp.					X		X	X						X						X				
Mimella globosa					X		X	X					X							X				
Opikina parvula					X		X	X					X							X				
Oxoplecia sp. A					X		X	X					X							X				
Oxoplecia sp. B					X		X	X					X							X				
Plectocamara sp. cf. erecta				X			X	X					X							X				
Rhipidomena tennesseensis					X		X	X						X						X				
Rostricellula ovata				X			X	X					X							X				
Strophomena medialis				X			X	X						X						X				
Strophomena inspeciosa				X			X	X						X						X				
Gastropod A					X	X		X							X						X			
Gastropod B					X	X		X							X						X			
Gastropod C				X		X		X							X						X			
Gastropod D				O	X	X		X							X						X			

Table B-3 (continued)

	Community					Salinity Tolerance		Relation to Bottom				Mobility Relationships Within the Benthos						Mode of Food Acquisition						
								Benthic				Epifaunal				Inf.		Filter Feeder						
	Supratidal-High Intertidal	Middle-Low Intertidal	Wave Baffle	Shallow Subtidal (nearshore)	Stable Subtidal (offshore)	Euryhaline	Stenohaline	Epifaunal	Infaunal	Nectobenthic	Nectonic	Encrusting	Attached	Sessile	Vagile	Sessile	Vagile	High (15-30cm)	Med (7-14cm)	Low (1-6 cm)	Deposit Feeder Scavenger	Browser	Predator (active)	Benthic Primary Producer
Gastropod E				X		X		X							X							X		
Gastropod F				X		X		X							X							X		
Gastropod G					X	X		X							X							X		
Cephalopod A					X		X				X												X	
Cephalopod B					X		X				X												X	
Cephalopod C					X		X				X												X	
Cephalopod D					X		X				X												X	
Endoceroid					X		X				X												X	
Bumastus sp.				O	X	X		X							X						X			
Calyptaulax (Calliops) sp.				X	X	X				?											?			
Ceraurus sp.					X	X		X							X						X			
Homotelus sp.					X	X		X							X						X			
Illaenus sp.				O	X	X		X							X						X			
Isotelus sp.					X	X		X							X						X			
Nanillaenus sp.				X	X	X		X							X						X			
Ostracods	X	X		X	X	X		X							X						X			
Anulocrinus latus					X		X	X					X							X				
Batherocystis appressa				X	O		X	X					X						?					
Canadocystis tennesseensis					X		X	X					X							X				
Carabocrinus micropunctatus					X		X	X					X					X						
Coronocystis angulatus				O	X		X	X					X					X						

Table B-3 (continued)

	Community					Salinity Tolerance		Relation to Bottom				Mobility Relationships Within the Benthos						Mode of Food Acquisition						
								Benthic				Epifaunal				Inf.		Filter Feeder						
	Supratidal-High Intertidal	Middle-Low Intertidal	Wave Baffle	Shallow Subtidal (nearshore)	Stable Subtidal (offshore)	Euryhaline	Stenohaline	Epifaunal	Infaunal	Necrobenthic	Nectonic	Encrusting	Attached	Sessile	Vagile	Sessile	Vagile	High(15-30cm)	Med.(7-14cm)	Low (1-6 cm)	Deposit Feeder Scavenger	Browser	Predator (active)	Benthic Primary Producer
Cyclocystoid				X			X	X					X					X						
Hybocrinus sp. cf. punctatocristatus					X		X	X					X					X						
Hybocrinus sp. cf. punctatus					X		X	X					X					X						
Meristochisma fayi					X		X	X					X					X						
Paleocrinus sp. cf. avondalensis					X		X	X					X					X						
Paleocrinus planobasilis					X		X	X					X					X						
Paradiablocrinus sp. cf. sinuorgosus					X		X	X					X					X						
Platycystites faberi					X		X	X					X					X						
Regulaecystis pyriformis					X		X	X							X				?	?				
Ulrichocystis eximia					X		X	X					X					X						
Contexta					X		X																	X
Girvanella oncolites			X				X																	X
Kazahkstanelia			O		X		X																	X
Moniliporella					X		X																	X
Nuia					X		X																	X
Receptaculites					X		X																	X
Solenopora			X		O		O																	X
Vermiporella					X		X																	X
(Blue-green) algal mats	O	X				X																		X
Vertical burrowers	O	X				?	X		X							X				X				

APPENDIX C

Table C-1. Fossils present in EF'18-A.

Echinoderms	Brachiopods	Bryozoans	Trilobites	Algae	Other Classes
Platycystites faberi	Dactylogonia sp.	Ottoseetaxis sp.	Illaenus sp.	Receptaculites	Ostracods
Canadocystis tennesseenis	Cyrtonotella sp.	Helopora sp.	Nanillaenus sp.	Nuia	
		Constellaria sp.	Calyptaulax (Calliops) sp.	Girvanella	
		Phylloporinid			
		Batostoma sp.			
		Nicholsonella sp.			
		Leptotrypa sp.			
		Astreptodictya sp.			
		bifoliate A			

Table C-2. Fossils present in EF'18-B.

Echinoderms	Brachiopods	Bryozoans	Trilobites	Algae	Other Classes
Ulrichocystis eximia	Dactylognia sp.	Hallopora sp.	Nanillaenus sp.	Receptaculites	Ostracods
Paradiablocrinus sp. cf. sinuorugosus	Mimella globosa	Leptotrypa sp.	Bumastus sp.	Kazahkstanelia	
Paleocrinus sp. cf. avondalensis	Oxoplecia sp. A	Helopora sp.	Asaphidae	Contexta	
	Cyrtonotella sp.	Astreptodictya sp.		Girvanella	
	Opikina parvula	Phylloporinid			
	Lingulella sp.	bifoliate (?)			

Table C-3. Fossils present in EF'18-C.

Echinoderms	Brachiopods	Bryozoans	Trilobites	Algae	Gastropods	Other Classes
Canadocystis tennesseensis	Glyptorthis uniformis	Amplexopora sp.	Illaenus	Receptaculites	Gastropod D	Ostracods
Ulrichocystis eximia	Opikina parvula	Helopora sp.	Dalmanitacea	Contexta		
Paradiablocrinus sp. cf. sinuorugosus	Mimella globosa	Bythopora sp.		Kazahkstanelia		
		Phylloporinid		Nuia		
Carabocrinus micropunctatus	Cyrtonotella sp.	Hallopora sp.		Girvanella		
Paleocrinus avondalensis	Rhipidomena tennessensis	Nicholsonella sp.				
		Hemiphragma sp.				
Meristochisma fayi	Lingulella sp.	Ceramoporoid				
Coronocystis angulatus		Leptotrypa sp.				
		Astreptodictya sp.				

Table C-4. Fossils present in EF'18-D.

Echinoderms	Brachiopods	Bryozoans	Trilobites	Algae	Gastropods	Other Classes
Hybocrinus sp. cf. punctatus Hybocrinus sp. cf. punctatocristatus Paleocrinus planobasilis Anulocrinus latus Carabocrinus micropunctatus Ulrichocystis eximia Canadocystis tennesseensis Regulaecystis pyriformis Coronocystis angulatus	Glyptorthis uniformis Cyrtonotella sp. Mimella globosa Oxoplecia sp. B	Hallopora sp. Helopora sp. Batostoma sp. Astreptodictya sp. bifoliate (?)	Isotelus sp. Bumastus sp. Phacopacea	Receptaculites Kazahkstanelia Vermiporella Contexta Nuia Girvanella	Gastropod D	ostracods pelecypods

Table C-5. Fossils present in EF'18-E.

Echinoderms	Brachiopods	Bryozoans	Trilobites	Algae	Gastropods	Other Classes
Ulrichocystis eximia Canadocystis tennessensis Carabocrinus micropunctatus Hybocrinus punctatus Coronocystis angulatus Regulaecystis pyriformis	Cyrtonotella sp. Glyptorthis rara Mimella globosa Öpikina sp.	Helpora sp. Phylloporinid Batostoma sp. Astreptodictya sp.	Bumastus sp.	Receptaculites Nuia Girvanella	Gastropod E Gastropod D	ostracods pelecypods

Table C-6. Fossils present in EF'18-F.

Echinoderms	Brachiopods	Bryozoans	Algae
Coronocystis angulatus	Glyptorthis sp. Cyrtonotella sp. Mimella globosa	No data	Receptaculites

Only a few samples were obtainable from this interval.

Table C-7. Fossils present in EF'18-G.

Echinoderms	Brachiopods	Trilobites	Bryozoans	Cephalopods	Gastropods
Hybocrinus punctatocristatus Carabocrinus sp. Regulaecystis pyriformis	Glyptorthis sp. Cyrtonotella sp. Mimella globosa	Homotelus sp. Bumastus sp. Ceraurus sp.	No data	Endoceroid Cephalopod A Cephalopod B Cephalopod C	Gastropod A

Table C-8. Fossils present in EF'18-H.

Brachiopods	Bryozoans	Trilobites	Algae	Gastropods	Cephalopods	Other Classes
Macrocoelia sp.	Helopora sp. Nicholsonella sp. Homotrypa sp. Batostoma sp. Ceramoporid Pachydictya sp. Astreptodictya sp.	Nanillaenus sp. Illaenus sp.	Contexta Solenopora type P Girvanella	Gastropod G Gastropod D Gastropod A	Cephalopod D Cephalopod A	ostracods pelecypods

Table C-9. Fossils present in EF'18-I.

Brachiopods	Bryozoans	Trilobites	Algae	Gastropods	Cephalopods	Other Classes
Glyptorthis sp. Cyrtonotella sp.	Coeloclema sp. Hallopora sp. Constellaria sp. Nicholsonella sp. Hemiphragma sp. Batostoma sp. Pachydictya sp. Astreptodictya sp. Phylloporinid	Nanillaenus sp. Illaenus sp. Bumastus sp.	Girvanella Moniliporella	Gastropod A Gastropod B	Endoceroid	ostracods pelecypods

Table C-10. Fossils present in EF'19-J.

Brachiopods	Bryozoans	Algae	Trilobites	Gastropods	Other Classes	Echinoderms
Mimella globosa Glyptorthis sp.	Hemiphragma sp. Nicholsonella sp. Ottoseetaxis sp. Ceramoporid Batostoma sp. Phylloporinid Pachydictya sp. Diplotrypa sp. Helopora sp. Astreptodictya sp.	Contexta Kazahkstanelia Girvanella Nuia	Illaneus sp.	Gastropod D	ostracods	Ulrichocystis eximia Carabocrinus sp.

Table C-11. Fossils present in EF'19-K.

Bryozoans	Algae	Sponges	Gastropods	Other Classes
Phylloporinid Ceramoporid Hemiphragma sp. Nicholsonella sp. Helopora sp. bifoliate (?)	Contexta Kazahkstanelia Girvanella	Allosaccus prolixus	Gastropod D	ostracods pelecypods

Table C-12. Fossils present in EF'19-L.

Bryozoans	Brachiopods	Algae	Gastropods	Other Classes
Phylloporinid Batostoma sp. Homotrypa sp. Hallopora sp. Bythopora sp. Helopora sp. bifoliate (?)	Glyptorthis sp. Mimella globosa Cyrtonotella sp.	Kazahkstanelia Vermiporella Contexta Nuia Girvanella	Gastropod D Gastropod G	ostracods

Table C-13. Fossils present in EF'19-M.

Echinoderms	Brachiopods	Trilobites	Bryozoans
Coronocystis angulatus Carabocrinus sp.	Rhipidomena tennessensis Macrocoelia sp.	Illaenid	No data

Table C-14. Fossils present in EF'19-N.

Echinoderms	Bryozoans	Brachiopods	Algae	Gastropods	Other Classes
Batherocystis appressa	Ceramoporid Helopora sp. Bythopora sp. Nicholsonella sp. Phylloporinid bifoliate (?)	Glyptorthis sp. Rhipidomena tennesseensis	Receptaculites Vermiporella Contexta Girvanella	Gastropod D	ostracods

Table C-15. Fossils present in EF'23-A.

Brachiopods	Bryozoans	Algae	Trilobites	Coral	Echinoderms	Trace Fossils
Strophomena sp. cf. inspeciosa Camerella sp. cf. plicata Hesperorthis sp. cf. tricenaria	Ceramoporid Hallopora sp. Coeloclema sp. Hemiphragma sp. Helopora sp. Nicholsonella sp. Pachydictya sp. Escharopora sp.	Kazahkstanelia Girvanella	Bumastus sp.	Tetradium sp.	Cyclocystoid	"Unidentified burrowing deposit feeder"

Table C-16. Fossils present in EF'23-B.

Brachiopods	Bryozoans	Algae	Trilobites
Hesperorthis sp. cf. tricenaria	Hallopora sp.	Girvanella	Illaenus
Strophomena sp.	Hemiphragma sp.		
	Nicholsonella sp.		
	Phylloporinid		
	Amplexopora sp.		
	Helopora sp.		
	Pachydictya sp.		
	Escharopora sp.		

Table C-17. Fossils present in EF'23-C.

Brachiopods	Bryozoans	Algae	Coral	Gastropods	Trilobites
Hesperorthis sp. cf. tricenaria	Hemiphragma sp.	Girvanella	Tetradium	Gastropod C	Bumastus sp.
Strophomena sp. cf. inspeciosa	Helopora sp.			Gastropod D	
	Batostoma sp.				
	Ottoseetaxis sp.				
	Constellaria sp.				
	Hallopora sp.				
	Pachydictya sp.				
	Coeloclema sp.				
	Escharopora sp.				

Table C-18. Fossils present in EF'23-D.

Brachiopods	Bryozoans	Algae	Trilobites	Echinoderms	Gastropods	Coral
Strophomena inspeciosa Hesperorthis sp. cf. tricenaria Plectocamara sp. cf. erecta	Hallopora sp. Helopora sp. Nicholsonella sp. Ottoseetaxis sp. Hemiphragma sp. Constellaria sp. Amplexopora sp. Diplotrypa sp. Pachydictya sp. Escharopora sp.	Solenopora type R Girvanella	Calyptaulax (Calliops) mesleri	Coronocystis angulatus	Gastropod C Gastropod E	Tetradium

Table C-19. Fossils present in EF'24-A.

Brachiopods	Bryozoans	Algae	Corals	Gastropods
Chaulistomella sp. Strophomena sp.	Hallopora sp. Helopora sp. Ottoseetaxis sp. Hemiphragma sp. Constellaria sp. Nicholsonella sp. Phylloporinid	Solenopora type R Girvanella Kazahkstanelia	Tetradium	Gastropod D

Table C-20. Fossils present in EF'24-B.

Brachiopods	Bryozoans	Algae	Corals	Gastropods
Strophomena sp.	Hemiphragma sp. Hallopora sp. Amplexopora sp. bifoliate (?)	Girvanella Kazahkstanelia	Tetradium	Gastropod E

Table C-21. Fossils present in EF'24-C.

Bryozoans	Algae	Coral	Gastropods
Helpora sp. Constellaria sp. Pachydictya sp. Nicholsonella sp. Amplexopora sp. Hallopora sp. Escharopora sp.	Girvanella Kazahkstanelia	Tetradium	Gastropod E

Table C-22. Fossils present in EF'25-A.

Brachiopods	Bryozoans	Algae	Trilobites	Echinoderms	Gastropods	Trace Fossil
Strophomena medialis Chaulistomella inaequistriata	Helopora sp. Phylloporinid Batostoma sp. Hemiphragma sp. Hallopora sp. Amplexopora sp. Ottoseetaxis sp. Escharopora sp. Pachydictya sp. Constellaria sp. Nicholsonella sp.	Girvanella	Nanillaenus sp. Calyptaulax sp.	Batherocystis appressa	Gastropod C	"Unidentified burrowing deposit feeder(s)"

Table C-23. Fossils present in EF'25-B.

Brachiopods	Bryozoans	Algae	Trilobites	Echinoderms	Gastropods
Strophomena medialis Chaulistomella inaequistriata Plectocamara sp. cf. erecta	Hallopora sp. Helopora sp. Bythopora sp. Hemiphragma sp. Escharopora sp. Pachydictya sp.	Girvanella	Calyptaulax sp. Illaenus sp.	Batherocystis appressa Coronocystis angulatus	Gastropod D

Table C-24. Fossils present in EF'25-C.

Brachiopods	Bryozoans	Echinoderms
Chaulistomella inaequistriata	Helopora sp.	Batherocystis appressa
Strophomena medialis	Pachydictya sp.	
	Escharopora sp.	

Table C-25. Fossils present in EF'25-D.

Brachiopods	Bryozoans	Echinoderms	Gastropods
Chaulistomella inaequistriata	Helopora sp.	Batherocystis appressa	Gastropod D
Strophomena sp.	Hallopora sp.		
	Hemiphragma sp.		
	Escharopora sp.		

Table C-26. Fossils present in EF'26-A.

Brachiopods	Echinoderms	Trilobites
Chaulistomella inaequistriata	Batherocystis appressa	Nanillaenus sp.
Strophomena sp. cf. medialis		

Table C-27. Fossils present in EF'26-B.

No fossil shells, but abundant vertical burrows, some cryptalgal laminate structures, micrite sediment laminae and clay laminae.

Table C-28. Fossils present in EF'26-C.

Brachiopods
Strophomena sp. cf. medialis

Micrite and clay laminae, some laminations appear to be cryptalgal.

Table C-29. Fossils present in EF'26-D.

Brachiopods	Echinoderms	Bryozoans
Strophomena sp. cf. medialis	Batherocystis appressa	Phylloporinid Hallopora sp. Helopora sp. Escharopora sp.

Table C-30. Fossils present in EF'26-E.

Brachiopods	Bryozoans
Strophomena sp. cf. medialis Rostricellula ovata	No data available

Table C-31. Fossils present in EF'26-F.

Brachiopods	Bryozoans
Strophomena sp. Rostricellula sp.	Amplexopora sp. Phylloporinid Helopora sp. Escharopora sp. Hallopora sp.

Table C-32. Fossils present in EF'26-G.

Brachiopods	Bryozoans	Trilobites	Gastropods	Ostracods
Rostricellula sp.	Amplexopora sp. Escharopora sp.	Calyptaulax sp.	Gastropod F	Ostracod A

Plate C-1. Gymnolaemata (Bryozoans).

A. Nicholsonella sp., Photomicrograph of thin section, longtudinal view, 25X (sample EF' 54-B).

B. Amplexopora sp., Photomicrograph of acetate peel, longitudinal and transverse view, 25X (sample EF' 26-10).

C. Diplotrypa sp., Photomicrograph of acetate peel, longitudinal view, 25X (sample EF' 25).

D. Hemiphragma sp., Photomicrograph of thin section, longitudinal view, 100X (sample EF' 54-B).

E. Batostoma sp., Photomicrograph of acetate peel, transverse view, 40X (sample EF' 25-1).

F. Ottoseetaxis sp., Photomicrograph of thin section, transverse view, 100X (sample EF' 58).

G. Helopora sp., Photomicrograph of thin section, transverse view, 100X (sample EF' 57).

H. Bythopora sp., Photomicrograph of thin section, transverse view, 100X (sample EF' 57).

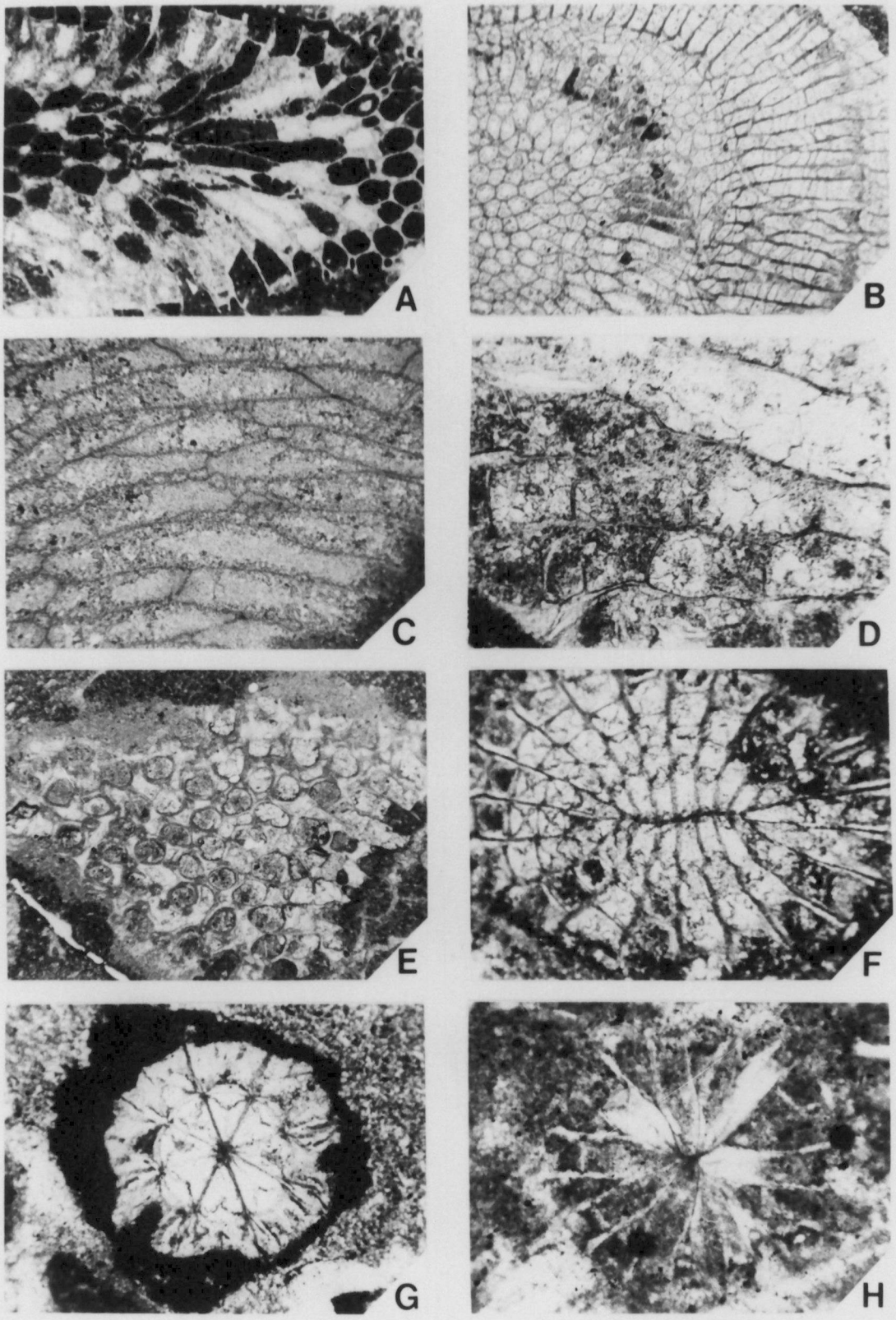


Plate C-1

Plate C-2. Gymnolaemata: Cryptostomata and Trepostomata (Bryozoans).

A. Escharopora sp., Photomicrograph of acetate peel, transverse view, 100X (sample EF' 25-2).

B. Pachydictya sp., Photomicrograph of thin section, longitudinal view, 25X (sample EF' 89).

C. Astreptodictya sp., Photomicrograph of thin section, transverse view, 100X (sample EF' 51).

D. Phylloporinid, Photomicrograph of thin section, transverse view, 100X (sample EF' 91).

E. Leptotrypa sp., Photomicrograph of thin section, longitudinal view, 100X (sample EF' 51).

F. Constellaria sp., Photomicrograph of thin section, transverse view, 25X (sample EF' 49).

G. Coeloclema sp., Photomicrograph of thin section, transverse view, 25X (sample EF' 57).

H. Homotrypa sp., Photomicrograph of thin section, longitudinal view, 100X (sample EF' 57).

I. Hallopora sp., Photomicrograph of thin section, longitudinal view, 25X (sample EF' 50).

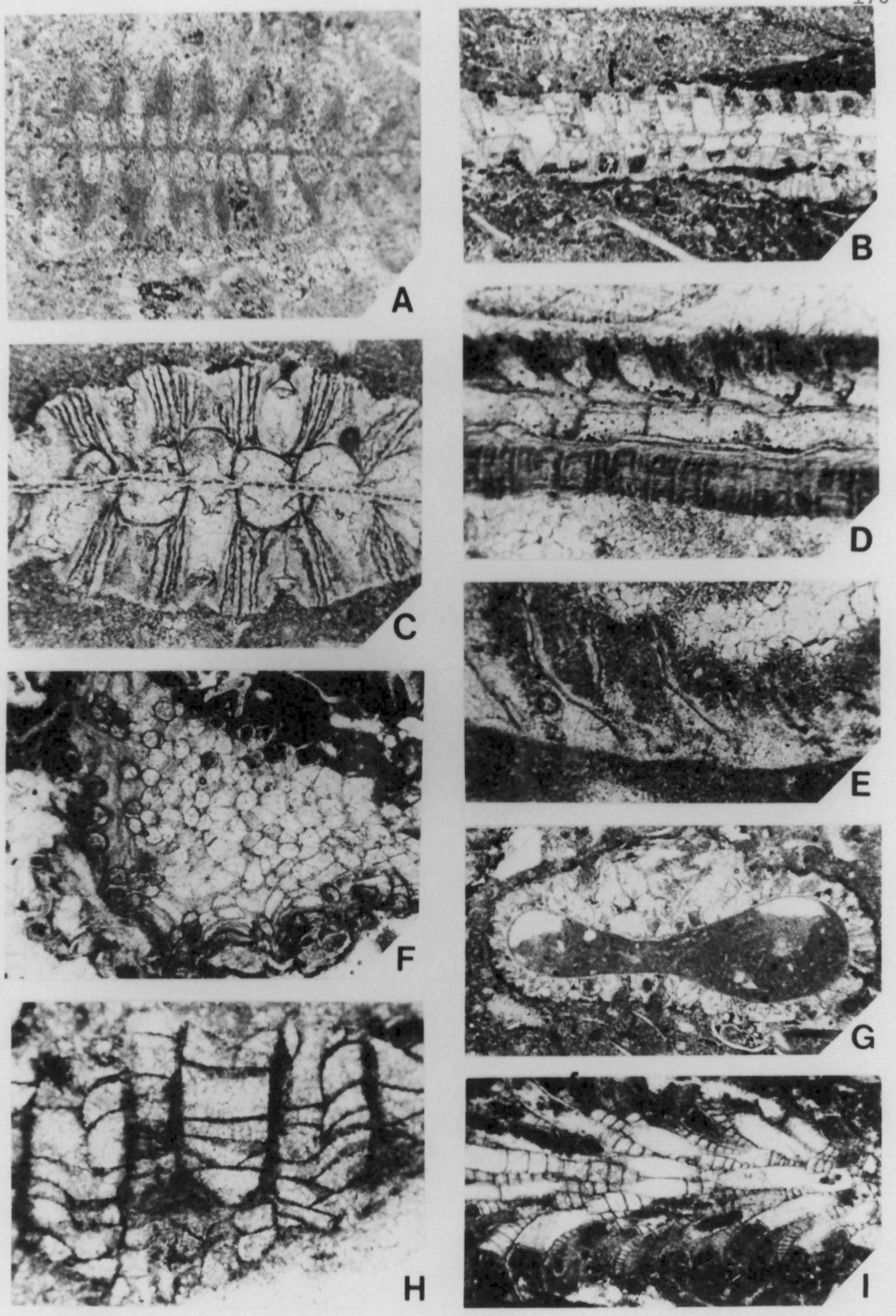


Plate C-2

Plate C-3. Inarticulata and Articulata (Brachiopods).

A,E,F. Camerella sp. cf. plicata; A,E brachical and anterior view of specimen on rock slab; 2X, 3X (sample EF' 23-2a,s); F side view of specimen on rock slab, 3X (sample EF' 23-2a,s).

B. Plectocamara sp. cf. erecta, brachial view of specimen on rock slab, 4X (sample EF' 25-9,s).

C. Glyptorthis rara, pedicle view of specimen in matrix, 5X (sample EF' 18-D3,i).

D. Glyptorthis uniformis, brachial view of specimen on rock slab, 4.5X (sample EF' 19-N,s).

G. Glyptorthis sp., pedicle view of specimen in matrix, 4X (sample EF' 18-E2,i).

H. Lingulella sp., inarticulate, interior view of pedicle valve (?), 5X, (sample EF' 18-E2,i).

I-K,N. Hesperorthis sp. cf. tricenaria; I,J interior and exterior of pedicle valve, 2X (samples EF' 23-12 and 23-6c,s); K,N brachial views, latter exhibiting attached pedicle valve, 2.5X (samples EF' 23-12 and 23-11,s).

L,M. Dactylogonia sp., pedicle and brachial view of specimens in matrix, 4X, 3X (samples EF' 18-A3a,s and 18-B1,i).

O. Oxoplecia sp. A, interior view of pedicle valve, 3X (sample EF' 18-B2,s).

P,Q,S. Mimella globosa; P posterior view, 3.5X (sample EF' 18-B3,i); Q,S interior and exterior of pedicle valve, 2.5X, 3X (samples EF' 18-B3,i and 18-D2,i).

R. Oxoplecia sp. B, pedicle view of specimen on rock slab, 4X (sample EF' 18-D2,s).

T. Rostricellula ovata, interior view of pedicle valve, 4X (sample EF' 26-9,s).

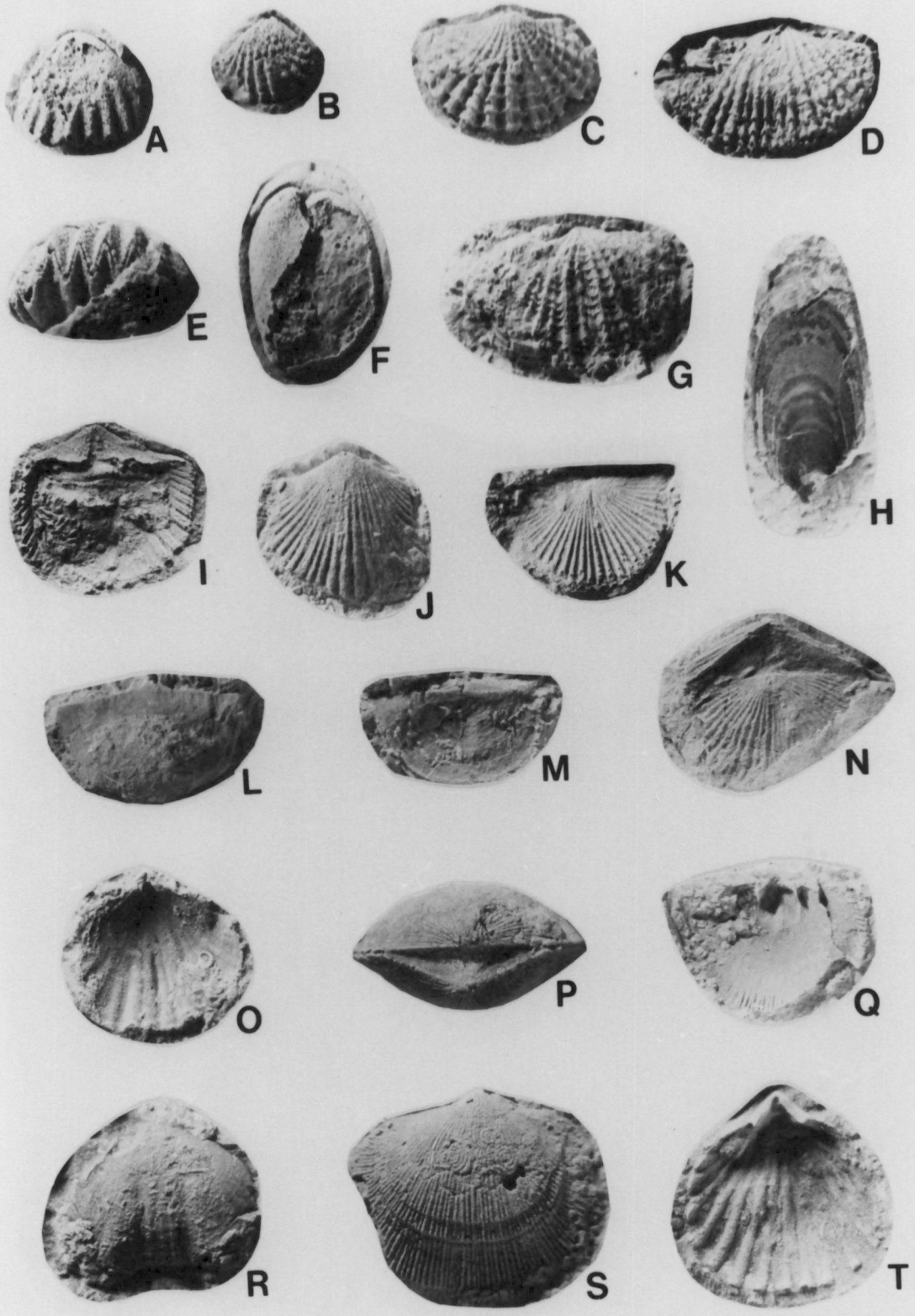


Plate C-3

Plate C-4. Articulata (Brachiopods).

A,D,G. Cyrtonotella sp., posterior, pedicle and brachial views of same specimen, 2.5X, 3X and 3X (sample EF' 18-B4,i).

B,C,E,H. Chaulistomella inaequistriata; B,C brachial and posterior views of same specimen, 2X (sample EF' 25-4,i); E,H interior views of brachial and pedicle valves, 2X (samples EF' 25-9 and 25-12,s).

F,I,J. Opikina parvula, F pedicle view of specimen, note oblique wrinkles at posterior margin, 2X (sample EF' 18-B4,i); I,J interior and exterior of brachial valve, latter with articulated pedicle valve, 2X (samples EF' 18-E1 and 18-C3,i).

K. Macrocoelia sp., pedicle view of weathered specimen in matrix, 2X (sample EF' 18-H,i).

L,M,P,S. Strophomena inspeciosa, L pedicle view of narrow interarea, 2X (sample EF' 23-15,s); M,P interiors of pedicle and brachial valves, 2X (sample EF' 23-15,s); S pedicle view of specimen on rock slab, 2X (sample EF' 23-15,s).

N,Q,T. Strophomena medialis, N interior view of pedicle valve, note wide interarea, 2X (sample EF' 25-15,i); Q,T brachial and pedicle views of same specimen, 2X (sample EF' 25-3,i).

O,R. Rhipidomena tennesseensis, brachial and pedicle views, 2X (sample EF' 19-N,i).

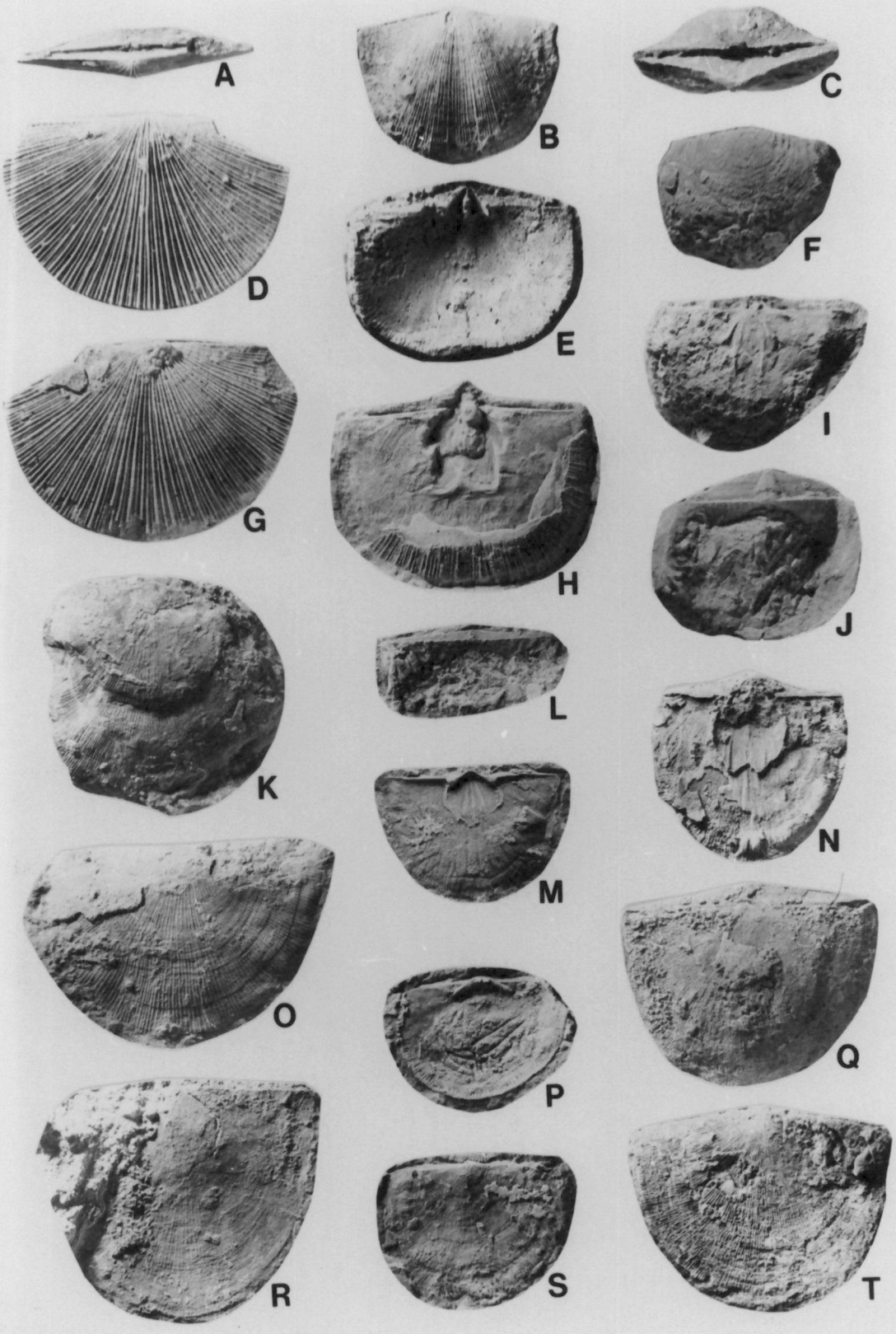


Plate C-4

Plate C-5. Cephalopoda and Gastropoda.

A. Cephalopod A, stenosiphonate, marginal siphuncle, 1X (sample EF' 18-H,i).

B. Cephalopod D, widely spaced sutures, 1X (sample EF' 18-H,i).

C. Cephalopod B, slightly flexed phragmacone, 2X (sample EF' 18-G,i).

D. Endoceroid, eurysiphonate, marginal siphuncle, 1X (sample EF' 18-G,i).

E. Gastropod A, prominent shoulders, 2X (sample EF' 18-G,i).

F. Cephalopod C, marginal siphuncle, depressed cross section, 2X (sample EF' 18-G,i).

G,H. Gastropod B, abapertural and apertural views of same specimen, 2X (sample EF' 18-G,i).

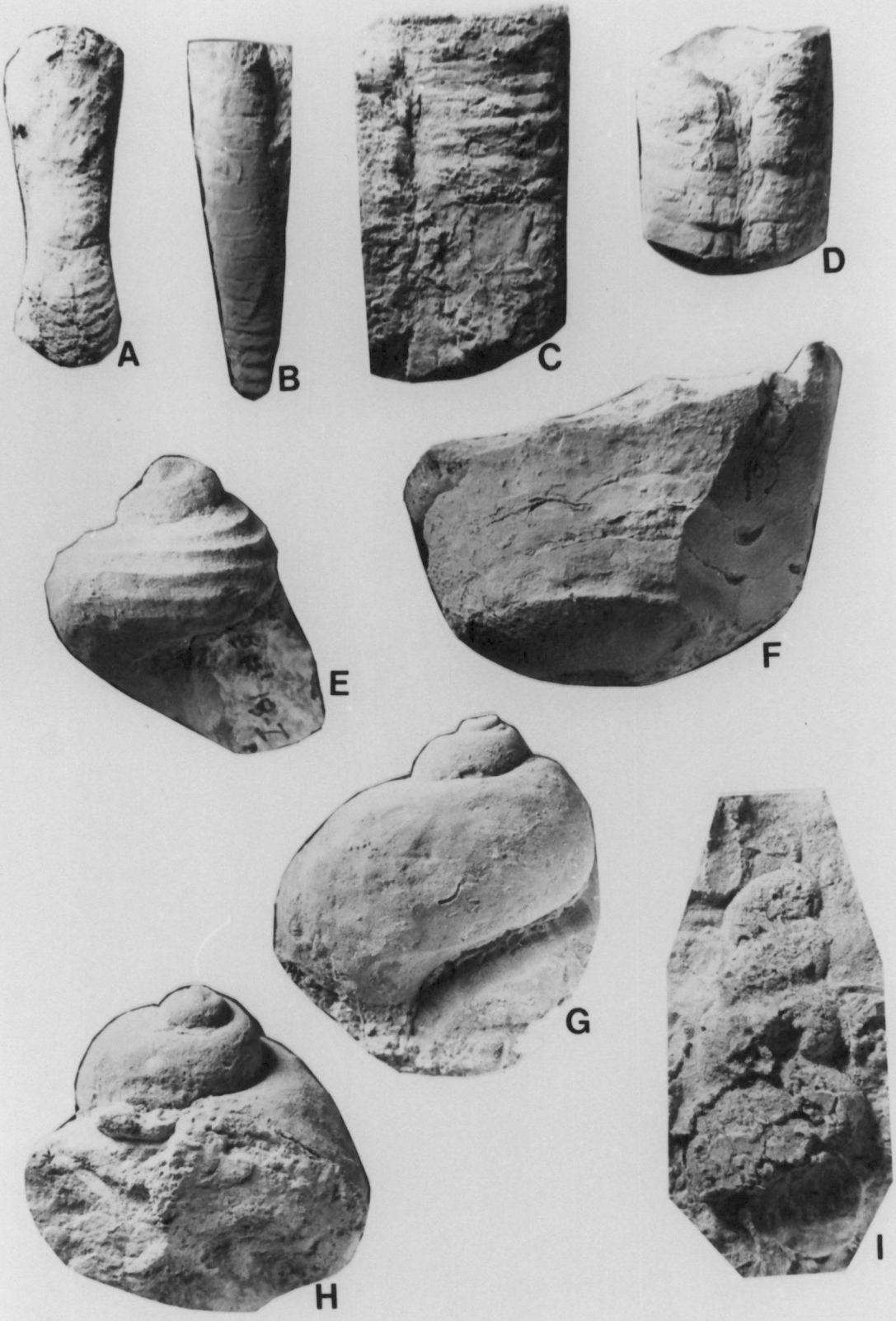


Plate C-5

Plate C-6. Trilobita.

A. Ceraurus sp., dorsal view of cephalon, 3X (sample EF' 18-G,i).

B. Isotelus sp., dorsal view of cephalon, 2X (sample EF' 18-D2,i).

C. Calyptaulax (Calliops) mesleri(?), dorsal view of cephalon, 2X (sample EF' 23-21,s).

D-F. Bumastus sp.; D,E dorsal views of two pygidia, 2X (samples EF' 18-G,i and 18-I3,s); F dorsal view of cephalon, 2X (sample EF' 23-6c,s).

G. Calyptaulax (Calliops) sp., dorsal view of pygidium, 3X (sample EF' 25-7,s).

H-J,L.N. Nanillaenus sp.; H-J dorsal views of pygidia, 2.5X, 2X and 2X (samples EF' 26-3,s; 18-H3,s and 18-I,i); L dorsal view of thorax, pygidium attached, 4X (sample EF' 25-1,s); N oblique dorsal view of thoraxial segments, 2.5X (sample EF' 18-A3,s).

K,M. Illaenus sp., dorsal views of two cephala, 2X (samples EF' 18-H,i and 18-A2,i).

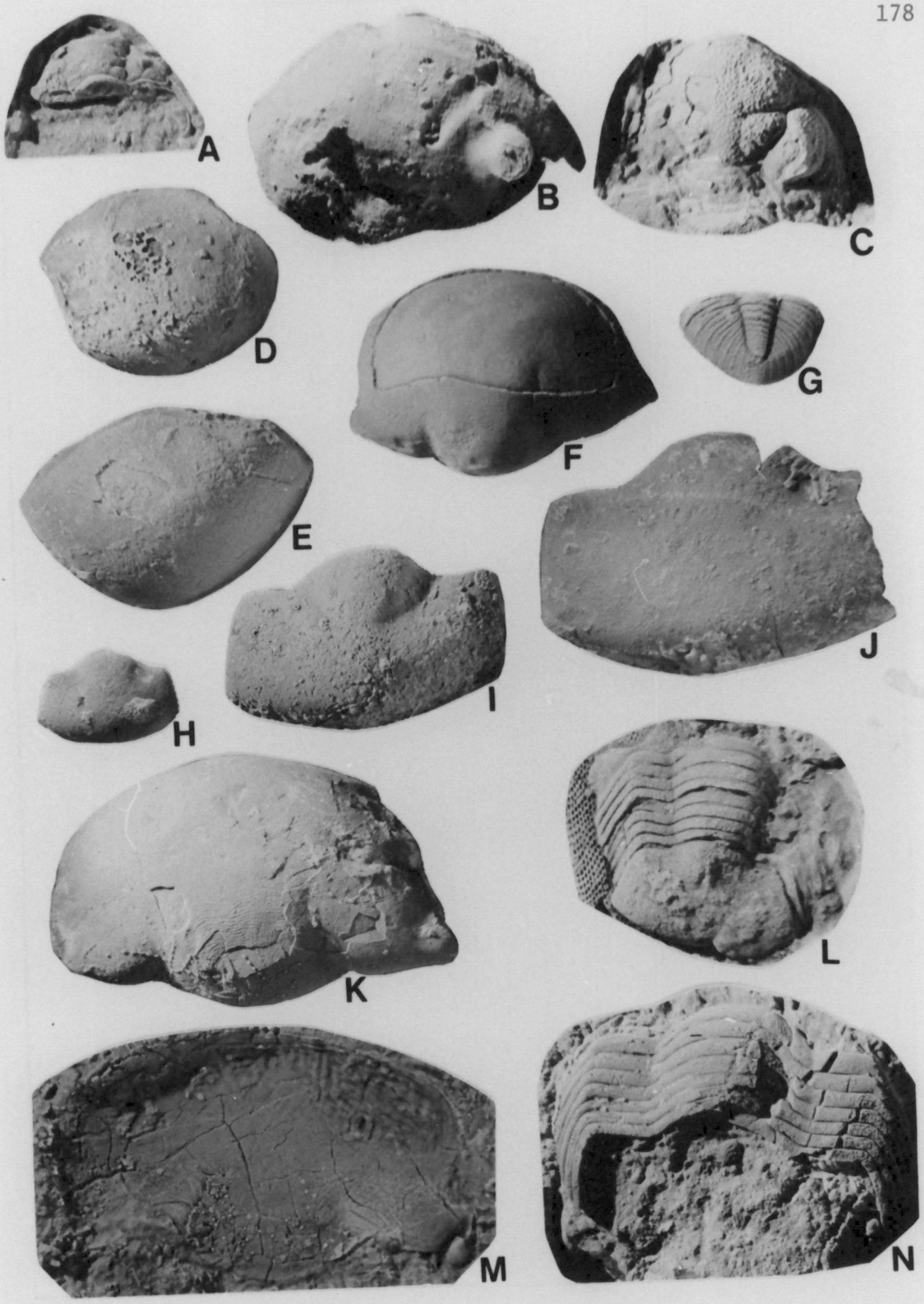


Plate C-6

Plate C-7. Rhombifera, Paracrinoidea, Eocrinoidea, Parablastoidea and Cyclocystoidea (pelmatozoan echinoderms).

A. Regulaecystis pyriformis, plate, Rhombiferan, 7X (sample EF' 18-E1,s).

B,C. Meristochisma fayi, plates, Parablastoid, 2.5X (samples EF' 18-C1 and 18-C3,i).

D. Coronocystis angulatus, radial plate, Rhombiferan, 4X (sample EF' 18-C2,i).

E. Batherocystis appressa, calyx and one attached columnal, Eocrinoid, 1.5X (sample EF' 25-11,s).

F,I. Canadocystis tennesseensis, both sides of calyx from same specimen, Paracrinoid, 3X (sample EF' 18-A3,i).

G. Cyclocystoid, marginal plate, 5X (sample EF' 23-2a,s).

H. Platycystites faberi, calyx, Paracrinoid, 3X (sample EF' 18-A3,i).

J. Ulrichocystis eximia, three adjoining plates in matrix, Paracrinoid, 6X (sample EF' 18-E4,i).

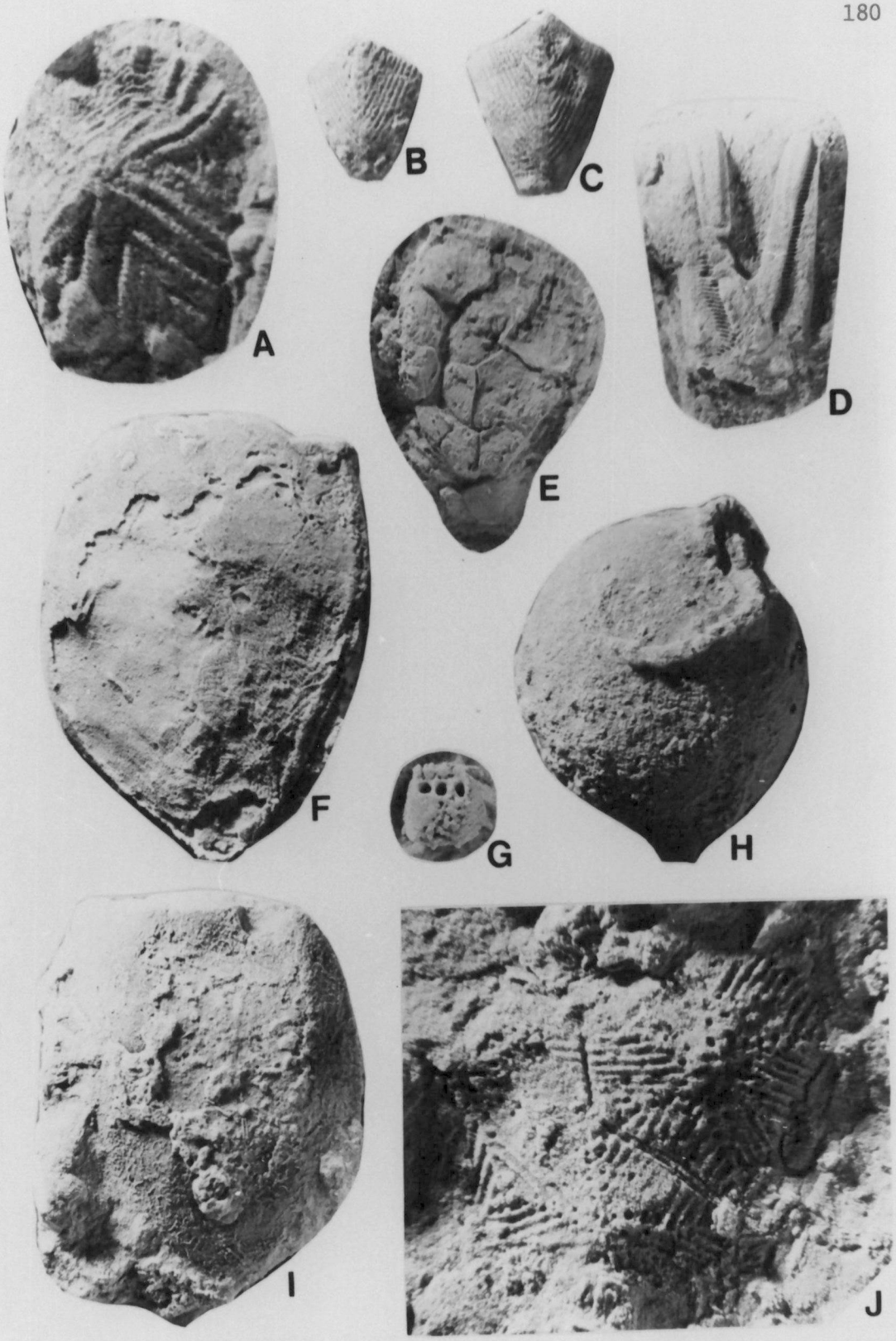


Plate C-7

Plate C-8. Crinoidea.

A. Paleocrinus planobasilis, radial plate, 4X (sample EF' 18-D3,i).

B. Paleocrinus sp. cf. avondalensis, plate, 4X (sample EF' 18-C1,i).

C. Anulocrinus latus, portion of calyx, 4X (sample EF' 18-D3,i).

D. Hybocrinus punctatus, calyx, 4X (sample EF' 18-E4,i).

E. Hybocrinus sp. cf. punctatocristatus, calyx, 1.5X (sample EF' 18-D1,s).

F. Paradiablocrinus sp. cf. sinuorugosus, base of calyx, 4X (sample EF' 18-B1,i).

G. Carabocrinus micropunctatus, plate, 8X (sample EF' 18-E2,s).

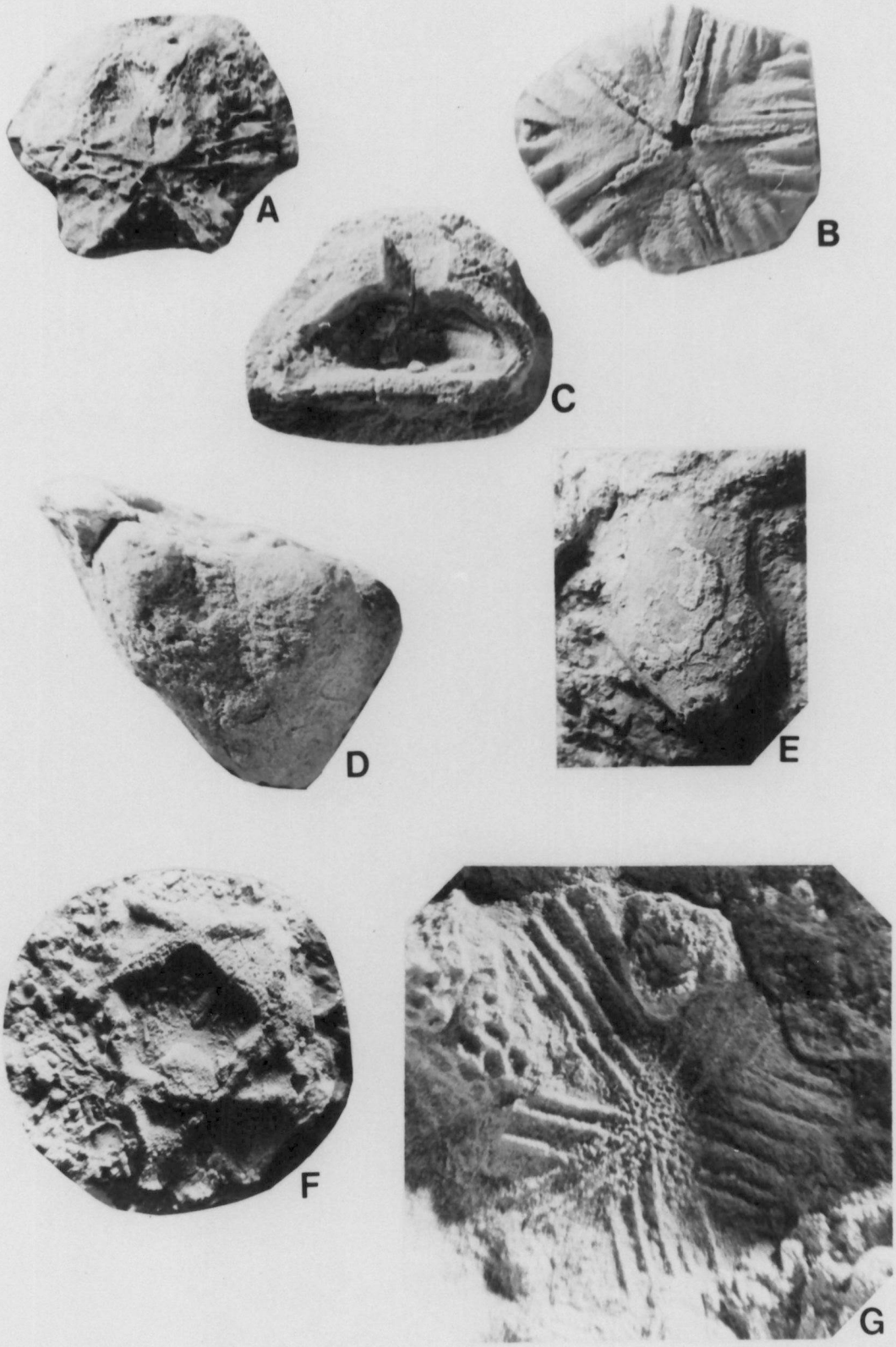


Plate C-8

Plate C-9. Chlorophyceae, Problematical algae, Rhodophyceae and Schizophyceae (algae).

A. Moniliporella sp., longitudinal view of single branch, Rhodophyceae, 30X (sample EF' 48).

B. Nuia sp., transverse and oblique views, Problematical algae, 100X (sample EF' 15-B).

C. Girvanella sp., loose tubules, Schizophyceae, 125X (sample EF' 22).

D. Solenopora type R, slice exhibiting transverse and longitudinal views, Rhodophyceae, 50X (sample EF' 90).

E,F. Contexta sp., oblique and transverse views of partly recrystallized thalli, Rhodophyceae, 30X, 40X (sample EF' 50).

G. Solenopora type P, slice exhibiting transverse and longitudinal views, Rhodophyceae, 25X (sample EF' 54-A).

H. Vermiporella sp., transverse view of recrystallized thallus, Chlorophyceae, 125X (sample EF' 71).

I. Receptaculites sp., view of opposite sides of two specimens, Chlorophyceae, 1X (samples EF' 18-B3 and 18-D1,i).

J. Kazahkstanelia sp., transverse view of thallus, Chlorophyceae, 30X (sample EF' 80).

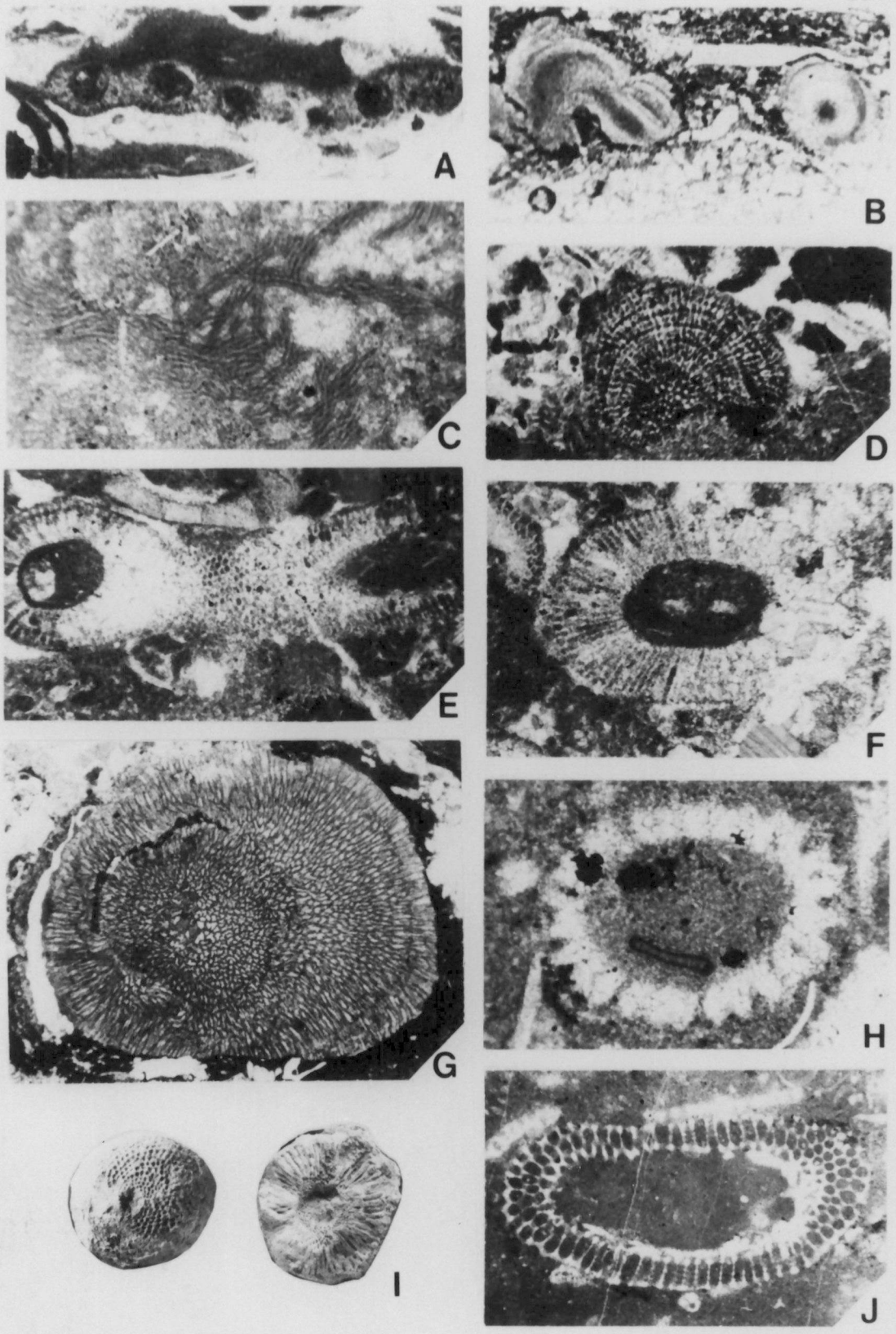


Plate C-9

VITA

Donald Kim Sickafoose was born in Easton, Maryland, on October 26, 1954. He attended elementary, junior high, and senior high schools in Lutherville, Maryland, and graduated from high school in June 1972. He entered Campbell College, North Carolina, in August 1972, and graduated in May 1976 with a Bachelor of Science degree. In September 1976, he entered the University of Tennessee at Knoxville and graduated with a Master of Science degree in June 1979. He started work for the Exxon Oil Company, New Orleans, Louisiana, in April 1979.